RSC Advances

REVIEW

View Article Online
View Journal | View Issue

Cite this: *RSC Adv.*, 2026, **16**, 3909

An overview on emerging green organic corrosion inhibitors: sustainable solution for oil and gas industrial applications

Nikhil Kumar, *[ad] Pranav Anunay,[b] Sunil Kumar,[cd] Lalit Kumar Meena [ad] and Dharmender Singh [e]

Corrosion remains a significant challenge across various industrial sectors, resulting in substantial economic losses, environmental hazards, and safety risks. Traditional corrosion inhibitors, though effective, often pose toxicity and environmental concerns, prompting the need for sustainable alternatives. The demand for eco-friendly and sustainable chemical species is increasing as industries seek to replace conventional toxic substances. This review emphasizes organic inhibitors derived from natural sources, such as amino acids, biopolymers, plant extracts, and environmentally benign synthetic compounds. Additionally, compounds synthesized through ultrasound and microwave irradiation, polyethylene glycols, ionic liquids, and multicomponent reactions are also considered environmentally friendly potential candidates to inhibit corrosion. The chemicals or compounds synthesized using water, ionic liquids, and supercritical carbon dioxide are also green corrosion inhibitors (CIs). Industrial processes such as oil extraction and gas transportation, where equipment are exposed to highly acidic environments, face significant corrosion challenges. Therefore, organic, green, eco-friendly, and cost-effective CIs are the primary demands of industry, researchers, and society. The development of new efficient green CIs can lead to the current research towards a sustainable pathway for future generations. In this context, researchers are continually working to develop more efficient CIs with the least hazardous environmental effects. The mechanisms of action, structural characteristics, and adsorption behaviour of OCIs are discussed in detail, along with their applicability in corrosive environments, such as oil wells, pipelines, and marine systems. This review provides a comprehensive overview of corrosion fundamentals, different classes of OCIs, key factors responsible for corrosion inhibition, mechanistic pathways, molecular modelling, and artificial neural networks for determining the rate of corrosion, followed by a future prospective. This review aims to support ongoing research efforts towards the sustainable corrosion control, offering valuable insights for scientists, engineers, and industries striving for greener and more cost-effective corrosion mitigation strategies.

Received 24th October 2025
Accepted 22nd December 2025

DOI: 10.1039/d5ra08166a

rsc.li/rsc-advances

Introduction

Corrosion in offshore platforms, oil wells, pipelines, and other infrastructure is a significant problem that has existed for a long time. It accounts for billions of dollars in annual production losses and repairs in oil and gas sectors as well as the loss of valuable lives.[1,2] Further, the oil and gas industrial processes employ hazardous gases and acidic solutions, which are extremely corrosive and aggressive. Acids can cause the evolution of hydrogen gas (H_2), which further results in hydrogen embrittlement and failures of metallic structures due to corrosion. One such industrial procedure is acid pickling, which is used to clean metal plates, wires, pipes, and machinery such as heat exchangers, cooling systems, and boilers of rust and surface contaminants. Many acids are frequently employed for this function, including HCl, H_2SO_4, H_3PO_4, HNO_3, H_3NSO_3, $C_6H_8O_7$, and HF acids.[3,4] Descaling is another industrial process that is utilized to remove hard-to-remove metal oxides from the

[a]*Advanced Materials & Corrosion (AMC) Division, CSIR-National Metallurgical Laboratory (NML), Jamshedpur, Jharkhand-831007, India. E-mail: kumar.nikhil@nml.res.in*

[b]*Department of Metallurgical and Material Engineering, Indian Institute of Technology Kanpur, Uttar Pradesh – 208016, India*

[c]*Materials Engineering (MTE) Division, CSIR-National Metallurgical Laboratory (NML), Jamshedpur, Jharkhand-831007, India*

[d]*Academy of Scientific and Innovative Research (AcSIR), Ghaziabad, Uttar Pradesh-201002, India*

[e]*Chemical Division, National Test House (NTH-NR), Ghaziabad, Uttar Pradesh-201002, India*

surface, such as high-temperature scale and rust, by mechanical or chemical means, and is often followed by pickling. Oil well acidification involves injecting extremely concentrated acidic solutions down a well through metallic pipes to increase the oil productivity by dissolving all acid-soluble components within underground rock formations or removing material at the wellbore face. A conventional method, namely well-acidizing, is employed to increase the productivity of pipelines. It involves dissolving rock formations like calcite, limestone, and dolomite by introducing acids under high pressure into their pore spaces. This process aims to increase the size of current flow channels and develop new ones, which will improve the flow of water or natural resources to the wellbore. Acidizing is often combined with matrix acidizing procedures and hydraulic fracturing. Acids are also used to remove scale from newly drilled wells and to repair drilling mud damage. Since the tubular materials and equipment used in the acidizing process are exposed to temperatures up to 200 °C, as well as chemicals like H_2S and CO_2, effective corrosion prevention is required. The characteristics of the groundwater reservoir determine the choice of acids applied in acidizing. Acids like HCl, HF, acetic acid, formic acid and their combination with other substances are often utilised. For instance, HF is suitable for sandstone deposits whereas HCl is regularly used for carbonate-based reserves. Mud acid, a solution of HCl and HF, is sometimes used in particular applications. The type, concentration, temperature, fluid velocity, and formation material of the acid are responsible factors for its reactivity. Heterocyclic compounds are utilised as CIs to reduce corrosion of the metallic tubes used in such operations. To reduce the adverse effects of acids and safeguard the metallic structures engaged, CIs must be carefully chosen and used.[4–6] The combination of two dissimilar metals used in pipelines leads to different forms of corrosion, including uniform corrosion, localised corrosion, internal corrosion, stress corrosion cracking, and galvanic corrosion, which occur in the petroleum sector. CIs must thus be used to reduce the corrosive effects, assuring the safety and efficiency of the acidizing process. Although regular chemical treatments are required for corrosion control, carbon steels (CS) are the most often used type of steel in the petroleum sector due to their affordable cost. Alternatives that are more resistant to corrosion can be used, such as austenitic or duplex stainless steels, although they are costlier and prone to chloride corrosion.

Nikhil Kumar

Dr Nikhil Kumar is a Scientist in Advanced Materials and Corrosion Division, CSIR-National Metallurgical Laboratory (NML), Jamshedpur, India. He obtained a BSc chemistry (H) from University of Delhi, India and a PhD in Inorganic and Materials Chemistry at the Department of Chemistry, National Institute of Technology (NIT) Kurukshetra, Haryana, India. Afterwards, he joined as a Postdoctoral Fellow, the Center of Hydrogen Fuel Cell Research, Korea Institute of Science and Technology (KIST), Seoul, South Korea. His research is mainly focused on the synthesis and design of functional materials for energy generation (OER & HER), conversion (Fuel Cell), storage (Supercapacitors), corrosion and coating applications. He has published 40 research articles, book chapters and patents. Dr Nikhil received several National and International awards for his academic achievements including Excellence Postdoctoral Fellowship, Israel and Shanghai Cooperation Organization-Young Scientist Conclave (SCO-YSC), Department of Science & Technology (DST) India.

Pranav Anunay

Mr Pranav Anunay is pursuing an MTech in Materials Science & Engineering from the Indian Institute of Technology (IIT), Kanpur, India. He has obtained a BTech in Metallurgical and Materials Engineering from Malaviya National Institute of Technology (MNIT), Jaipur, India. His research interests involve development of corrosion inhibitors and coatings for steel and other metallic substrates. He also has an experience in quenching and partitioning of steel and non-destructive testing.

Sunil Kumar

Dr Sunil Kumar is a Principal Scientist at the CSIR-National Metallurgical Laboratory (NML), Jamshedpur, India. He obtained his PhD and MTech in Chemical Engineering from IIT Delhi, India, and his BTech in Chemical Engineering from UIET Kanpur, India. His research focuses on atomistic simulations and advanced computational techniques, including density functional theory, molecular dynamics and reactive molecular dynamics, computational fluid dynamics, and the discrete element method for modelling metals, alloys, nanocomposites, polymers, corrosion, hydrogen production, and CO_2 conversion. He has published more than 50 scientific papers in reputed international journals and contributes extensively to the field of computational materials science.

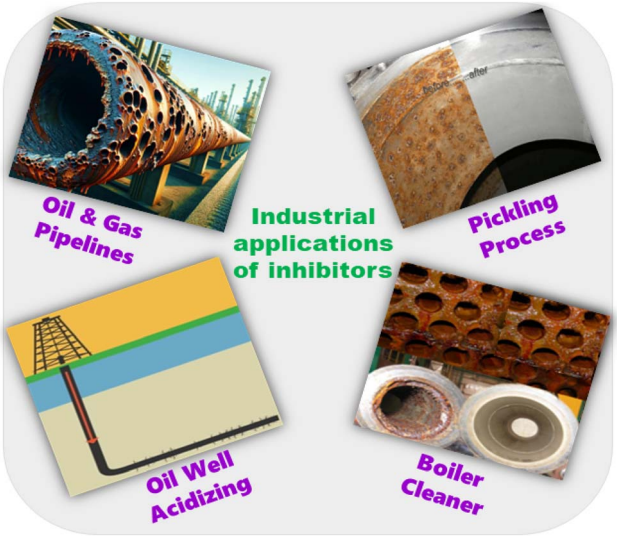

Fig. 1 Some well-known industrial applications of corrosion inhibitors.

Since API N80 CS is a steel that is often used for downhole tubular, flow lines and pipelines, the majority of research on CIs has been conducted on this material. At temperatures exceeding 93.3 °C, the corrosion resistance of various steel types might vary by up to 35%.[5] Different type of industrial applications of CIs are portrayed in Fig. 1.

A large number of organic and inorganic reagents like ammonia, thiourea, and heterocyclic compounds containing oxygen (O), nitrogen (N), sulphur (S), or phosphorus (P) are utilized in the HCl pickling of mild steel and carbon steel. Similarly, sulphuric acid pickling uses organic amines, quaternary ammonium salts, urea derivatives, and other substances to fight corrosion. The development of CIs is difficult as nitric acid pickling is extremely oxidizing, yet substances like hydrazine, Na_2S, NH_4SCN, thiourea, and others are utilized. Heterocyclic substances such as triazole, quaternary amines, benzotriazole, derivatives of urea, polyvinylpyrrolidone, imidazoline, and polyethyleneimine are needed for phosphoric acid pickling.[3–7] The research and development (R&D) fraternity across industries and academia has been continuously putting efforts into minimizing the economic and environmental impact of corrosion through various innovative solutions. Green inhibitors are commonly referred to as environmentally friendly corrosion inhibitors (CIs), which prevent corrosion of metals and alloys while reducing their detrimental effect on the environment. The current demand is to replace traditional CIs, which are associated with hazardous environmental impact, with a newer class of non-toxic CIs. More precisely, inorganic CIs incorporate either heavy metals or other hazardous substances, which pose a danger to humans and the ecological system. Besides direct

Lalit Kumar Meena

Mr Lalit Kumar Meena serves as a Principal Scientist in the Advanced Materials and Corrosion Division at CSIR-National Metallurgical Laboratory (NML), Jamshedpur. With over a decade of experience in corrosion science and advanced materials engineering, his work focuses on flow-assisted, microbial, and high-temperature corrosion, protective coatings, surface engineering, and failure analysis. An alumnus of the Indian Institute of Technology, Roorkee, he holds a BTech and MTech in Metallurgical and Materials Engineering, and is pursuing a PhD on Flow Assisted Pipeline Corrosion. Since joining CSIR-NML in 2015, he has contributed to several nationally significant projects with industries such as TATA Steel, SAIL, ONGC, BPCL, NTPC, DRDO, and IFB, addressing critical challenges in materials reliability and corrosion protection. He has authored numerous peer-reviewed publications in reputed journals, contributed book chapters, and is co-inventor of a granted Indian patent on a closed-loop system for simulating and monitoring corrosion in continuous flow conditions. Currently, his research focusses on elucidating the mechanisms of flow-assisted corrosion in pipeline steels, microstructure–corrosion relationships, and corrosion mitigation strategies for industrial applications.

Dharmender Singh

Dr Dharmender Singh is serving as a Scientific Officer (Chemical) at the National Test House (NTH), Ghaziabad, India. He received his BSc from Hindu College, University of Delhi, and his MSc in Chemistry from Kurukshetra University, India. He joined as a Research Associate at Jubilant Chemsys, R&D Centre, Noida. Hereafter, he obtained his PhD from the Department of Chemistry, Dr B. R. Ambedkar National Institute of Technology (NIT) Jalandhar, India. Dr Dharmender also worked as a Chemist at the Central Revenues Control Laboratory (CRCL), New Delhi, India. His research interests focus on the development of organic molecules and high-performance corrosion resistant conducting polymer/nanomaterial based hybrid coatings.

influence, these compounds may leak into the environment during usage or disposal, resulting in soil contamination or water body pollution.[8] Additionally, inorganic inhibitors may not offer appropriate multipurpose protection in various corrosive conditions or for range of metals and alloys since they are developed for specific types of corrosion or metal/alloy substrates. This inherent specificity or lack of multipurpose protection limits their use in particular fields or environments where a broader spectrum of corrosion protection is necessary. Stability problems may also affect the performance of inorganic inhibitors, as few substances are likely to degrade or decompose over time, reducing their effectiveness and necessitating regular reapplication. Such limitations pose a significant concerns for long-term applications like infrastructure or offshore industries that require long-term corrosion preventive solution. In addition, inorganic inhibitors could also face compatibility issues with other type of coatings, paints, or protective layers, which can diminish the overall performance, impair adhesion, or trigger adverse chemical interactions that accelerate corrosion.[1,2,8]

To ensure that CIs are effective and suitable for a range of applications, various criteria must be considered while choosing them for corrosion protection. It should be inexpensive *i.e.* economically feasible, easy to obtain, and readily available. CIs should be regulated by environmental laws to support sustainable practices and be in agreement with environmental protection and conservation. Additionally, the CIs should preferably be made from renewable resources, which will lessen dependence on scarce resources and ensure a continuous supply of inhibitors. Researchers and enterprises may use CIs that offer efficient protection while reducing environmental impact and support sustainable practices by taking these considerations into account.[7,9] A variety of CIs are used to prevent corrosion of metals and alloys; scavenging inhibitors are one kind and it works by eliminating aggressive chemicals from the corrosive medium by trapping or reacting with volatile gaseous substances to capture them or inhibit oxygen-induced corrosion. In packaging for storage or display, scavenger inhibitors are frequently utilized. Another type is interface inhibitor which prevents rusting by establishing a barrier at the metal–environment contact point. This interface inhibitor can be divided into two groups: liquid phase inhibitors and vapour phase inhibitors. Furthermore, vapour phase CIs are employed for the prevention of small atmospheric corrosion particularly in enclosed situations by establishing a protective environment by lightly saturating wrapping paper inside a closed container. The most often used kind of CIs are liquids, which may be further divided into anodic, cathodic or mixed types depending on the type of reaction. Overall, these innumerable CIs either remove aggressive materials, create protective layers, or modify electrochemical processes at the metal surface to effectively prevent corrosion.[3,7] The individual corrosion scenario and the intended level of protection must be taken into account when choosing an inhibitor. This review demonstrates basic corrosion and its types, background and current scenario of OCIs, factors affecting corrosion, mechanistic pathway, molecular modelling, artificial neural network to determine the rate of corrosion and future applications of organic CIs especially in oil well and pipelines.

Corrosion in oil and gas industries

In the oil and gas sector, corrosion is a major problem because it may result in the deterioration of pipelines, infrastructure, and equipment, posing a risk to public safety, causing environmental harm, and resulting in financial losses. The infrastructure of oil and gas industries is under constant threat due to several types of corrosion, such as uniform corrosion and different types of localized corrosion. Uniform corrosion is the most predictable type of corrosion that happens evenly throughout the metal surface, and it is controllable with protective coatings and routine maintenance. On the other hand, localised corrosion comprises galvanic, pitting, crevice, inter-grannular, filiform corrosion and stress corrosion cracking. Pitting corrosion is recognized by the formation of small and deep holes on the metal surface, which are often challenging to detect until severe damage has occurred. In small areas where the corrosive environment becomes trapped, crevice corrosion happens due to the formation of differential aeration or concentration cells. The filiform corrosion typically occurs on painted or coated surfaces and results from inadequate surface preparation. Further, galvanic corrosion occurs when two dissimilar metals are electrically coupled in a conductive electrolyte, causing the more anodic (less noble) metal to undergo accelerated dissolution relative to the cathodic counterpart. The inter-grannular corrosion (IGC) is another form of corrosion that preferentially occurs along the grain boundaries of metals/alloys and can crumble a structure without causing much weight loss. In the oil and gas sector, crack initiation and propagation can occur in corrosive environments under the influence of sustained tensile stresses, a phenomenon referred to as Stress Corrosion Cracking (SCC).[1,2] At many places, this cracking phenomenon involves a hydrogen sulphide gas environment called sulphide stress cracking (SSC), and if somewhere hydrogen atoms seep into the metal, creating internal fractures called hydrogen-induced cracking (HIC). In some cases, the gas pipelines may contain fungus, bacteria, or algae, which can lead to a particular type of corrosion, *i.e.*, microbiologically influenced corrosion (MIC). Also, the high velocities of corrosive fluids in pipelines may vastly accelerate the rate of material loss, and this phenomenon is known as erosion corrosion (EC) or flow assisted/accelerated corrosion (FAC). Further, the corrosion mechanisms and various forms of corrosion are discussed in the forthcoming section.

Basic definition & classification of corrosion

The corrosion is a natural degradation process of metals/alloys resulting from chemical and eletcrochemical interactions with the surrounding environment. This progressive phenomenon gradually compromises the physicochemical and structural properties of the metallic components, often leading to severe consequences if left uncontrolled. Metals are particularly susceptible to corrosion, which typically occurs upon exposure to certain aggressive species oxygen, sulphur, chlorides, and other

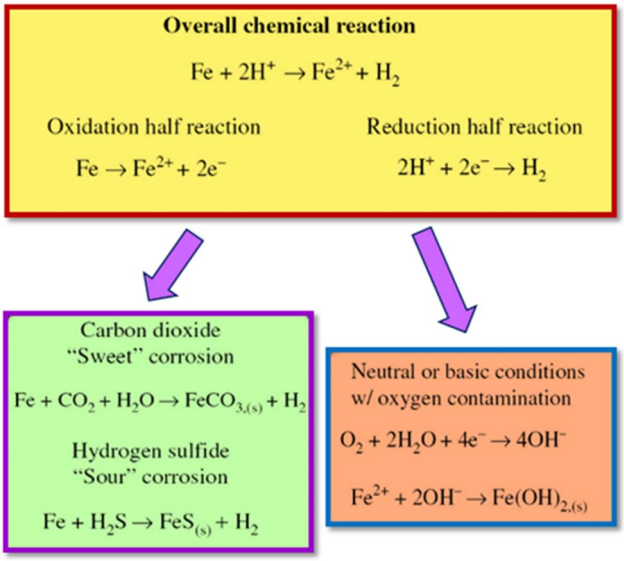

Fig. 2 Pictorial representation of relevant chemical equations to corrosion investigation, reproduced from ref. 11 with permission from [Elsevier] [*React. Funct. Polym.*, 2015, **95**, 25–45] copyright 2015.

chemicals in presence of water.[10] The interactions between metal and it's surrounding can produce corrosion products *i.e.* oxides, hydroxides or salts-that are thermodynamically more stable than the parent metal. The chemical reactions take places at cathode and anode in different kind of corrosions are displayed in Fig. 2. The type of corrosion that occurs relies on the factors such as the metallurgical charcteristics of componenets, environmental chemistry and the external forces. Having a comprehensive understanding of the corrosion causes and mechanisms facilitates the creation of efficient defences against this expensive and natural process. As reported in literature, corrosion can appear in various ways, comprising galvanic corrosion, uniform corrosion, pitting corrosion, crevice corrosion, intergranular corrosion and many others as discussed below.

Uniform corrosion. The most prevalent and simple form of corrosion, which is uniform corrosion. It happens when an exposed surface of metal corrodes uniformly over time. Uniform corrosion typically occurs in a stable environment or in presence of air, water, and other certain chemicals. Generally, uniform corrosion increases as acidity of the environment increases and often promoted in presence of different gases such as carbon dioxide (CO_2), oxygen (O_2), ammonia (NH_3) or hydrogen sulphide (H_2S). The metal steadily losses material, which causes a consistent loss in thickness. Even while uniform corrosion may be predictable, it can nevertheless harm buildings significantly, especially if the metal thickness is crucial for the stability of the structure. As it increases very slowly, hence its corrosion rate or weight loss of metal is also measured as mm per year (mm $year^{-1}$).

Galvanic corrosion. When two dissimilar metals come into contact with one other and an electrolyte (such as a conducting liquid like seawater), galvanic corrosion occurs. In such sceneries, a galvanic cell is established, wherein the metal having less noble electrochemical potential acts as an anode and the other acts as a cathode. The anodic metal corrodes quickly, while the cathodic metal is comparatively protected, this type of corrosion is frequently observed in plumbing systems, as well as in marine or outdoor environments where dissimilar metals are used in conjunction.

Pitting corrosion. Pitting corrosion is a localised form of corrosion that produces small pits and cavities on the metal surface. It initiates when a specific site on the surface becomes chemically more active than its surroundings, resulting in accelerated localized attack. This local active dissolution may also results from breakdown of a passive film at specific site, which often promoted by chloride ions, oxygen concentration cells, or surface contaminants as seen in active–passive metals. Despite low overall corrosion rates, it is difficult to detect and can cause penetration through the thickness and ultimate failure of the structural.

Crevice corrosion. Crevice corrosion is a type of localised attack that occurs in the occluded areas of metallic components. The attack is produced by a shift in the crevice's environment in comparison to the bulk solution. Often, crevice corrosion start to occur when mass transport of the electrolyte is hindered, resulting in conditions such as oxygen depletion and acidification, which can activate the passive surface and aggrevate the dissolution rate of materials. Typically, the term crevice corrosion occurs in passive metals and alloys (*e.g.*, stainless steels); however, in a broader sense, the corrosion of nonpassive metals and alloys (*e.g.*, carbon steel) by differential aeration can also be considered a form of crevice corrosion. Crevices exist in many designed buildings, hence crevice corrosion is a frequent kind of corrosion in most, if not all, industries. Crevices can be either man-made by design, such as in washers and pipe flanges in structures, or they can occur naturally as a result of biofouling, deposits, and debris over the metallic surface.

Intergranular corrosion (IGC). IGC is an another localized form of corrosion which preferentially occurs at and adjacent to the grain boundaries (GBs) between crysatallites, which a little or nil attack within the grains. It occurs when specific grain boundary regions are more prone to corrosion as a result of changes in composition (enrichment or depletion of alloying elements) or impurities presence at GBs. A very well-known case is intergranular corrosion of stainless steels, owing to precipitation of chromium-rich carbides in the temperature range of ≈450–850 °C (as can be encountered for instance in the heat-affected zones of weld joints) at the grain boundaries, and as a consequence the formation of chromium-depleted zones in the vicinity of the grain boundaries. As chromium in solid solution is the alloying element crucial for the passivation ability of Fe–Cr alloys, the chromium-depleted zones will activate and hence preferentially dissolve. The remaining passive surface of the matrix acts as a large cathode to drive the dissolution of the grain boundary zones. Other alloys prone to intergranular corrosion owing to metallurgical effects are certain aluminium alloys in specific heat treatment conditions. This kind of corrosion, which is frequently related to incorrect heat treatment or welding procedures, can result in structural weakness and material failure.

Stress corrosion cracking (SCC). SCC is the brittle cracking of a typically ductile metal caused by the combined effects of tensile stress and a particular corrosive environment, culminating in sudden and unexpected catastrophic failure. The tensile stresses can be present as residual stresses due to machining and fabrication process or as operating stresses in service. The SCC involves small cracks which propagate quickly, either along the grain boundaries (intergranular) or through the grains (transgranular), under the influence of tensile loads (applied or residual) and a sensitive environment like chlorides or hydrogen sulphide. SCC failures are a significant concern in the industries such as nuclear, petrochemical, and aviation sectors.

Erosion corrosion. Erosion corrosion is a accelerated degradation of metals and alloys due to combined action of mechanical wear and chemical or electrochemical reactions. Mechanical erosion and corrosion are combined to form corrosion. It takes place when an abrasive fluids (gas, liquid or solids) with particles or impurities is exposed to a metal surface in presence of corrosive environments. The protective layer of oxide on the metal surface is physically removed by the particles, exposing the underlying metal to corrosive environments thereby accelerated corrosion of the metals/alloys. The erosion corrosion is characterized by directional surface features and common phenomenon in areas like pump impellers and pipe inlets which carry corrosive fluids at high velocity along with the suspended particulates.

Selective leaching corrosion (SLC). Selective leaching corrosion is also known as de-alloying, demetalification, parting and selective dissolution, is also a form of corrosion in some specific solid solution alloys. SLC is a process where a more anodic/active alloying element/component of an alloy is prefentially dissolved in an electrolyte, leaving behind the cathodic/nobler alloying element/component behind in the structure, thereby reducing the mechanical properties of the alloy a common example is dezincification of brass, zinc having more negative electrochemical potential is selectively leached out in an electrolyte, leaving a nobler porous copper structure behind in the structure. The de-aluminification and graphitic corrosion in specific environments are another example of selective leaching corrosion. The pictorial representation of different forms of corrosion is provided in Fig. 3.

If the corrosion is not controlled or stopped, the metal deterioration continues and may result into component failure ultimately. Thus, corrosion control is very much crucial and should be achieved carefully through viable means. The corrosion control can achieved by various techniques, like as the usage of corrosion-resistant materials, protective coatings, cathodic protection, and appropriate design and maintenance procedures. The various protection methodologies are discussed briefly below.

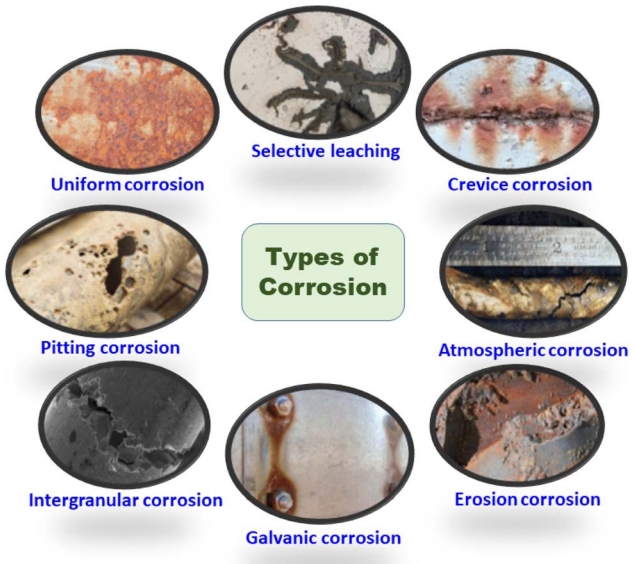

Fig. 3 Various forms of corrosion which frequently take place in industries.

Corrosion protection methodologies

To date, several corrosion mitigation methodologies have been systematically adopted to protect metals/alloys with particular emphasis on pipelines in the oil, gas, and related industrial sectors. The appropriate choice of more corrosion-resistant alloys (nickel, titanium-based alloys, and stainless steel) is an important protection method owing to their superior resistance to harsh conditions encountered in the oil and gas industries. It is also important to make sure that different materials used in combination do not promote galvanic corrosion, which necessitates the careful selection of components with compatible electrochemical properties. Another widely employed corrosion protection approach involves the application of surface coatings, such as polymer linings, paints, and epoxy-based systems, which serve as protective barriers between the metal substrate and the corrosive environment.[3,7] These coatings enhance durability by minimizing direct chemical interaction and improve resistance to abrasion, chemical attack, and moisture ingress, thereby extending the service life of critical infrastructure such as pipelines and process equipment.

Further, the metallic coatings, such as galvanizing (Zn coatings) and aluminizing (Al coatings), proved efficient in protecting the underlying material, where a sacrificial layer (Zn/Al) corrodes preferentially and cathodically safeguards steel structures.[12] Another important and most widely used corrosion protection method is cathodic protection, where the structural component that needs to be safeguarded is made cathode of the electrochemical system either by connecting to more anodic/reactive materials (in case of iron/steel, sacrificial anode; zinc, aluminium, or magnesium) or by supplying additional electrons to the system from an external DC power source thus hindered anodic reaction and reduced corrosion of the structure. Another corrosion protection technique is anodic protection, where an external electrical current is applied to the metallic structure to uphold it at sufficiently high anodic potentials (passivation zone), where a stable, passive, and protective oxide layer forms onto the surface. This technique is less popular than cathodic protection in the oil and gas

industries, because it is restricted mainly to active-passive types metals/alloys and applied in some specialised circumstances, *e.g.* safeguarding the storage tanks that contain corrosive acids. An important methodology to control corrosion processes is adding chemicals to the corrosive environment, which are chemicals named as CIs (amines, phosphates, chromates or molybdates).[13] These inhibitors develop a protective or barrier layer through a very thin coating and decrease the corrosiveness of the contiguous environment or hinder the electrochemical process of corrosion. The advantages and different types of inhibitors are as follows:

Usage of corrosion inhibitors

Several reasons offer the usage of appropriate CIs in terms of industrial suitability. CIs are economically cost-effective chemicals when considering the possible costs of maintenance, equipment failure and downtime. CIs are very easy to apply in any industrial process as it does not require any significant changes to existing systems and may be implemented simply. CIs are very flexible towards their surrounding environment, it may be acidic, oil, gas, aqueous. They also provide extra shielding to metal and alloys when combined with other well-known corrosion inhibition techniques like cathodic protection and coatings. Another important factor regarding CIs is the suitable place where it works. CIs are extensively used in boiler water systems, water injection systems and cooling water systems to stop the internal corrosion of pipelines and equipment. Inhibitors are the most recommended candidates employ to shield the tubing and well casing from H_2S and CO_2 in wells of oil and gas production.[14,15] Furthermore, pipelines to carrying natural gas, crude oil and processed fluids are packed with inhibitors to stopover internal corrosion triggered by impurities and corrosive agents of fluid. Even, when machine or equipment is being shutdown, inhibitors are used due to the presence of stagnant fluids and surrounding environment which can accelerates corrosion. Inhibitors provide an alternate kind of protection in such circumstances when it is difficult to apply some protective coatings.

Types of corrosion inhibitors

Numerous types of CIs are reported in literature with their applicability in various industrial sectors. Anodic inhibitors, which lowers the anodic reaction by producing a protective oxide layer on the metal sites through oxidation. Molybdates, nitrates, chromates and phosphates are well known examples and often used in aquatic situations where metals are susceptible to anodic corrosion such as cooling water systems. Cathodic inhibitors are also a well-recognized class of inhibitors, which also slow down the cathodic process, to create a protective layer on the cathodic regions *via* precipitation or by lowering the availability of reducible species such as oxygen. Examples include calcium bicarbonate, polyphosphates, and zinc salts. These inhibitors are widely used in boiler water treatment, cooling systems and other places where cathodic reactions must be regulated. Mixed type inhibitors works by affecting both the cathodic and anodic processes through creating a protective layer over the whole metal surface. Most common examples are phosphates, amine and nitro compounds based organic inhibitors, which are employed in various oil production activities as well as in cooling systems. Volatile CIs include mixtures of nitrite, phosphate and amine compounds utilized to prevent corrosion in metal parts during transportation and storage in enclosed systems such as pipelines, boilers and packaging. A popular class of inhibitor is organic inhibitors, which are renowned to make a hydrophobic (water-resistant) layer on the substrate metal surface and stops corrosive species from penetrating the metal. Some industrially active organic inhibitors are amines, thiols, imidazolines and certain surfactants and vastly incorporated as additives in water treatments, protective coatings and oil and gas production.[16] Similarly, another class named inorganic inhibitors work effectively by forming a protective oxide film or passive coating on the metal surface to stops the corrosion. Chromates, silicates, molybdates, phosphates are few examples which frequently utilised as paint and coating additives, industrial water treatment systems and cooling systems. In addition, oxygen scavengers remove dissolved oxygen from the

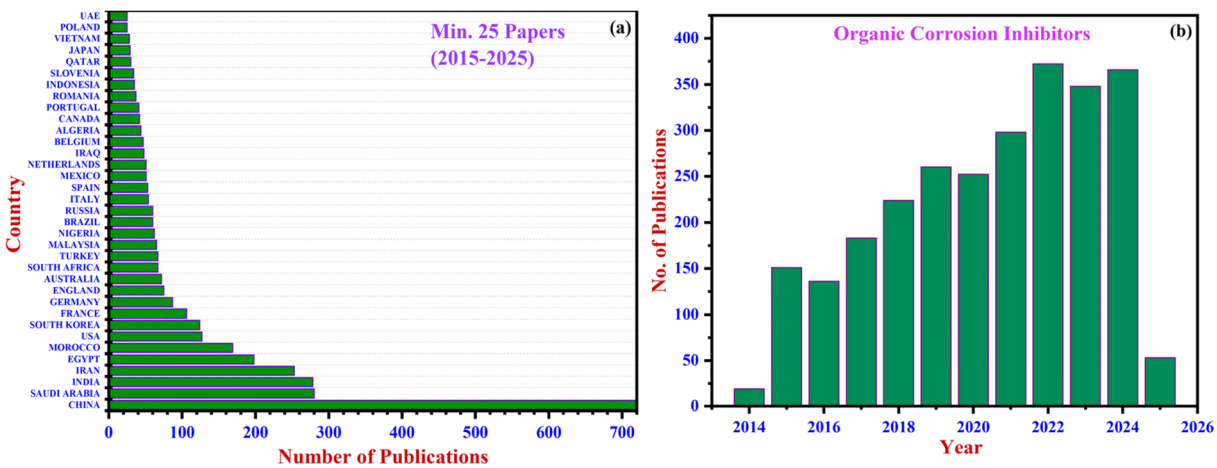

Fig. 4 Classification of OCIs since 2015–2025 (ten years): (a) country wise and (b) year wise.

surrounding environment, thereby reducing the risk of oxygen-induced corrosion. Hydrazine, ascorbic acid and sulphites are well-known oxygen scavengers often applied in boiler water treatment systems.[17] Another class of inhibitors is film-forming inhibitors, which works well by making a thin protective film that blocks corrosive species to come on the surface of metal, usually by chemical reaction or adsorption. Phosphate esters, fatty amines and polymers are utilised as film-forming inhibitors in pipelines carrying oil and gas, water treatment systems and producing wells. Last ten year and country wise classification of OCIs are portrayed in Fig. 4.

Background of organic corrosion inhibitors

Organic compounds are recognized as potential CIs for different kind of metal and their alloys for last three decades (thirty years). A plethora of research has been done to explore the corrosion efficiency/anti-corrosion potential of different organic compounds and molecules. In this context, I. E. Uwah *et al.* reported an inhibitive action of ethanol extracts from leaves (LV), bark (BK) and roots (RT) of *Nauclea latifolia* on mild steel corrosion in H_2SO_4 solutions at 30–60 °C.[6] A series of different fatty acid triazoles was developed by another research group (Quraishi and Jamal) and also evaluated them in HCl as CIs for cold-rolled mild steel (CRMS) and N-80 steel. Importantly, these substances recognized as highly safe for environment, show minimal toxicity and worked well as mixed-type inhibitors.[18] Additionally, Quraishi and Jamal also reported an eco-friendly and economical 4-salicylideneamino-3-hydrazino-5-mercapto-1,2,4-triazolefor CRMS and N-80 steel. It demonstrated mixed-type inhibition using propargyl alcohol as the standard CI and does not release any harmful vapours.[19] A class of oxadiazoles and dianils has been investigated as CIs for MS and CRMS. These substances have shown strong inhibition, with different inhibitory methods and performances depending on the substance.[20] Yildirim and Cetin synthesized acetamide, isoxazolidine, and isoxazoline derivatives and found them to be very effective CIs for cold rolled low carbon steel. However, their practical use in oil-field applications may be limited due to the use of acetone and abrasive cleaning.[21] Other researchers also synthesized various compounds such as mercapto-triazoles, isoxazolidines, 3,5-bis(*n*-pyridyl)-4-amino-1,2,4-triazoles, 3,5-bis(2-thienyl)-1,3,4-thiadiazole, gemini surfactants, thiosemicarbazides, quinoline derivatives, imidazolines, thiocarbohydrazides and tested their corrosion inhibition efficiency for different metals and acid environments. On the contrary, naturally occurring plants-based Henna extract and its key constituents such as α-D-glucose, lawsone, gallic acid, and tannic acid have been studied as CIs. They act as mixed-type inhibitors and can prevent corrosion, but their efficiency decreases with increasing temperature.[22] *Justiciagendarussa* plant extract contains components such as friedelin,β-sitosterol, lupenol, *ortho*-substituted aromatic amines, phenolic dimmers, and flavonoids. It also acts as aninhibitor of mixed-type, but its corrosion inhibition effectiveness decreases at higher temperatures due to compound decomposition.[23] Three important amino acids (glycine, alanine, and leucine) have also been investigated as efficient CIs at certain concentrations. However, at lower concentrations, they may promote corrosion, potentially due to complexation with iron (Fe).[24] A detailed literature review was carried out for already reported OCIs (Table 1, Appendix A), inhibitor source with protective metals (Table 2, Appendix B). For additional details please refer to the Appendix.

Different classes of OCIs

Biopolymers. Biopolymers are recognized as environmental benign due to their origination and derivation. As it is well known that natural polymers are made from plant and animal cells. A large number of qualities of these biopolymers are make them useful for a range of uses, including the prevention of corrosion. Biopolymers also have some other characteristics such as they are non-bio accumulative, which lessens their influence on ecosystems, and biodegradable, which means they may be broken down by natural processes easily. These particular materials also have a delaying impact on anodic and cathodic processes, making them effective at preventing corrosion in different conditions. The ability of biopolymers to be used as inhibitors at the interface, establishing a barrier at the metal-environment contact. Polysaccharides like starch, cellulose, and chitosan as well as nucleic acids (RNA & DNA), polypeptides, lignin, and natural rubber are examples of biopolymers. These include the carbohydrate-based biopolymers like chitosan and cellulose, as well as their derivatives, which are frequently employed to suppress corrosion. *N*-acetyl-D-glucosamine (acetylated groups) and D-glucosamine (deacetylated units), which are randomly dispersed and linked together by α-β-1,4-glycosidic bond, make up a linear chain polysaccharide known as chitosan.[5] Chitin is a chemical component of the shell of crustaceans (such as prawns and crabs) and fungi cell walls, is deacetylated to produce it. For commercial purposes, chitin is partially deacetylated to make chitosan. Chitosan possesses characteristics like high molecular weight between 3800 and 20000 Da, a degree of deacetylation ranging from 60% to 100%, and the presence of polar components ($-CH_2OH$, $-NHCOCH_3$, –OH, and –O–) which facilitate efficient bond formation with metallic surfaces. Adding a polar functional group can make chitosan more soluble in polar electrolytes, despite the fact that it typically has low solubility. Functional groups increase solubility and enhance corrosion inhibition efficiency by enhancing the number of donor sites extensively responsible for adsorption process and by increasing the molecular size, effective adsorbed area increases. A comprehensive study has been done on chitosan as a CI, especially for Mild Steel in acidic environments. The usage of chemical, surface characterization, and electrochemical techniques, the effectiveness of chitosan as a corrosion inhibitor has been studied thoroughly and it shows highly effective corrosion inhibition rates of 96% at 60 °C and 93% at 70 °C. Its adsorption behaviour on mild steel surfaces is explained through the Langmuir adsorption isotherm model, and further examined using SEM and AFM. Chitosan has also been proven to be successful in preventing copper corrosion in both acidic

an as well as in neutral electrolytes. Chitosan and potassium iodide (KI) have been found to work synergistically to enhance efficiency when compared to chitosan alone. Chitosan has a number of derivatives that are used to prevent corrosion. 2% NaCl solution has been used with water-soluble chitosan to prevent corrosion on tin plates, with efficiencies ranging from 72.73% to 91.41%, depending on whether the chitosan was generated from prawn shell waste or mussel shell waste. Schiff's bases, which are substances made from chitosan aromatic aldehydes, have exceptional anti-corrosive qualities. Due to their greater density of active donor centres, they are highly soluble in polar solvents and exhibit excellent protection efficiency. Chitosan and PEG get cross-linked to provide for cathodic type corrosion inhibition of around 94% in sulfamic acid. Chitosan combined with Thio-carbo-hydrazide also acts as slight cathodic inhibitor that was observed by SEM and EDX methods. Chitosan clubbed with polyaniline in acidic medium provides for improved surface morphologies and so therefore it behaves as a good mixed-type interface inhibitor. Another type of biopolymer used for corrosion inhibition is cellulose.[25] Besides having biological importance, they are industrially important as a corrosion inhibitor. They are also linear polysaccharides and are carbohydrate based D-glucose units joint by glycosidic linkage. In nature it is found in plant cell walls and also in algae. Majorly Carboxyl Methyl Cellulose and Hydroxy Methyl Cellulose are used. They are sometimes used in association with Ag nanoparticles. One more biopolymer utilized for same kind of purposes is starch, which comprises of linear and branched chain of amylose and amylopectin respectively. Although it has low solubility but it shows good corrosion inhibition property. The basic chemical structure of cellulose and starch is displayed as Fig. 5.

Plant extracts. Plant extracts are very important class of CIs due to their distinctive characteristics. First of all, they are eco-friendly and provide a viable substitute for corrosion inhibition. These extracts include complex phytochemicals with electron-rich centres that function as efficient adsorption sites. Plant extracts have high solubility despite their complexity as they contain wide variety of functional groups, which are polar in nature. These extracts also exhibit synergistic enhancements, which increase their effectiveness. Their widespread availability, which makes them affordable alternatives, is an additional advantage. Plants may be extracted from a variety of components, including leaves (which are very efficient since they synthesize phytochemicals), bark, fruit, flowers, and peels.[26] Plant extracts are made in a biphasic technique for maximum stability and have to be frozen before use. Due to their low toxicity relative to synthetic inhibitors, low cost, and environmental friendliness, plant extracts were often used as potential CIs. A variety of organic substances are found in plants and these organic molecules have strong inhibitive capabilities and making them proficient CIs for metals in a range of different conditions. Polyphenols are a popular family of plant extracts used as CIs. These substances, such as tannins, flavonoids, and lignin, are widely distributed in a variety of plants.[27] By establishing a protection barrier on the surface of metal by the adsorption of their molecules, polyphenols effectively prevent corrosion. Through interacting with the metal surface, polyphenols functional groups, such as the hydroxyl (–OH) and carbonyl (C=O) groups, prevent corrosion. Alkaloids are a different class of well-known plant extracts that are utilised as CIs. Alkaloids have aromatic structures and nitrogen-containing heterocyclic rings that offer good inhibitory characteristics. Inhibiting corrosion processes and blocking the passage of hostile species like oxygen and water, they make a stable complex with the metal surface. A subclass of polyphenols called flavonoids has also demonstrated incredible promise as a CI. Strong adsorption onto the metal surface is made possible by the complex aromatic ring structures of these molecules, which contain a variety of functional groups including hydroxyl, methoxy, and carbonyl. They can also prevent some well-known forms of corrosion (pitting corrosion and stress corrosion cracking), in accumulation to acting as anodic/cathodic inhibitors.

Through experimental techniques together with weight loss test, electrochemical measurements, and surface analysis methods like scanning electron microscopy (SEM) and X-ray photoelectron spectroscopy (XPS), the inhibitive capabilities of these plant extracts have been investigated and validated. Plant extracts can be applied directly to the metal surface as coatings to prevent corrosion or combined with other protective agents to increase their potency. To generate hybrid materials that provide prolonged and regulated corrosion protection, plant extracts can also be added to polymer coatings or nanocomposites. The stability and solubility of plant extracts in the targeted environment must be taken into account. Under

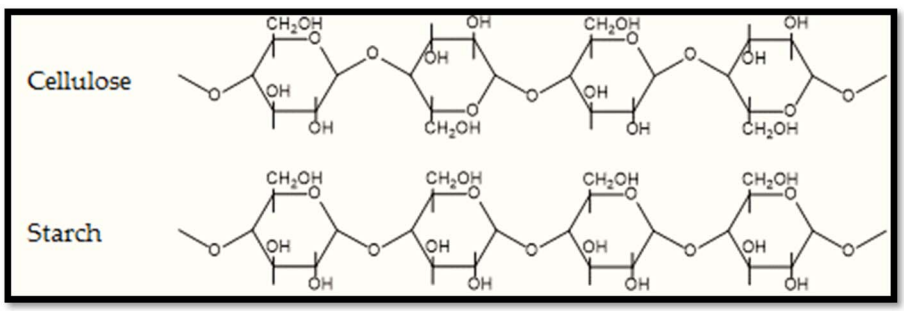

Fig. 5 The basic chemical structure of biopolymers (cellulose and starch) which utilized as corrosion inhibitors, reproduced from ref. 25 with permission from [MDPI] [*Polymers* (Basel), 2017, **9**, 523] copyright 2017.

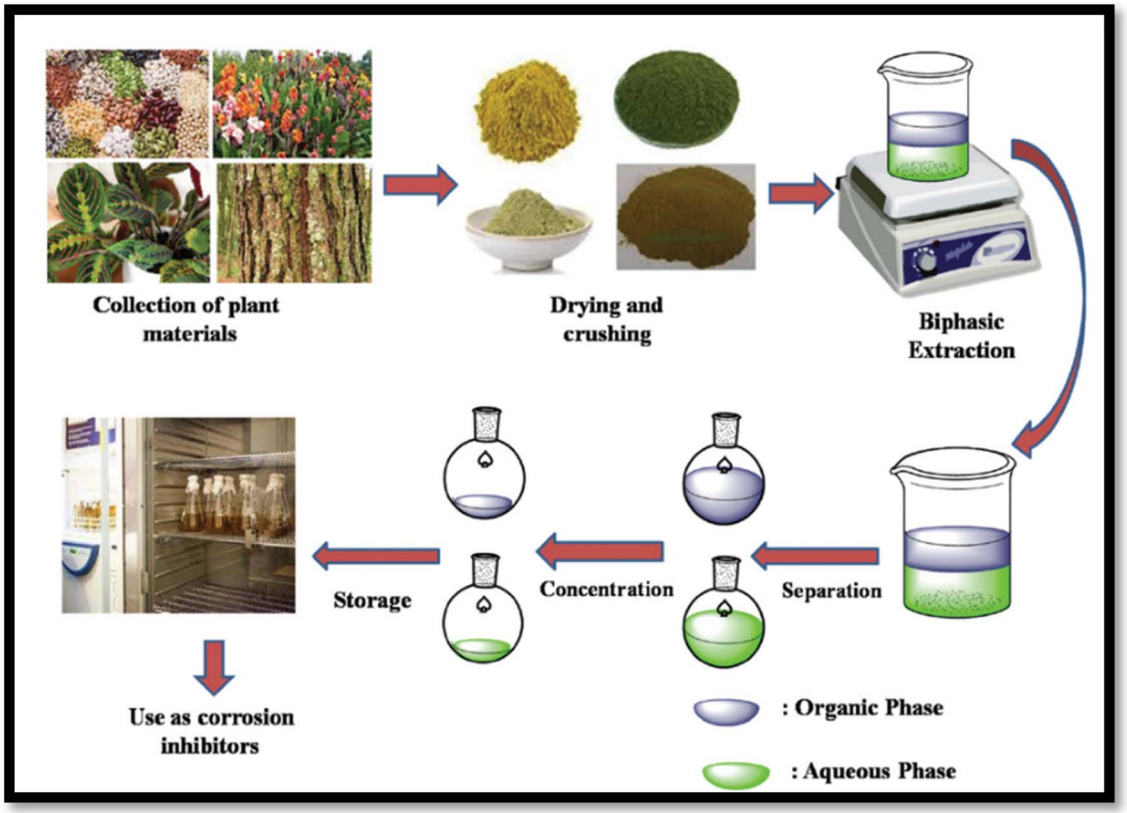

Fig. 6 The laboratory process for the formation of corrosion inhibitors from plants extract, reproduced from ref. 5 with permission from [RSC] [*Mater. Adv.*, 2021, **2**, 3806–3850] copyright 2021.

certain circumstances, some plant extracts may deteriorate quickly, reducing their long-term inhibitive power. As a result, research is still being done to improve their functionality and create formulations that are appropriate for certain uses. Overall, the use of plant extracts as efficient and environmentally benign CIs has shown significant potential.[28] The usage of these natural chemicals in corrosion prevention for diverse sectors and applications is anticipated to acquire greater momentum as the globe looks for sustainable and environmentally friendly alternatives. A schematic diagram for the process used to make plant extracts as CIs is demonstrated in Fig. 6.

Chemical medicines and drugs. Chemical pharmaceuticals and treatments have a relationship to the organic world since they come from biological and natural origins. These are complex molecules with several electron-rich centres that can form many bonds and make attachment to different functional groups easier. They have a unique capacity to display strong anti-corrosion capabilities due to their chemical complexity and also exhibits innumerable qualities, including bio-tolerance, biocompatibility, and non-bio-accumulation.[5] Their large chain size along with macromolecular structure and provide large surface area coverage, which increases the effectiveness of protection. The high price of chemical medications is a significant drawback, because it requires multistep synthesis and ultra-purification methods. Therefore, examining expired medications is one solution to this problem as they are biologically worthless but yet could be useful in other situations. Due to their distinct chemical characteristics and interactions with metal surfaces, chemical medications and medicines have also been investigated as possible CIs. Some of these substances have also shown inhibitory effects against metal corrosion,

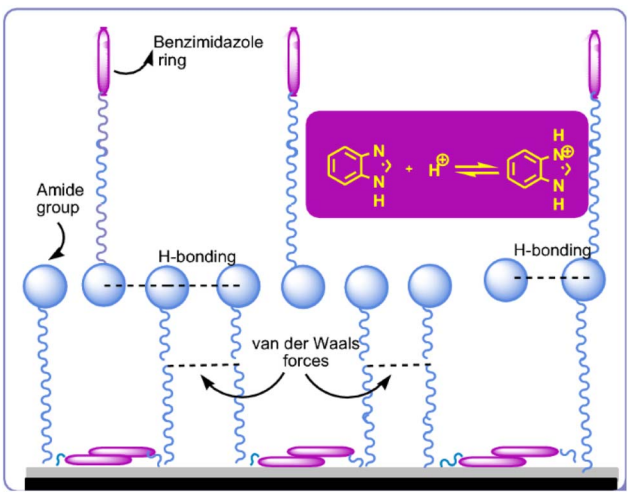

Fig. 7 The responsible functional groups of imidazole family as corrosion inhibitors, reproduced from ref. 29 with permission from [Springer] [*BMC Chem.*, 2019, **13**, 136] copyright 2019.

despite the fact that their principal use is frequently tied to healthcare and treating various medical ailments. Particularly in applications where their dual functioning is advantageous, these chemical inhibitors can provide an alternative to conventional corrosion prevention techniques. Pharmaceutical substances encompassing active heteroatoms (nitrogen, oxygen, or sulphur) are one family of chemical medications employed as CIs. These heteroatoms have free electrons (lone pairs), which can coordinate with surface-located metal atoms to create a shield-like layer. Examples include the investigation of amine-containing medications like chlorpheniramine and aminophylline as CIs for metals like CS.[29] Their amine groups interact with positively charged metal cations to produce complexes that prevent corrosion.

Nonsteroidal anti-inflammatory drugs (NSAIDs), for example, and other pharmaceuticals and medications that include aromatic rings have also demonstrated inhibitive characteristics. Stable adsorption layers can emerge as a result of interactions between the pi-electrons (Π electrons) of aromatic rings and surfaces of metal substrates. On metals like steel and aluminium, the ability to reduce corrosion by substances like ibuprofen and naproxen has been investigated. Some drug molecules feature functional groups, as carboxylate (–COOH) and hydroxyl (–OH) groups, that allow them to chemisorb or physisorb on the metal surface.[30] A medication having carboxyl groups that has demonstrated inhibitory efficacy against aluminium and carbon steel is aspirin (acetylsalicylic acid). The responsible functional groups for corrosion inhibition in a medicine is portrayed in Fig. 7.

CIs can also be found in inorganic medicines and substances. For instance, the ability of substances containing phosphorus, nitrogen, and sulphur atoms, such as phosphates, amines, and thiols, to suppress corrosion on metals like iron and copper has been studied. Chemical medications inhibitive methods include adsorption phenomenon onto the metal surface, resulting in the creation of a barrier that stops corrosive species alike oxygen, water molecule, and ions from reaching to the metal. Anodic, cathodic, or mixed inhibitory effects may be responsible for the inhibition process, liable on the particular drug and metallic system,[31,32] which is significant to highlight that while some chemical medications may have qualities that reduce corrosion, their usage as specific CIs are not common for a variety of reasons. First off, the dosage needed to effectively prevent against corrosion may go over safe therapeutic limits. To guarantee long-term efficacy as CIs, it is also necessary to properly analyse the medications stability and compatibility in various settings and applications. In conclusion, due to their distinct chemical compositions and interactions with metal surfaces, chemical medications and medicines have shown potential as CIs. To maximise their inhibitory effects and determine their viability in certain corrosion prevention applications, more study is required.

Ionic liquids. Salts that exist in a liquid or molten form below 100 °C are known as ionic liquids containing both inorganic anions and organic cations. Ionic liquids (ILs) can be divided into categories according to the ability to interact with both organic and inorganic substances, pH, and functional groups.[2] They are less toxic with high polarity, moderately low melting point, lower vapour pressure, strong thermal and chemical resistance, high solubility, and excellent protective efficacy are just a few of their standout qualities. Furthermore, they have the capacity to impart superior surface morphologies and their characteristics may be adjusted to meet particular needs. Donor–acceptor interactions and mixed and interface-type behaviour in ionic liquids cause the creation of planar orientations. In terms of mechanics, the anionic moieties bind to anionic sites whereas the cationic moieties attach to cathodic sites; the type of anion that forms the site determines the type of inhibition that occurs. Ionic liquids may be studied using methods including potentiodynamic polarization, scanning

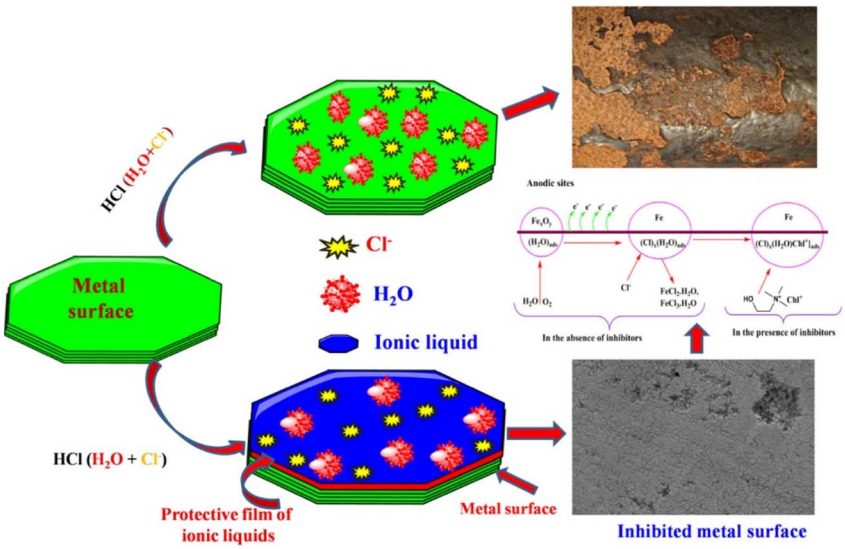

Fig. 8 Representation of ionic liquids as corrosion inhibitors, reproduced from ref. 34 with permission from [Elsevier] [*J. Mol. Liq.*, 2021, **321**, 114484] copyright 2021.

electron microscopy, and atomic force microscopy.[5] ILs interact with metal surfaces *via* hydrophobic alkyl chains and polar hydrophilic imidazole groups, preventing water from coming into touch with the surface of the metal. Longer hydrophobic chain lengths improve the inhibitory effectiveness, while increased hydrophobicity decreases solubility and lessens the inhibitory impact on corrosion. Due to their distinct characteristics and adaptability in a variety of applications, ILs have recognized as potential CIs. Organic cations and inorganic or organic anions combine to form ionic liquids, which are liquid salts. They are appealing options for corrosion prevention because their design makes it possible to modify their chemical structure to obtain certain qualities. The ability of ionic liquids to establish a robust and durable adsorption layer on metal surfaces is one of its main benefits as CIs. Through interactions between the charged ions and metal atoms, ILs are able to chemisorb upon the metal surface. This adsorption creates a layer of protection which precludes the metal from coming into touch with corrosive species like oxygen and water. Specific functional groups can be added to ionic liquids to target particular forms of corrosion. For example, ILs containing ions of nitrogen, sulphur, or phosphorus have been explored for their ability to stop pitting corrosion since these heteroatoms can coordinate with metal cations and prevent localised corrosion. By forming protective oxide layers on the metal surface, ILs with oxygen-containing ions, on the other hand, have demonstrated efficiency against general corrosion. Ionic liquids may also be tuned for specific uses by altering their solubility, volatility, and viscosity. ILs can be applied directly as liquids or as a component of polymer coatings to offer an extra layer of security. They are useful for high-temperature situations where traditional organic inhibitors may decay or evaporate due to their low volatility and strong thermal stability. In addition, ionic liquids frequently have lower environmental impact and are non-toxic than traditional OCIs owing to their low volatility and ease of recovery and recycling for reuse, they pose a lower risk of emissions. In the creation of CIs, ILs can also function as green solvents, providing a sustainable substitute for traditional organic solvents. This characteristic is very helpful since it helps to lessen the negative environmental effects of corrosion inhibition processes. ILs enormous potential for application as CIs is still not without obstacles, though. A constraint may be the price of manufacturing several ILs that are specifically created for a user. Their interactions with various metal surfaces and surroundings are very complicated, necessitating in-depth investigation and testing for each individual application.[33,34] A schematic representation of ionic liquid act as CIs is depicted as Fig. 8.

Polyethylene glycols (PEGs). PEGs have significant industrial and biological value. Their low flammability, low vapour pressure, affordability, low toxicity, environmental friendliness, and biocompatibility are only a few of their many advantageous qualities. PEGs have a large molecular weight and are easily modifiable; they are non-volatile and display mixed and interface type behaviour.[5] They have a synergistic effect when KI > KBr > KCl and act as superior CIs in comparison to polyvinyl alcohols and natural polymers. PEGs perform well when applied

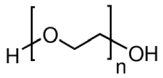

Fig. 9 Chemical structure of polyethylene glycol.

to steel in 3 N H_2SO_4, exceeding 90% at a concentration of 0.1 M H_2SO_4. Through methods like EIS, their interfacial behaviour has been studied, and SEM has verified their smoothness, which is attributable to their high molecular weight. PEGs have also been shown to work well with 0.5 M HCl on carbon steel. Due to their distinctive chemical characteristics and efficiency in a variety of applications, polyethylene glycols (PEGs) are adaptable and often employed as CIs. The PEG family of synthetic polymers is made up of ethylene glycol repeats as displayed in Fig. 9. They are ideal for corrosion prevention since they are water-soluble, non-toxic, and have good film-forming properties. PEGs capacity to create a shielding coating on the metal surface is one of their primary advantages as CIs. PEGs stick strongly to the metal surface after being applied, forming a thin and continuous barrier.[35] The corrosion process is slowed down by this barrier, which effectively blocks the entry of corrosive chemicals like water molecules, ions and oxygen to the metal surface. PEGs function superbly as CIs for both widespread and localised corrosion. They are particularly efficient in stopping pitting corrosion, a type of corrosion in which localised assault can cause quick and significant material damage. PEGs reduce the beginning and spread of pitting corrosion by providing a homogeneous protective layer. The structure and molecular weight of PEGs can be changed to increase their inhibitory effects. PEGs with higher molecular weights likely to offer more effective protection because they have thicker films and greater adherence to metal surfaces. PEGs can also be used with other CIs or additives to have synergistic effects that enhance performance as a whole. For instance, PEGs can be used with conventional inhibitors like sodium benzoate or nitrite to increase the effectiveness of protection. To stop steel from corroding in reinforced buildings, PEGs are also used in a variety of sectors, such as metalworking, oil and gas, water treatment, and concrete and cement-based products. They are very useful for diverse corrosion protection applications owing to their great adaptability towards various materials and simplicity of application. It is crucial to remember that variables like concentration, temperature, and the environment in which they are utilised might affect how well PEGs work as CIs.[1] Therefore, to choose the best PEG formulation for a certain corrosion protection application, extensive testing and assessment are required.

Multi-component reaction inhibition. The benefit of multi-component reactions (MCRs) is the ability to produce complex molecules in a single step, which increases their efficiency and benefits the environment. The synthesis of heterocyclic rings with nitrogen (N) or oxygen (O) as the heteroatoms occur in many MCRs. These reactions have a number of attractive qualities, including short preparation time requirements, excellent selectivity, profitability, and high yield.[1] MCRs can be

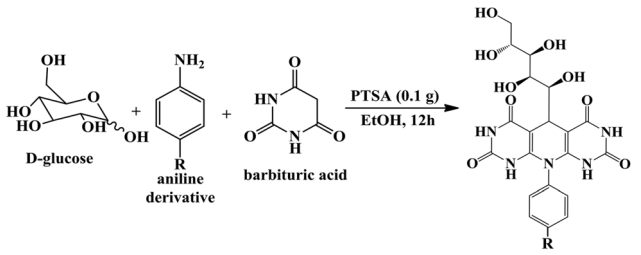

Fig. 10 Chemical substance synthesized by MCRs utilized as corrosion inhibitor, reproduced from ref. 38 with permission from [Springer] [*Sci. Rep.*, 2017, **7**, 44432] copyright 2017.

categorized according to how many reactants are used in each stage. Additionally, the MCR-produced compounds have excellent bonding properties with metallic surfaces, which makes them potentially useful for catalysis or surface modification. Overall, MCRs provide a practical and useful method for streamlining synthesis procedures and providing access to a wide variety of molecules. Due to their effectiveness, variety, and environmental friendliness, multi-component reactions (MCRs) have taken on a key role in the production of OCIs.[5] MCRs are single-step synthetic processes that include the simultaneous reaction of three or more basic elements to produce complex compounds as demonstrated in Fig. 10. This potent synthetic technique has transformed the area of organic synthesis and has a wide range of uses, including the development and manufacture of CIs. One of MCRs' key benefits in the production of OCIs is their quick generation of a variety of chemical structures. Chemists can access a wide range of chemical space and swiftly synthesise a library of possible inhibitors by mixing a number of starting components in a single process. This high-throughput method expedites the identification and improvement of efficient CIs, enabling a more effective screening procedure. MCRs also offer a resource-efficient and sustainable method for synthesising CIs. These reactions only require one pot, which decreases the amount of waste production and increases the sustainability of the operation. MCRs are appealing for the large-scale, environmentally and economically sustainable manufacture of CIs due to the better overall yields, cheaper costs, and less environmental impact.[36] Because of MCRs adaptability, different functional groups may be included into the inhibitor compounds. The ability to customise the chemical characteristics and adsorption behaviour on metal surfaces is very helpful when designing CIs. MCRs, for instance, can add groups including nitrogen, sulphur, or phosphorus, which are known to improve the inhibitive efficacy against certain forms of corrosion. Through MCRs, CIs chemical structures may be altered to create specialised inhibitors with increased efficacy and selectivity. MCRs also make it possible to make hybrid CIs by fusing many functions into a single molecule. This strategy may result in synergistic effects, where several moieties cooperate to increase the effectiveness of inhibition and offer improved corrosion protection. Inhibitors with enhanced adsorption, film-forming, and stability can be produced by combining different functional groups, which increases their effectiveness in preventing corrosion.[37] In conclusion, the production of OCIs has been transformed by MCRs. They are crucial in the creation of CIs due to their quick generation of a variety of chemical structures, fast atom efficiency, and environmental friendliness.[38] MCRs allow for the customization of inhibitor molecules to suit certain corrosion conditions and offer improved corrosion protection by adding different functional groups and producing hybrid inhibitors. We may anticipate future developments in the synthesis and functionality of OCIs as MCR research progresses, which will upsurge corrosion prevention in applications of different industrial sectors.

Derived from US and MW irradiations. Non-traditional heating techniques, which arise from ultrasonic (US) and microwave (MW) irradiations, are favoured over conventional heating techniques because of their quick response times and even heating. With sluggish activation rates and uneven heating, conventional heating techniques can take many minutes, hours, or even days to complete a reaction. Contrarily, unconventional techniques like microwave irradiation and ultrasound can finish processes in a matter of seconds.[5] These techniques have been used to catalyse various chemical processes and multi-component reactions (MCRs), improving selectivity and facilitating the production of heterocyclic compounds with corrosion-inhibitory characteristics. Chemical procedures can be accelerated and made more effective with the use of ultrasonic and microwave irradiation, which has benefits for both reaction time and product quality. OCIs are made using cutting-edge processes including ultrasound and microwave irradiations. They provide a number of benefits over conventional synthesis methods, making it possible to produce inhibitors with improved characteristics quickly and effectively. High-frequency sound waves can be used to apply ultrasound irradiation to a reaction mixture. A localised hotspot is created and mass transport and mixing are improved because to the mechanical impact of ultrasound, which also causes cavitation, the creation of microbubbles, and their collapse. In the synthesis of CIs, this encourages quicker reaction rates and greater yields.[1,2] Due to the gentle conditions and selectivity of ultrasound-assisted processes, it is possible to synthesise certain inhibitor structures with less adverse side effects. Additionally, the application of ultrasound may result in the creation of nanoparticles and nanocomposites, which provide exceptional prospects for modifying the inhibitory characteristics. EM waves are used in microwave irradiation to heat reaction mixtures. When compared to conventional heating techniques, microwave irradiation offers quick and uniform heating, resulting in faster reaction kinetics and shorter reaction durations. High product purity and selectivity may be produced by the efficient and well-controlled heating used in microwave-assisted synthesis. In addition, microwave irradiation makes it possible to create greener synthesis pathways by using less energy and solvent. They have been used effectively to create a variety of OCIs. These methods enable the creation of inhibitors with enhanced selectivity, inhibitive efficacy, and custom molecular architectures. The screening and optimisation of possible CIs is made easier by the quick and effective

synthesis provided by ultrasonic and microwave irradiations, hastening the identification of new and powerful inhibitors.

Additionally, scalability and cost-effectiveness are advantages of ultrasonic and microwave-assisted synthesis. These methods are appropriate for industrial applications since they are easily modified for mass production. Cost reductions in the production process are also a result of faster reaction times and higher yields. In conclusion, potent instruments for producing OCIs include ultrasonic and microwave irradiations. They are useful in the synthesis of various inhibitor structures with enhanced characteristics because of their capacity to increase reaction rates, selectivity, and scalability.[39] Researchers may definitely anticipate more progress and advancements in the designing of OCIs for more effective and long-lasting corrosion resistance as research on these approaches continues.

Green solvents. Green solvents provide many beneficial features and serve a vital part in many chemical processes. Research has proved that green solvents act as catalyst for multiple multi component single step reactions so as to better process and produce green and organic CIs. First of all, compared to conventional solvents, they have a less detrimental impact on ecosystems and human health. Green solvents frequently come from sustainable sources or regenerative sources are biodegradable with less toxicity. Second, they are reasonably priced, making them good choices for industrial procedures.[1,2] Green solvents may also quickly dissolve a broad variety of compounds, promoting effective and efficient reactions. They are appealing substitutes for traditional solvents given their positive features, which support sustainable and ecologically friendly practices in the field of chemistry. Owing to their lesser toxicity, biodegradability, and marginal negative environmental effects, green solvents, often referred to as environmentally friendly solvents or eco-friendly solvents, are rapidly being researched and used as CIs. Green solvents are an appealing alternative to standard solvents for a variety of uses, including corrosion prevention since they are safer and more environmentally friendly. The environmental friendliness of green solvents makes them ideal CIs. These solvents often come from renewable sources and do not harm the environment too much. They frequently contain little to no volatile organic compounds (VOCs), which minimises emissions and air pollution while being applied. Green solvents are more sustainable and in line with ecologically friendly practises since they also leave a less carbon footprint. Another benefit of using green solvents is their low toxicity. Green solvents are less toxic to human health and have less dangerous to consumers and employees than traditional solvents. This factor is especially important in professions like oil and gas, maritime, and construction where worker safety is a top priority. They fall within the categories of supercritical fluids, terpenes, ionic liquids, and bio-based solvents (Fig. 11). Bio-based solvents are sustainable and renewable alternatives since they are made from biomass sources like plants and agricultural waste. As was already noted, ionic liquids are salts that are liquid and have special qualities that make them both CIs and solvents.[5] Under specified temperature and pressure circumstances, supercritical fluids, such supercritical carbon dioxide, have special

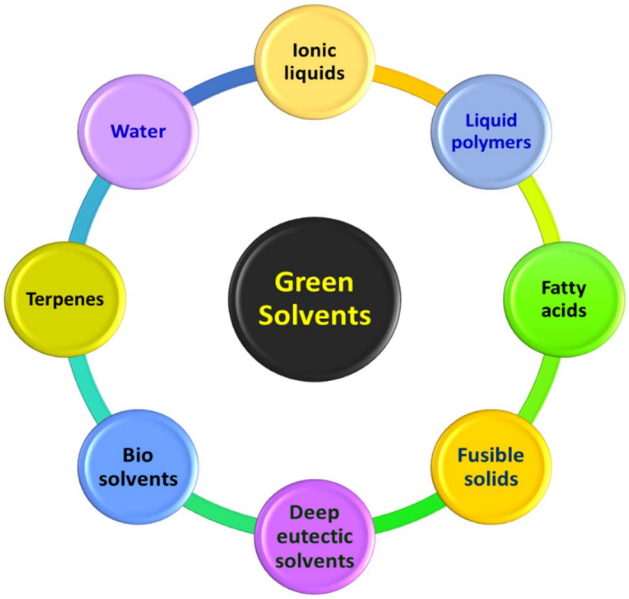

Fig. 11 Various types of green solvents.

solvent characteristics, providing an ecologically acceptable alternative.

In line with the ideals of green chemistry, the usage of green solvents as CIs promotes more environmentally friendly and long-lasting corrosion prevention techniques. By using environmentally friendly solvents, businesses may lessen their impact on the environment and cut back on the production of hazardous waste. It is crucial to remember that depending on the exact application and environment, green solvents may or may not work as CIs. To assure their effectiveness and compatibility with various metal surfaces and corrosion conditions, thorough testing and assessment are required. In conclusion, green solvents provide a more ecologically responsible and long-lasting method of corrosion inhibition. They are appealing substitutes for traditional solvents due to their low toxicity, biodegradability, and renewable nature.[40] Industries may support a greener, more sustainable future while successfully protecting their metal assets from corrosion damage by implementing green solvents in corrosion protection.

Factors responsible for inhibition

An OCIs molecular framework is an essential variable in determining how efficient it is. Amino ($-NH_2$), hydroxy (–OH), and carboxylate (–COOH) groups, among other functional groups, improve the inhibitor capacity to adsorb upon the metallic surface. These functional groups interact chemically with the metal to create chemical reactions that result in the development of a barrier. The inhibitor species or molecules connect with the metal surface by chemical bonding or weak contact, depending on the adsorption method, which might be physical or chemical.[1,2] A graphic representation of all the responsible key factors for the performance of any CI (Fig. 12).

Adsorption strength. An OCIs capacity to adhere firmly to the metallic surface is determined by robust adsorption strength. A

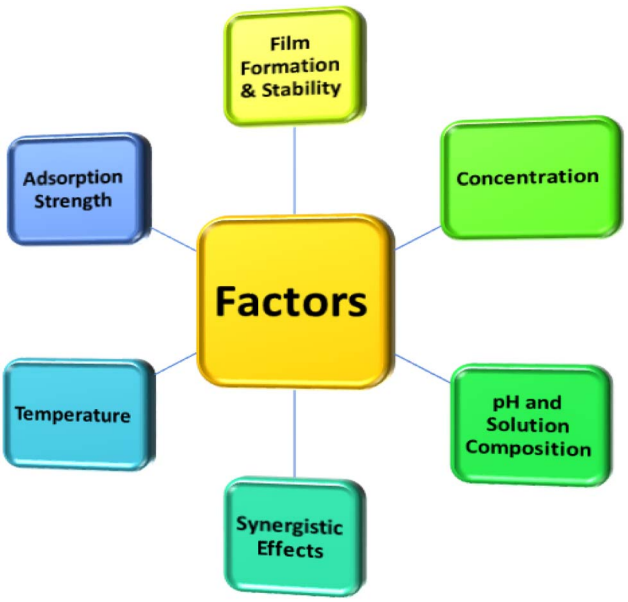

Fig. 12 Factors responsible for organic corrosion inhibitors.

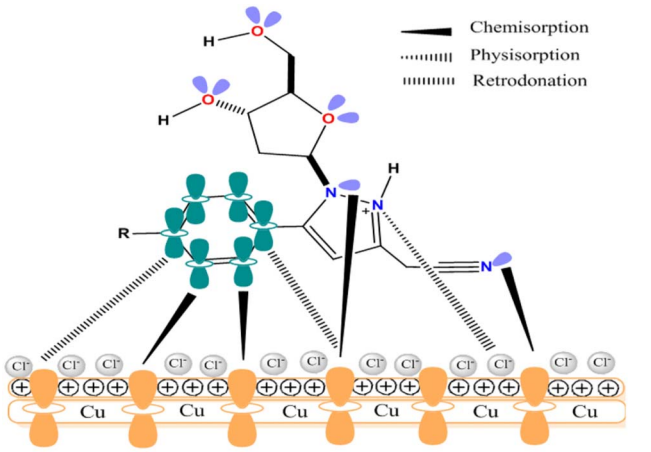

Fig. 13 Representation of types of adsorption and their strength for corrosion inhibitors, reproduced from ref. 41 with permission from [Springer] [*Sci. Rep.*, 2021, **11**, 3771] copyright 2021.

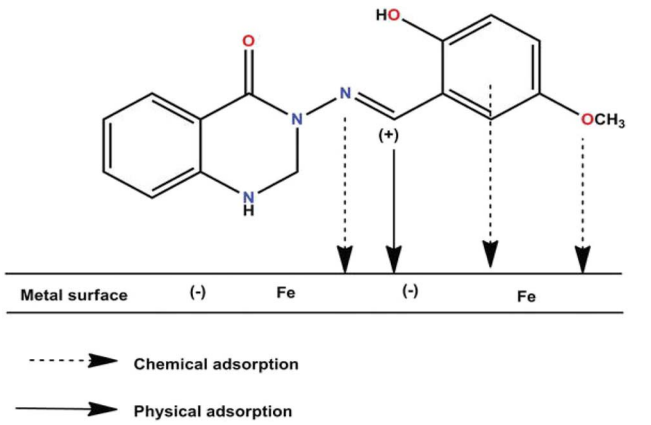

Fig. 14 Representation of concentration effecting efficiency of corrosion inhibitors, reproduced from ref. 42 with permission from [Elsevier] [*J. Colloid Interface Sci.*, 2017, **502**, 134–145] copyright 2017.

tight, continuous protective coating is ensured by strong adsorption, which is desirable. The interaction between inhibitor and metal, the presence of adsorption sites on the metallic surface, and the electronic characteristics of the inhibitor species/molecules are some of the variables that affect the adsorption strength. Interactions such coordinate bonding, charge transfer, hydrogen bonds, or weak van der Waals interactions may be involved in the adsorption mechanism. The mechanism is hence linked with the surface chemistry and follows Langumir adsorption isotherm.[41] It hence depends on the reactivity as in surface roughness, more the roughness better the adsorption efficiency. A representation of types of adsorption along with their strength and extensively responsible for corrosion inhibition (Fig. 13).

Concentration. Concentration is generally expressed in the form of molarity, molality, formality and normality. Gram equivalent is one of the common linking factors between these terms. The efficacy of the OCIs is closely linked to the quantity of the inhibitor in the corrosive solution. In general, efficiency is improved as the inhibitor concentration is amplified, which clearly indicates that more inhibitor molecules are accessible to bind to the metal surface at larger concentrations.[42] Each inhibitor does, however, have a specific concentration range over which severe film formation or agglomeration may happen, decreasing the inhibitor's potency. The corrosion efficiency affecting by concentration of corrosion inhibitor is displayed in Fig. 14.

pH and solution composition. The effectiveness of OCIs depends on the pH and solution composition of the corrosive solution. The inhibitors and the metal surface ionization states can be impacted by the pH, changing the adsorption behaviour.[1] The stability of the inhibitor coating and the adsorption phenomenon can be affected by the solution composition, *i.e.,* the presence of particular ions or additions. For instance, some inhibitors work by precipitating or complexing with metal ions in the solution to produce a protective coating. The pH of any solution depends on constituents of the organic compounds and also the solution. All the different types of acid and base compositions have different formulation to calculate pH of solution.

Temperature. The efficiency of OCIs is greatly impacted by temperature, which is an important variable in corrosion processes. Corrosion rates are accelerated at higher temperatures, hence it is critical to choose inhibitors that are stable and effective under these conditions.[1] The stability of the film formed by inhibitor, the rate of inhibitor breakdown, and the adsorption kinetics can all be impacted by temperature. As temperature increases the bonding changes to chemical due to decomposition and rearrangement of molecules. Hence inhibition effect is drastically reduced.

Film formation and stability. The efficiency of organic corrosion inhibitors (OCIs) is primarily governed by their ability

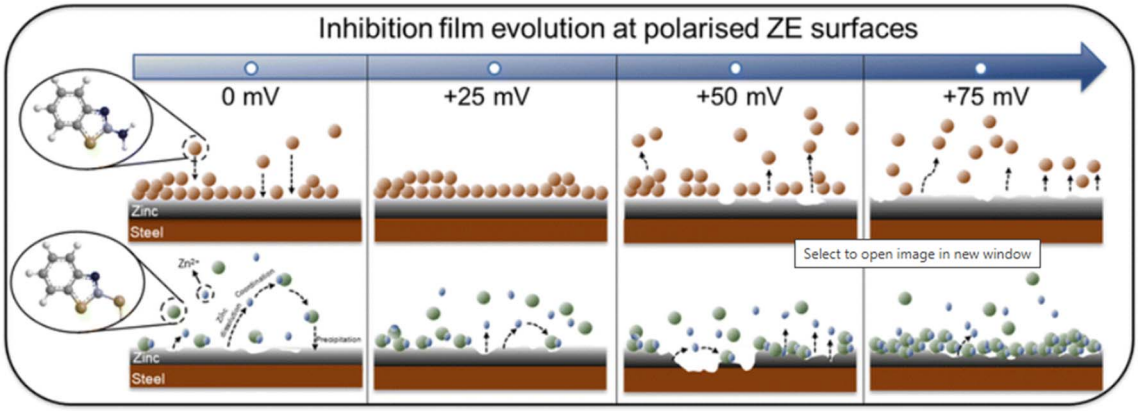

Fig. 15 Schematic illustration of inhibition film formation and sustainability at the ZE surface with surface over potentials ranging from 0 to +75 Mv, reproduced from ref. 43 with permission from [RSC] [*Mol. Syst. Des. Eng.*, 2024, **9**, 29–45] copyright 2024.

Fig. 16 Representation of synergism effect for corrosion inhibition efficiency, reproduced from ref. 44 with permission from [RSC] [*RSC Adv.*, 2020, **10**, 15163–15170] copyright 2020.

to generate and sustain a stable protective film on the metal surface, as shown in Fig. 15. This film functions as a barrier that restricts the ingress of corrosive species. The formation of such films may proceed *via* physical adsorption, chemical interactions with the metal substrate, or the self-assembly of inhibitor molecules. The long-term stability of the film is determined by the strength of inhibitor–metal interactions, the presence of aggressive species within the corrosive medium, and the mechanical robustness of the protective layer. In 2023, Deng *et al.*[43] have studied the inhibition performance of 2-aminobenzothiazole (2-ABT) and 2-mercaptobenzothiazole (2-MBT) against zinc electrode (ZE) corrosion, which highlights the critical role of molecular structure in adsorption and film stability. Electrochemical measurements confirmed that both compounds act as mixed-type inhibitors, simultaneously suppressing anodic and cathodic reactions, with inhibition efficiencies of 81% (2-MBT) and 77% (2-ABT) at 1 mM concentration. While 2-ABT forms a thin, uniform film through S-site chemisorption, 2-MBT coordinates with Zn^{2+} *via* N and thiol-S groups, producing heterogeneous surface deposits. DFT calculations reveal stronger Zn–inhibitor interactions for 2-MBT, including Zn displacement and complex formation. Importantly, 2-ABT loses protection at higher potentials due to desorption, whereas 2-MBT maintains stability by forming a compact protective layer. Collectively, these findings provide valuable mechanistic insight into structure–property relationships, underscoring the potential of rational molecular design for tailored corrosion inhibition strategies.

Synergistic effects. When two or more CIs or additives are combined, synergistic effects may occur, enhancing efficiency relative to the use of individual inhibitors alone. The synergistic advantages may arise from many mechanisms, such as enhanced adsorption, increased film stability, or complementary modes of action. To create a more effective and lifelong protective coating, one inhibitor, for instance, may facilitate the adsorption of another inhibitor onto the metal surface.[44] Synergistic effects significantly influence the total efficacy of the inhibitor systems in preventing corrosion as displayed in Fig. 16.

Several other factors responsible for influencing the performance of CIs includes: metal or alloy type with their chemical composition *i.e.* one CI works efficiently on steel but the same

might not work well for aluminium due to variations in surface characteristics and chemical reactivity. Surface condition of metal substrates is an important factor *i.e.* the inhibitor's ability to adsorb and, in turn, its ability to provide protection can be impacted by the presence of oxides, pollutants, or surface roughness. The presence of an aggressive ion in surroundings may also affect the performance of CIs particularly in chlorides, sulphates and saline conditions. The concentration of CIs including optimal dosage and intrinsic efficiency of inhibitor are vital parameters to measure the activeness of inhibitor. The stability and solubility of inhibitor in the media definitely decides the efficiency of any CIs. In addition, the interaction with other chemical species and competition for active adsorption sites may influence the performance of the CIs. Mass transfer and flow dynamics including flow rate may allow CIs to build up and offer more protection to metal substrates.

Inhibition efficiency validation

The corrosion is a thermodynamically driven process which progresses through chemical and electrochemical reactions between metals/alloys with surrounding environments. However, thermodynamics alone may not help to understand the kinetics of the process at which it occurs. Thus, different techniques have been employed to elucidate the corrosion mechanism, kinetics and efficacy of inhibitor in various environments. The gravimetric analysis/weight loss measurements are commonly and most widely utilized to define the efficiency of organic corrosion inhibitors due to ease of experimentation and no additional requirement of costly equipment. Further, some modern electrochemical techniques such as potentiodynamic polarization, electrochemical impedance spectroscopy (EIS) and electrochemical noise analysis, are also being employed to define the efficacy of the inhibitors and to divulge the protection mechanisms involved. These modern techniques are also proved equally comparative to the conventional weight loss measurements to define the efficacy of the inhibitors in the laboratory conditions in accelerated manner. Despite the theoretical differences among these methodologies, the results exhibit a consistent trend in magnitude, suggesting that they are acceptable and can substantiate the efficacy of corrosion inhibition as discussed below:

Conventional immersion exposures (CIE)

As mentioned above, the corrosion performance is largely monitored through the gravimetric analysis/weight loss method, which entails immersing/exposing the metal/alloy specimens in a simulated environment for a predetermined time duration. Following this exposure, the sample is retrieved, and the change in its weight before and after the exposure is measured[45] (Table 3, Appendix C). This method is fundamental, reliable, and exact for determining the rate of metal corrosion. The metal sample is initially subjected to a pretreatment process prior to the experiment, which involves grinding with emery paper, followed by cleaning with double distilled water, degreasing with acetone, and finally drying. The specimen utilised for the measurement is weighed on a balance with a sensitivity of ±0.01 mg. It is also noted in the methodology that after the metal sample is immersed in various test solutions at a specific temperature (avoiding temperature influence) for a specific duration with and without different quantities of inhibitors. Following the execution of the experiment, the sample was subsequently washed, dried, and weighed. The inhibitor concentration for weight loss and the electrochemical study was measured in mg L^{-1}. More often, the experiments are conducted with triplicate set of specimens as advised in the standard ASTM-G31 and the averaged values is taken into account.[46,47] Surface coverage (θ), inhibition efficiency (IE, %), and corrosion rate (CR) are determined using the following equations:

$$\theta = \frac{W_0 - W_i}{W_0} \quad (1)$$

$$\mathrm{IE}(\%) = \frac{W_0 - W_i}{W_0} \times 100 \quad (2)$$

where, W_0 represents the weight loss in the absence of an inhibitor, while W_i indicates the weight loss when inhibitor is present in the electrolyte. Further, corrosion rate (CR) is calculated as per the equation mentioned below:

$$\mathrm{CR} = \frac{87.6\ \Delta W}{StD} \quad (3)$$

In this context, ΔWrepresents the corrosion weight loss of metal/alloy specimens measured in milligram, S denotes the area of the coupon in square centimeter, t indicates the exposure time in hour, and D refers to the density of metal/alloy expressed in grams per cubic centimetre.[48–52]

As mentioned previously, the weight loss method is very much reliable and advantageous in determing the efficiency of organic inhibitors (by eqn (2)). Mahdi *et al.* examined the corrosion resistance of mild steel in 1 M HCl solutions, both with and without the inhibitor 2,2′-(1,4-

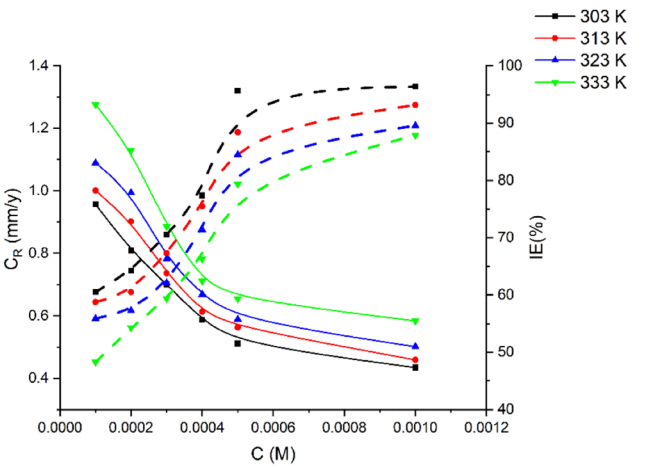

Fig. 17 Plot showing the trend in mild steel corrosion rate (CR, left side) and inhibitor efficiency (IE, right side) with increase in PMBMH concentration in HCl solution at different temperatures. Reproduced from ref. 52 with permission from [MDPI] [*Molecules*, 2022, **27**, 4857] copyright 2022.

phenylenebis(methanylylidene)) bis(*N*-(3-methoxyphenyl) hydrazinecarbothioamide) (PMBMH), at various temperatures (30, 40, 50, and 60 °C) using the weight loss method.[52] The weight change and corrosion rate derived for mild steel with varying quantities of corrosion inhibitors, found to indicate that the IE increases while the CR values decrease with increasing inhibitor concentrations irrespective of the exposure temperature as shown in Fig. 17. Further, the corrosion rate reported to increase and inhibition efficiency found to decrease with increasing temperature from 30 °C to 60 °C at all the inhibitor concentrations. The temperature-dependent reduction in IE is believed to result from diminished physical adsorption of the inhibitor on the mild steel surface, caused by an increase in hydrogen gas evolution with rising temperatures, leading to decreased physical attachment and elevated corrosion rates as compared to lower temperatures. However, the effect of temperature increase on IE is more pronounced at lower inhibitor concentrations as compared to higher concentrations where IE remained $\geq$ 90% at all temperatures (Fig. 17). The efficiency of inhibitors at higher concentrations across varying temperatures demonstrated consistency, which thought to be attributed to minimal or slight disturbance in adsorption and chemisorption occurance independently or in conjunction with physisorption.

Electrochemical techniques

Corrosion inhibitors are known to control the metal corrosion through slowing down or hindering the anodic and/or cathodic electrochemical reactions occurring during the process. The corrosion inhibition is accomplished by suppressing the rate of the cathodic reduction and/or obstructing the anodic oxidative dissolution of metal.[53] The use of cathodic inhibitors for corrosion inhibition entails multiple processes. Initially, these inhibitors elevate the overpotential of the cathodic reaction, thereby difficulty in the occurrence of corrosion and reduced rate of corrosion. Cathodic inhibitors obstruct the cathodic process *via* deposition at cathodic sites, either through the creation of insoluble compounds or by enhancing the metal's liability to hydrogen, thus, reduced corrosion due to low or non-availability of cathodic reactants. Cathodic inhibitors serve as a barrier, impeding electron passage and thereby diminishing the total corrosion rate. Anodic protection occurs when a corrosion inhibitor adsorbs onto the surface, creating an oxide layer on the metal surface. This protective film serves as a barrier, obstructing the anodic process. Anodic inhibitors which contains non-oxidizing ions, require external oxygen for safeguarding the metals against corrosion, whereas oxidising ions containing inhibitors can safeguard metals without the need for external oxygen. Further, there are certain inhibitors which supress both anodic and cathodic reactions to control the corrosion, known as mixed type of inhibitors. As, the inhibitors control the corrosion through electrochemical mechanisms, the electrochemical techniques are good tool to understand the type of inhibitors and subsequent mechanisms involved in the process.

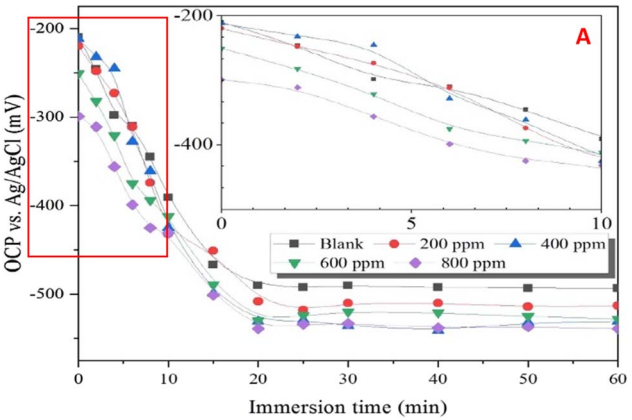

Fig. 18 The open circuit potential (OCP) variation with immersion time for mild steel exposed in uninhibited and inhibited 1 M HCl solution (Inhibitor; different quantities of *Ziziphora* leaves extract); inset shows the enlarged view of region 'A' marked in red colour, reproduce from ref. 54, with permission from [Elsevier] [*Constr. Build. Mater.*, 2020, **245**, 118464] copyright 2020.

Open circuit potential (OCP)

The open circuit potential (OCP), often reffered to as the self-corrosion potential (E_{corr}), represents the corrosion potential difference between the working electrode and reference electrode in the absence of current, is a crucial indicator of the corrosion or passivation state of the working electrode surface.[53] The OCP measurement at zero current and the stabilized values reflect the equilibrium between anodic (metal dissolution) and cathodic (reduction) reactions. An inhibitor either doesn't alter much or pushes this equilibrium towards a more noble (positive) or active (negative) potential side depending upon its nature of protection. The organic inhibitors which form a protective barrier (passivation) *via* adsorbing onto the metal surface and blocks the corrosive species to reach the metal/solution interface, thereby shifting the OCP to more positive side and reduce the corrosion rates. Further, a stable OCP indicates the uniform protective film formation over the surface while a fluctuating OCP suggests the unstable film formation onto the surface. The large positive stable OCP values are often regarded as log-lasting protection while a sudden drop towards more negative values is considered as inhibitor depletion or protective film failure during the corrosion process. In addition, sometime a negative shift in OCP is observed but the inhibitor film protects the metal well, these inhibitors are named as cathodic inhibitors. The mixed type inhibitors cause a smaller shift in OCP but supresses both the anodic and cathodic reactions but need to be validated with other electrochemical techniques (PDP) for their mechanisms. Thus, the OCP measurement, can offer valuable insight into the type of inhibitor based on the potential shift obtained with the incorporation of the inhibitor into the process (Table 3, Appendix C). Dehghani *et al.* monitored the OCP of mild steel specimens in 1 M HCl solution with varying concentration of *Ziziphora* leaves as an inhibitor before conducting the EIS and PDP experiments.[54] The OCP values reported to drop toward negative

(active) potential side up to 20 minutes and later on became relatively stable both in unhibited or inhibited solutions (Fig. 18). The stabilisation is attributed to the formation of a stable iron oxide/hydroxide coating on mild steel in the absence of inhibitors, while in the case of inhibited HCl solutions, it is due to the complete adsorption of inhibitor molecules (Fig. 18). Evidence showed that increasing the concentration of *Ziziphora* leaves extract in the electrolyte led to lower OCP values towards more negative side but a complete stabilization, which means that the molecules of *Ziziphora* leaves extract were able to adsorb well and cover a lot of iron surfaces. Though the potentials were observed towards negative side but the shift remained <82 mV, thus the inhibiter can be called as a mixed type inhibitor.

Electrochemical impedance spectroscopy (EIS)

This technique is often being deployed to obtain the additional details on corrosion mechanisms during the interaction of inhibitor and metals surface (Table 3, Appendix C). EIS is used to determine the material's resistance and capacitance characteristics in absence and presence of inhibitor by applying small alternating current (AC) perturbations. The EIS spectra is obtained through varying frequency in certain range at open circuit potential (OCP). The output of EIS is plotted in form of Bode and Nyquist plots, where impedance and phase angle is plotted on *y*-axis against frequency at *x*-axis, and imaginary part of impedance is plotted on *y*-axis against real part of impedance at axis, respectively. The spectra is fitted with a suitable electrochemical equivalent circuit (EEC) to obtain polarization/charge transfer resistance (R_{ct}) and double layer capacitance (C_{dl}). Also, the technique is utilized to determine the corrosion rates accurately in accelerated manner non-destructively. The inhibition efficiency is calculated through the equation mentioned below by utilizing the resistance data:

$$\mathrm{IE}(\%) = \frac{R_i - R_b}{R_i} \times 100 \quad (4)$$

where, R_b and R_i are the charge transfer resistance in absence and presence of the inhibitor in the medium, respectively.

When the concentration of the inhibitor is increased, the value of R_{ct} increases and the value of C_{dl} decreases if the inhibitor is well adsorbed.[55] As previously mentioned, typically, the data obtained from instruments to create two forms of

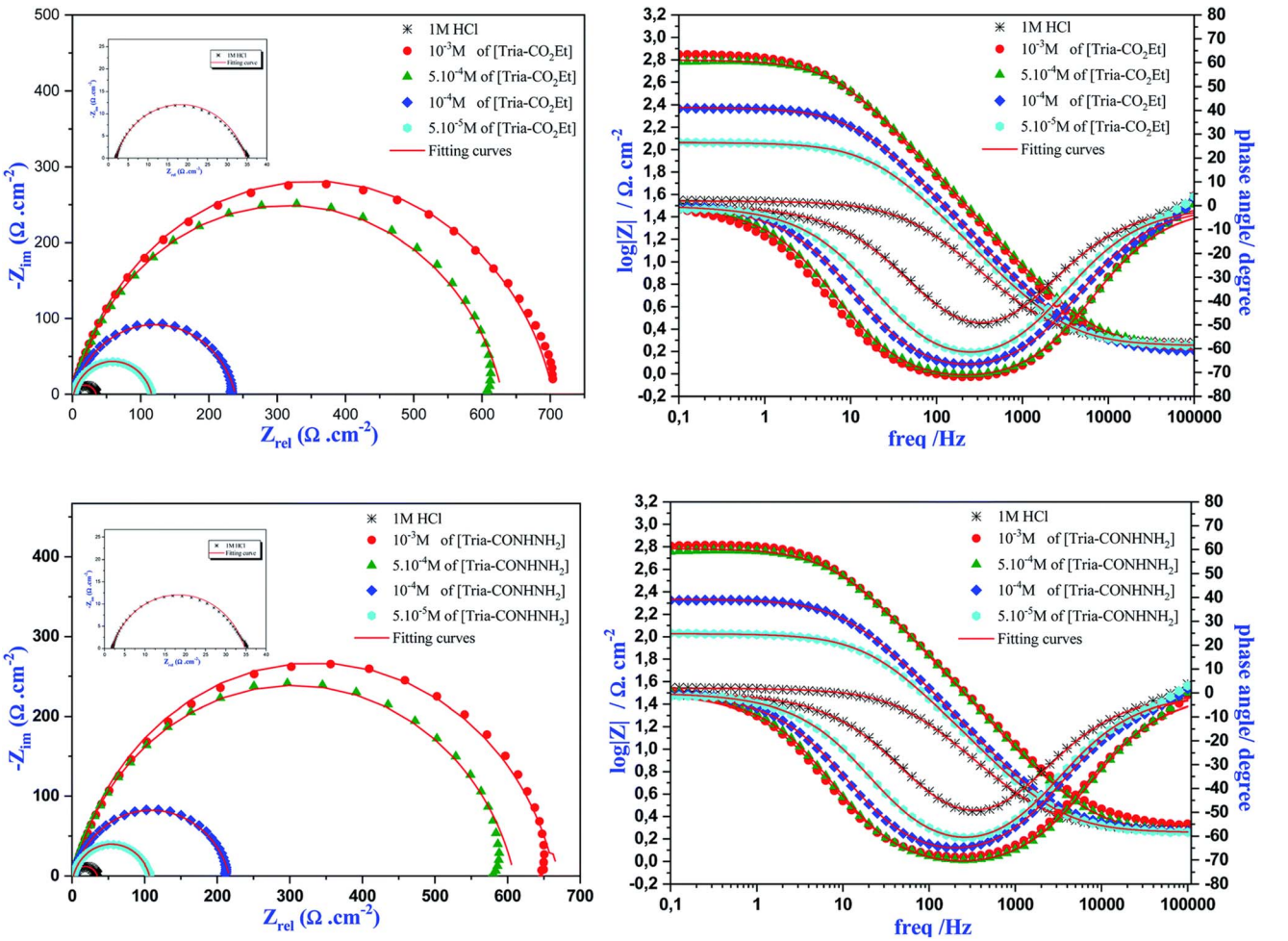

Fig. 19 Nyquist and Bode plots for mild steel in 1.0 M HCl with and without various [Tria-CO_2Et] and [Tria-$CONHNH_2$] concentrations, reproduced from ref. 56 with permission from [RSC] [*RSC Adv.*, 2021, **11**, 4147–4162] copyright 2021.

graphical representations that enhance the understanding of the corrosion inhibition process. To elucidate the graphical representation, an examples is taken for the EIS data derived from literature. The graphical representation comprises Fig. 19, Nyquist and Bode plots, pertaining to the two different inhibitors ethyl 2-(4-phenyl-1*H*-1,2,3-triazol-1-yl) acetate [Tria-CO_2Et], and 2-(4-phenyl-1*H*-1,2,3-triazol-1-yl) acetohydrazide [Tria-$CONHNH_2$] inhibitors utilised for the mitigation of MS corrosion.[56] These plots shown a depressed semicircle, non-ideal with their center, which is related to different physical phenomena such as surface heterogeneity. EIS measurements revealed that both inhibitors exhibited a high inhibition performance, achieving an inhibition efficiency of 95.3% for [Tria-CO_2Et] and 95.0% for [Tria-$CONHNH_2$] with a concentration of 1.0×10^{-3} M. The Bode plot showed that the impedance value is increased with increasing amount of inhibitor in the HCl media and derived highest for 1.0×10^{-3} M levels of inhibitor addition. Also, the phase angle values were found to be shifted towards higher values with the presence of inhibitor. This indicated that the inhibitor has covered the metallic surface fully as indicated by the increased phase angle values (approaching towards −90° *i.e.* much closer to capacitive behaviour thereby much uniform surface). Further, the capacitive loop diameter revealed the presence of a thin layer of inhibitor on metal surface. Further, Yousif *et al.* utilized the EIS technique to study the inhibition mechanism of newly synthesized (*S*,*E*)-2-((1-(4-minophenyl)ethylidene)amino) (3-(4-hydroxyphenyl)propanoic acid), "AEPA", and (2*S*,5*R*,6*R*)-3,3-dimethyl-7-oxo-6-propionamido-4-thia-1-azabicyclo[3.2.0] heptane-2-carboxylic acid, "DOCA", for carbon steel in 1 M HCl solution.[57] The fitted Bode and Nyqist plots obtained for various concentration of AEPA and DOCA are illustrated in Fig. 20a–d, respectively. The EIS data was fitted to the double time constant electrochemical equivalent circuit (EEC) as shown in inset of Fig. 20a and b. The EEC is comprised of circuit includes the solution resistance (R_s), film resistance (R_f), charge transfer resistance (R_{ct}), constant phase element of the adsorbed film (CPE_{film}) and double layer (CPE_{dl}) with phase shifts n_1 and n_2, respectively.

The imperefect dippresed semi-cricle shape of all the curves revealed the similar type of corrosion mechanism over the entire frequency range which is charge transfer mechanism. Further, the imperfection in the shape was correlated to the surface roughness factor of steel specimens. The diameter of the semi-circles was reported to increase with increasing the concentration of AEPA and DOCA in the solution. This increase was attributed to the increase in charge transfer resistance value and inhibitor efficiency, suggesting that the efficacy of the inhibitor may be directly proportional to the concentration of inhibitors. An increase in charge transfer resistance suggested that a greater number of inhibitor species were adsorbed onto the surface as concentration rise. The adsorption created a film onto the surface thereby increase in the resistance (R_f) as concentration increased. This can be ascribed to the

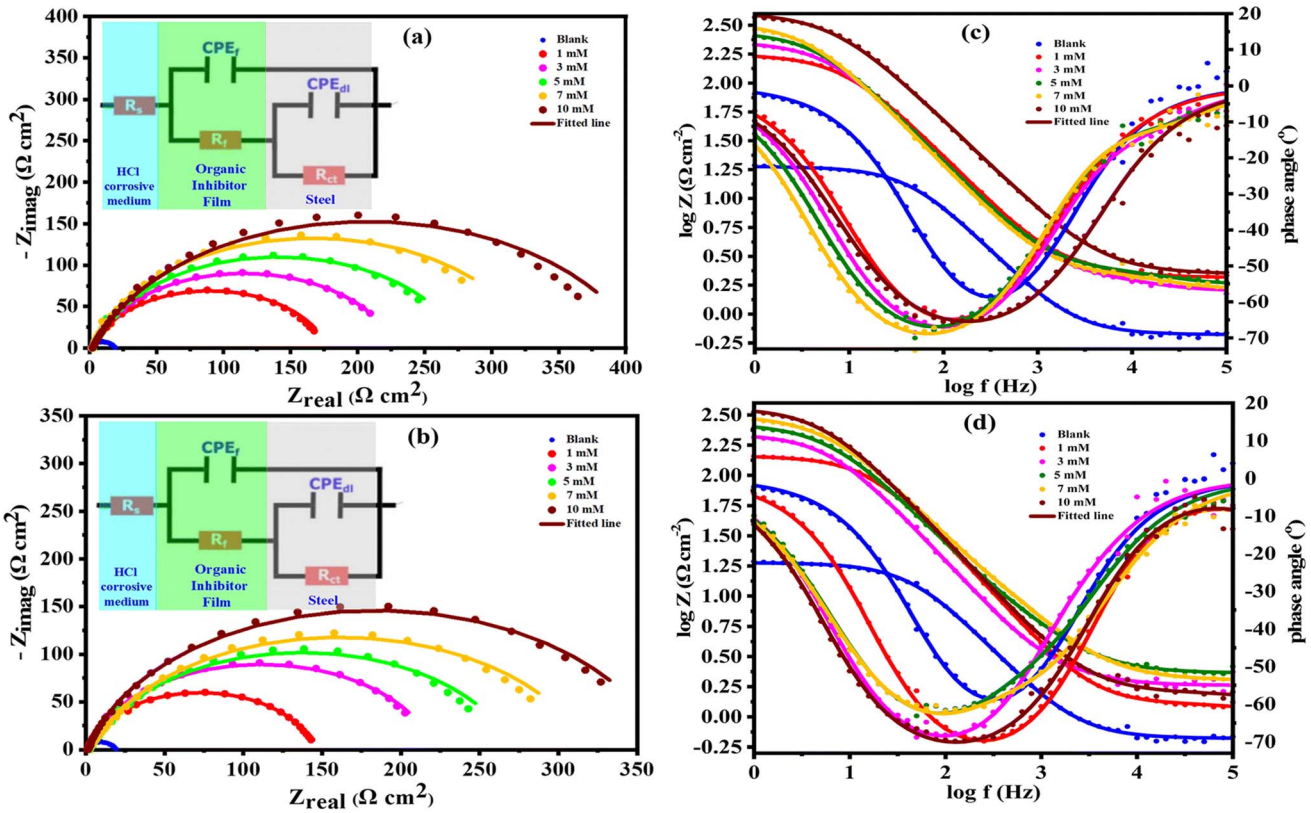

Fig. 20 Nyquist plots, Bode and phase angle plots for steel in 1.0 M HCl solution without and with different concentrations of AEPA (a and c), and DOCA (b and d) compounds at 30 °C, reproduced from ref. 57, with permission from [RSC] [*RSC Adv.*, 2025, **15**, 28666–28688] copyright 2025.

enhancement of local dielectric/insulation around the surface due to the augmented adsorption of the inhibitor. This adsorption of the inhibitor displaces water molecules and chloride ions from the surface, thereby reducing active corrosion sites and decreasing the corrosion rate. The 'n' values are often related to the electrolyte and metallic interface homoginity or hetroginity. The values of n_1 and n_2 in inhibited solution were determined much higher as compared to the blank solutions, which indicated a reduction in surface roughness due to the adsorption of inhibitor on to the surface, thereby reduced corrosion rates. The value of 'n' rises with an increase in inhibitor concentration, indicating that a superior anti-corrosion effect is achieved with higher inhibitor concentrations. This shows that the EIS is an effective tool to divulge the inhibition mechanism and efficacy of the inhibitors in an electrolyte.

Potentiodynamic polarization (PDP)

PDP is another healthy tool to study the corrosion mechanism and inhibitor efficacy in accelerated manner in the laboratory. This is carried out with the help of a potentiostat/Galvanostat and standard three electrode electrochemical cell comprising of working, counter and reference electrode. The specimens are scanned in a defined potential range at predetermined rates to obtain the cathodic and anodic current densities. The current response as a function of applied potential reveals several alterations, including the shape of polarisation curves and the positioning of anodic or cathodic current densities relative to the curve in absence of GCI, which can be utilised to assess the efficacy of GCIs in corrosion inhibition. Further, the kinetics of anodic and cathodic reactions can be comprehended by polarisation curves. Also, the PDP enables the measurement of corrosion kinetics and employed to determine the electrochemical parameters such as corrosion potential (E_{corr}), corrosion current density (i_{corr}), cathodic Tafel slope (β_c), anodic Tafel slope (β_a), and percentage of inhibition (IE, %) as a function of inhibitor concentration derived from the curves. The Tafel slopes (β_a) and (β_c) will be ascertained based on the mechanism of the process, which may involve inhibition through cathodic, anodic, or both types of reactions, while the E_{corr} value will indicate the nature of the inhibitor employed.[58,59] If the curve on the graph shifts towards a lower current density, it indicates a decrease in the corrosion rate.[60]

$$\mathrm{IE}(\%) = \frac{i_{corr} - i'_{corr}}{i_{corr}} \quad (5)$$

where, i_{corr} and i'_{corr} are the corrosion current density in absence and presence of the inhibitor in the medium, respectively.

The Tafel polarisation curves illustrated in Fig. 21 have been documented in the literature, where AEPA and DOCA were employed to mitigate the corrosion rate of carbon steel in an acidic environment.[57]

To study the mechanism of dissolution process of carbon steel, potentiodynamic polarization measurement were performed. Several parameters such as anodic and cathodic slopes (β_a and β_c in mV dec^{-1}), corrosion current density (in mA cm^{-2}),

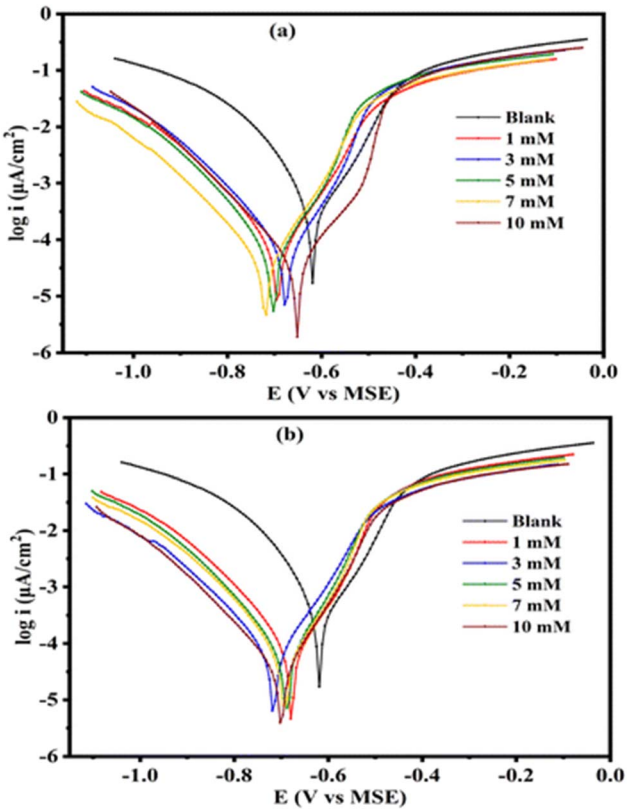

Fig. 21 Potentiodynamic polarization curves for the corrosion of carbon steel in 1.0 M HCl in absence and presence of different concentrations of AEPA (a) and DOCA (b) compounds at 30 °C, reproduced from ref. 57, with permission from [RSC] [*RSC Adv.*, 2025, **15**, 28666–28688] copyright 2025.

corrosion potential (in mV *vs.* SCE) and the inhibition efficiency (η_{PDP})(%) were calculated by analysis of PDP curves. A drop in current density was observed in the polarization curves after the addition of both the inhibitors. The anodic and cathodic curves were marked to suppressed towards less current density values and E_{corr} values were found to shift towards more negative side with incorporation of inhibitors. Also, the E_{corr} values were shifted to beyond 85 mV in both the cases thus inhibitors can be considered cathodic type. Further, inhibition efficiency was increased linearly on carbon steel surface as concentration of the inhibitors (AEPA and DOCA molecules) increased in the solution.

Corrosion protection mechnanisms

The efficacy of inhibitor is closely linked to the adsorption tendency of the inhibitor molecules onto the metal surface. Thus, it is imperative to understand the adsorption isotherm involved to get the better insight of the corrosion prevention mechanisms. As, the corrosion progresses through the galvanic/electrochemical cell formation onto the metallic surface. Thus, efficient inhibitor prevent the corrosion by disruptin the interaction between various components in an corrosion cell such as elimination of local anode, cathode, or hindering the path of an electrolyte necessary for electron transport by effectively

adsorbing onto the surface. Adsorption is influenced by various factors, including charge, ionic species, solvent adsorption, electrochemical potential at the solvent–solution interface, characteristics of the metal surface, reaction temperature, electronic properties, and the presence of electron-donating or electron-repelling groups of derivatives. Determining the degree of surface coverage by the inhibitor (θ) and assessing the adsorption isotherms through various mathematical models are crucial steps in comprehending corrosion mechanisms. The values of θ can be accurately derived using the gravimetric method of weight loss as mentioned in eqn (1).

There are various adsorption isotherms mentioned in the literature which are the key factors to describe the interaction between sample and inhibitor (Table 4, Appendix D). Adsorption is validated if surface coverage data conforms to any isotherm. The graphical depiction of the isotherm should yield a linear representation, and the regression coefficient must equal one. The intercept of the adsorption isotherm provides the value of the adsorption equilibrium constant (K_{ads}), which is subsequently utilised to characterise the free energy value.[61] The universal representation of all isotherms is shown below:

$$f(\theta,X)\exp(-2a\theta) = K_{ads}C \quad (6)$$

Where $f(\theta, X)$ is configurational factor, θ is surface coverage, C is inhibitor concentration, X is size ration, and a is molecular interaction parameter during the adsorption process.[62] All isotherms utilised to examine corrosion mechanisms are derived from above mentioned equation. Not all isotherms are suitable for corrosion investigations; however, a selective number, such as Langmuir, Freundlich, El-Awady, Temkin, and Flory-Huggins, can be utilised. The standard free energy of adsorption in corrosion ($\Delta G_{ads}{}^{0}$) is computed using the K_{ads} values derived from adsorption isotherms by the following equation:

$$\Delta G_{ads}{}^{0} = RT \ln K_{ads}\ C_{solvent} \quad (7)$$

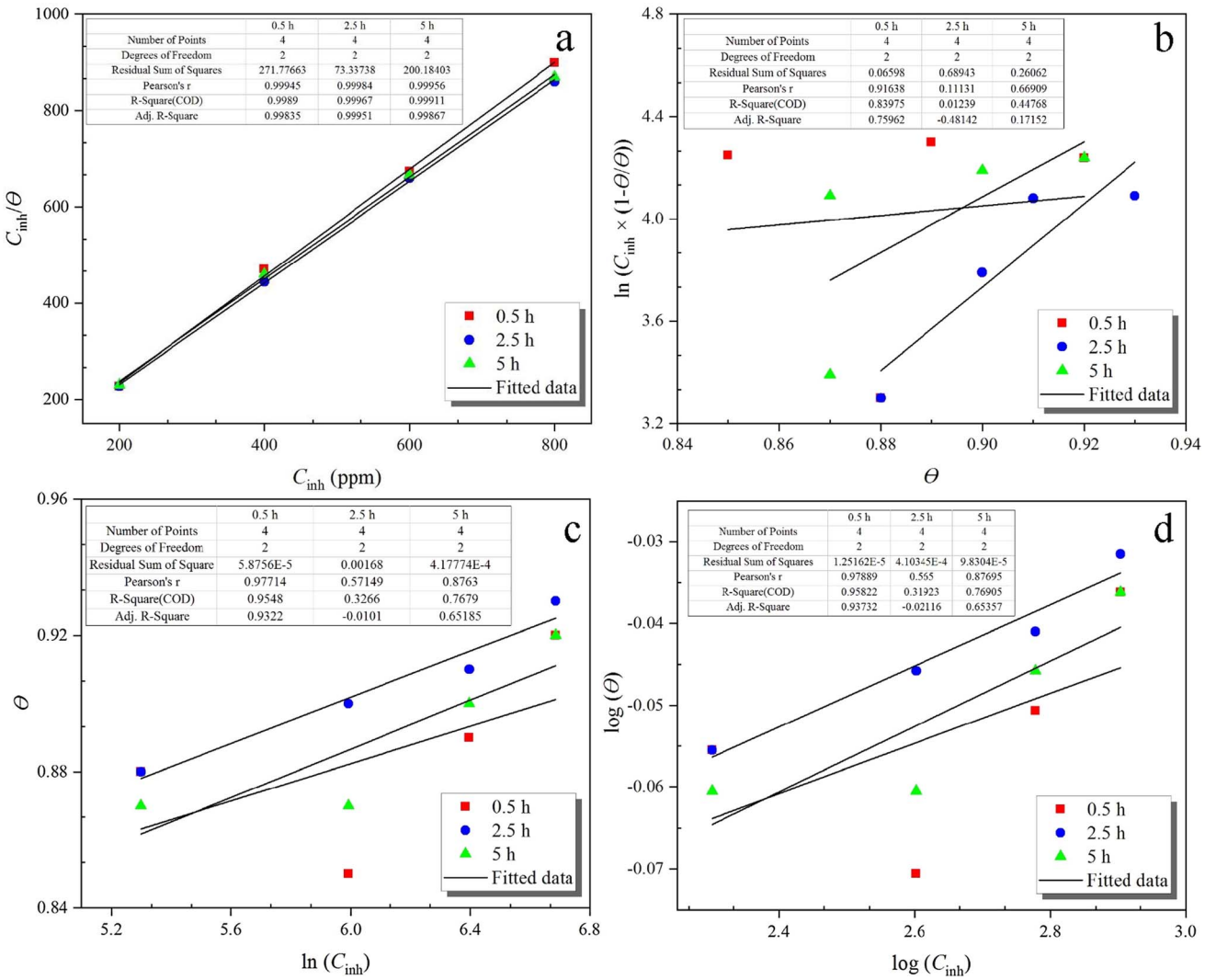

Fig. 22 Various adsorption isotherm parameters determined for adsorption of *Ziziphora* leaves extract to mild steel in 1 M HCl solution with different concentrations (a) Langmuir, (b) Frumkin, (c) Temkin and (d) Freundlich adsorption isotherms, reproduce from ref. 54, with permission from [Elsevier] [*Constr. Build. Mater.*, 2020, **245**, 118464] copyright 2020.

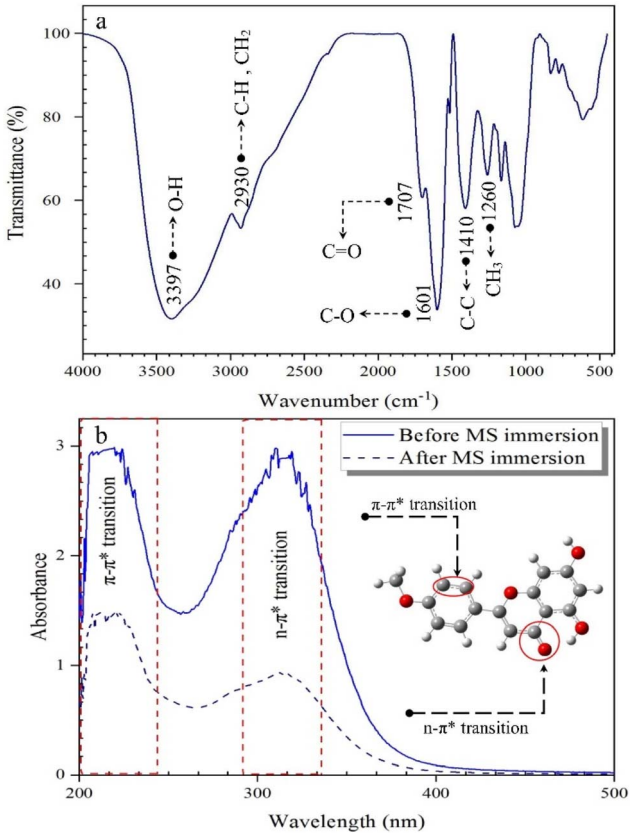

Fig. 23 (a) FT-IR and (b) UV-Vis spectra of *Ziziphora* leaves extract powder with and without MS substrate, reproduce from ref. 54, with permission from [Elsevier] [*Constr. Build. Mater.*, 2020, **245**, 118464] copyright 2020.

where $C_{solvent}$ is the molar concentration of solvent (in case of water the value is always 55.5 mol L^{-1}), K_{ads} is the value of the equilibrium constant of the adsorption process, R is Universal Gas Constant, and T is the absolute temperature.[63] Further, the other kinetic–thermodynamic parameters such as enthalpy, entropy, Gibb's free energy and activation energy of adsorption are also important to compute for the better understanding the protection mechanisms further. The physical significance of various parameters is explained in Table 5 (Appendix E) and the various equation for computing these parameters is mentioned in the literature.[64] Dehghani *et al.*[54] analysed the adsorption type of *Ziziphora* leaf extract components on mild steel surface in HCl solution. Various adsorption modes were evaluated and calculations were done for the desired adsorbent. The experimental findings were analysed using Langmuir, Frumkin, Temkin, and Freundlich isotherms, with the fitting outcomes illustrated in Fig. 22. The experimental results were very compatible with the Langmuir isotherm ($R^2 = 0.99$). Consequently, it can be deduced that the *Ziziphora* leaf extract safeguarded the MS substrate *via* a monolayer formation on to the surface. The adsorption parameters are presented in Table 6 (Appendix F). The summarised data in this table exhibited elevated adsorption equilibrium constant (K_{ads}) values, indicating the spontaneous adsorption of *Ziziphora* leaves extract onto the steel substrate. Moreover, it was determined that the standard Gibbs free energy (ΔG_{ads}) values varied between −33 and −35 kJ mol^{-1}. There are previous studies which also indicated that if the ΔG_{ads} is calculated above 20 kJ mol^{-1}, the adsorption occurs physically, but for the values below 40 kJ mol^{-1} then the adsorption occurs *via* chemical interactions.[65] Thus, it was concluded that the molecules of the *Ziziphora* leaf extract were adsorbed by chemical and physical interactions, including electrostatic forces and charge sharing.

This adsorption was further confirmed by FT-IR and UV-Vis spectrophotometry characterization techniques. The FT-IR and UV-Vis spectra are portrayed in Fig. 23. The FT-IR elucidated the presence of polar functional groups and heteroatoms in the adsorption of inhibitor compounds onto the iron surface. The vibrations of O–H (3397 cm^{-1}), C–H (2930 cm^{-1}), C=O (1707 cm^{-1}), C–O (1601 cm^{-1}), C–C (1410 cm^{-1}), and CH_3 (1260 cm^{-1}) were identified in the structure of *Ziziphora* leaves extract, which may facilitate the adsorption of extract molecules on the MS surface, thereby enhancing their anti-corrosion efficacy against corrosion. The extract of *Ziziphora* leaves contains several heteroatoms (*e.g.*, O) that can be readily protonated and adsorbed by electrostatic interactions. The UV-Vis spectrum illustrated two distinct peaks prior to MS immersion in HCl (Fig. 21b). The initial peak at 225 nm indicates a π–π* transition, signifying the absorption of the C=C bond (aromatic). The second peak, centred at 331 nm, corresponds to the n–π* transition, demonstrating the absorption capacity of C=O groups. After the immersion of MS substrate, the π–π* and n–π* transition peaks shifted to 221 and 326 nm, respectively. These differences indicated the sequential interaction of C=C and C=O bonds with iron cations, thereby successful adsorption on to the surface.

Numerous studies have illustrated that the adsorption of inhibitor molecules results into a protective film formations containing specific chemical orientations, thereby no or very minimal corrosion of underlying substrate. The development of a protective film on metal surfaces is correlated with open circuit (OC) or self-corrosion potential of the metals/alloys. The moment open circuit potential becomes relatively stable, indicated the full surface coverage and development of the protective layer onto the substrate.[66,67] Several surface characterization techniques including X-ray photoelectron spectroscopy (XPS), scanning electron microscopy (SEM), atomic force microscopy (AFM) were used to characterize these organic thin films which forms on to the surface of the carbon-steel while immersed in inhibitor containing mediums. Song *et al.*[68] examined the production of protective films on metal surfaces utilising XPS technique. According to the XPS spectra in Fig. 24a, the protective layer was mostly made up of iron oxide, hydroxyl oxide, and organic compounds that contained carbon. The XPS analysis led them to conclude that an organic coating with carbon formed on the steel surface, indicating that the plant extract may improve the steel sample's corrosion resistance. Simovic *et al.*[69] examined the effectiveness of green corrosion inhibitors derived from black pine (*Pinus nigra*) oil for carbon steel. The contact angle measurements were utilized to look at the hydrophilic properties of inhibited and non-inhibited carbon steel samples according to ASTM standards [ASTM,

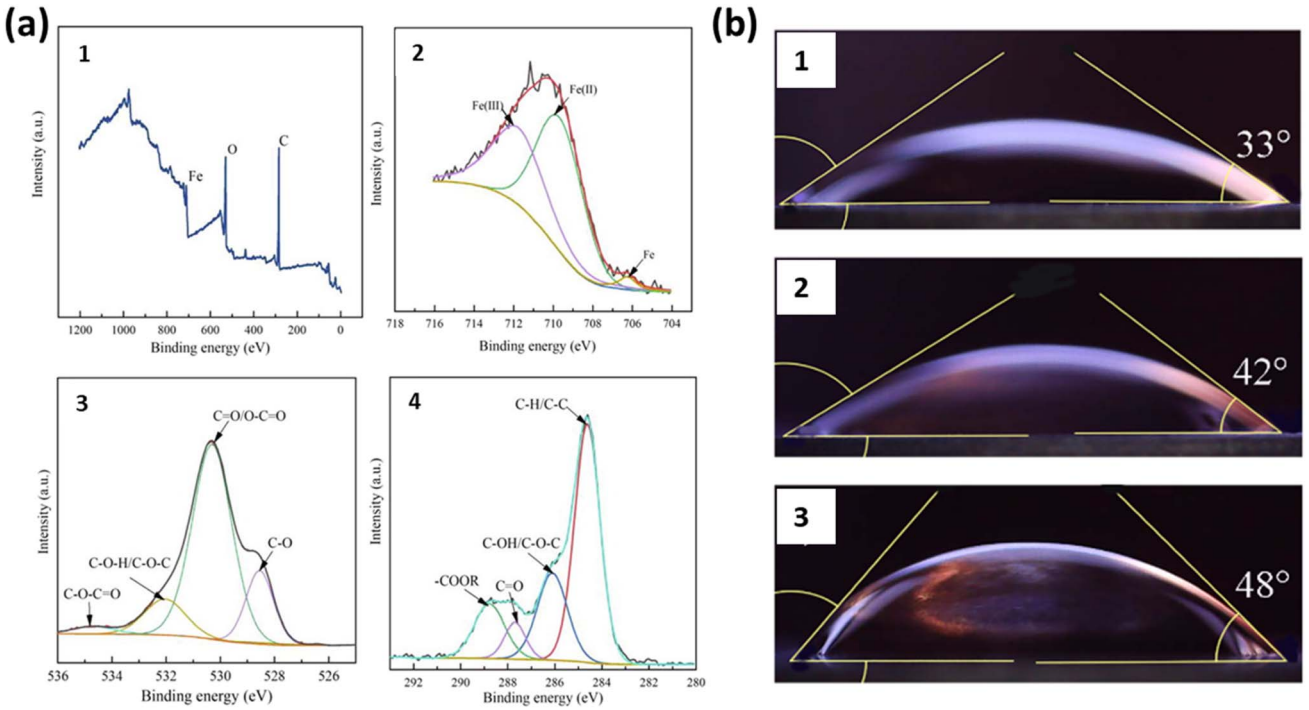

Fig. 24 (a) XPS spectra of steels with plant extract added to the corrosive solution (1): wide-scan spectrum; (2) Fe 2p spectrum, (3) O 1s spectrum and (4) C 1s spectrum, reproduced from ref. 68, with permission from [Elsevier] [*J. Ind. Eng. Chem.*, 2022, **111**, 464–479] copyright 2022 and (b) Carbon steel contact angle measurements after being immersed in (1) 1 M HCl for 1 h; (2) 1 M HCl with 50 ppm PN for 1 h; (3) 1 M HCl with 50 ppm PN for 4 h, reproduced from ref. 69, with permission from [MDPI] [*Metals*, 2023, **13**, 508] copyright 2023.

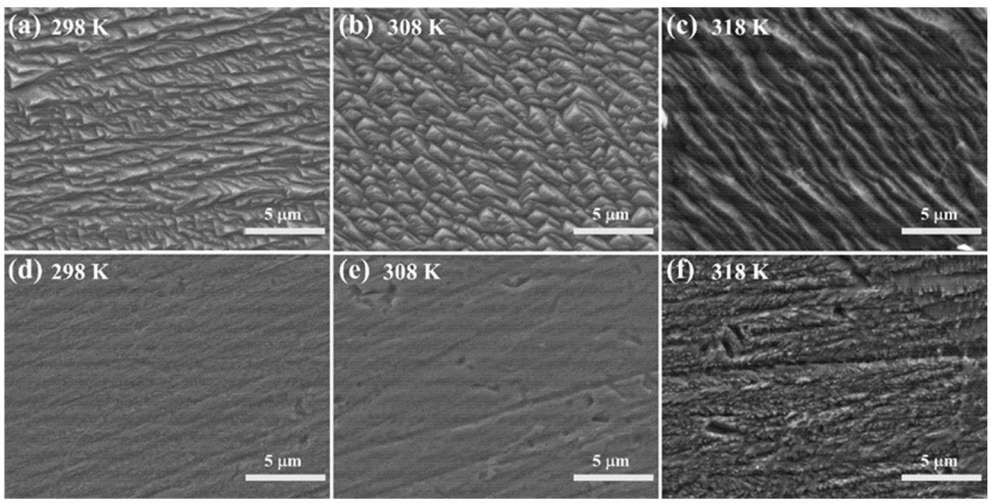

Fig. 25 FE-SEM micrographs of the X70 steel specimens immersed in 1 M HCl solution (a–c) without and (d–f) with 200 mg L^{-1} GLE for 4 h at different temperatures, reproduced from ref. 70 with permission from [Elsevier] [*Corros. Sci.*, 2018, **133**, 6–16] copyright 2018.

D7490–13 standard test method for measurement of the surface tension of solid coatings, substrates and pigments using contact angle measurements, B ASTM Stand. 6 (2013) 1–5]. Fig. 24b shows the results of the contact angle test on metal that was in inhibitors for 1 and 4 hours and carbon steel that was in 1 M HCl for one hour. The higher contact angle of the inhibited sample compared to the non-inhibited one shows that there is an organic inhibitor barrier coating on the metal surface. The data also demonstrated that the hydrophobicity of the inhibited samples got better with time, showing that an inhibitor layer works as a shield against harsh conditions. They infered that the creation of a hydrophobic layer of inhibitors on the metallic surface.

Qiang *et al.*[70] examined the uninhibited and inhibited steel specimens for the developed surface films under SEM and AFM. They saw that the exposed steel surface had a lot of damage and

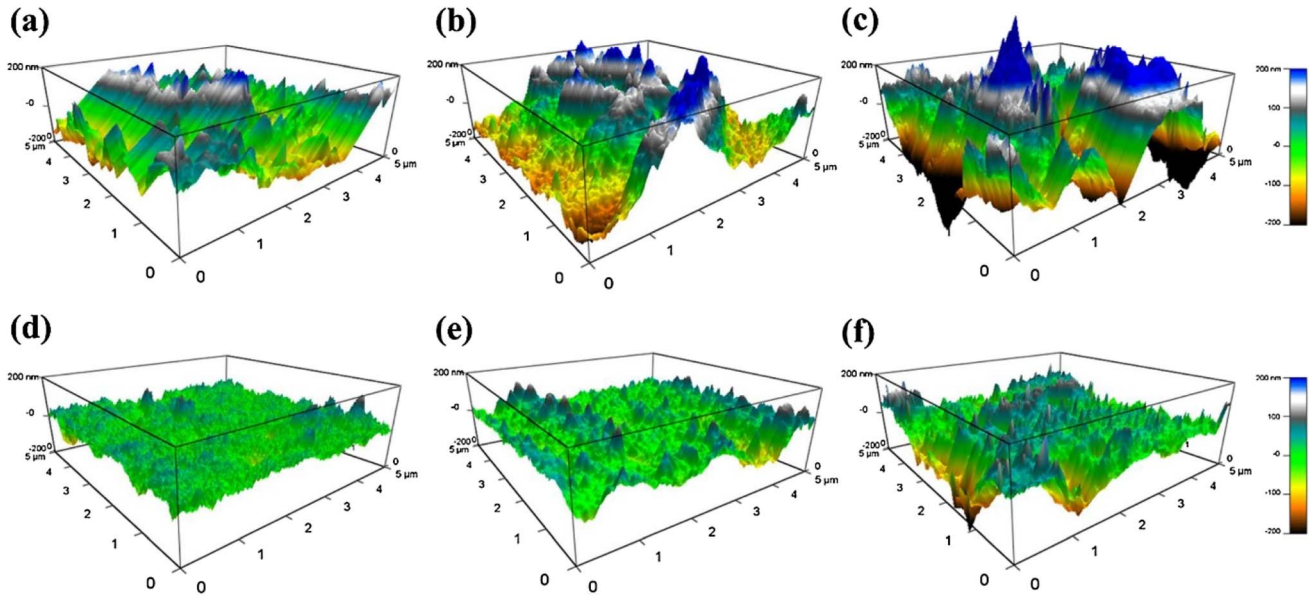

Fig. 26 3D AFM images of the X70 steel specimens immersed in 1 M HCl solution without GLE for 0.5 h at (a) 298 K, (b) 308 K, and (c) 318 K; 3D AFM images of the X70 steel specimens immersed in 1 M HCl solution with 200 mg L^{-1} GLE for 0.5 h at (d) 298 K, (e) 308 K, and (f) 318 K, reproduced from ref. 70, with permission from [Elsevier] [*Corros. Sci.*, 2018, **133**, 6–16] copyright 2018.

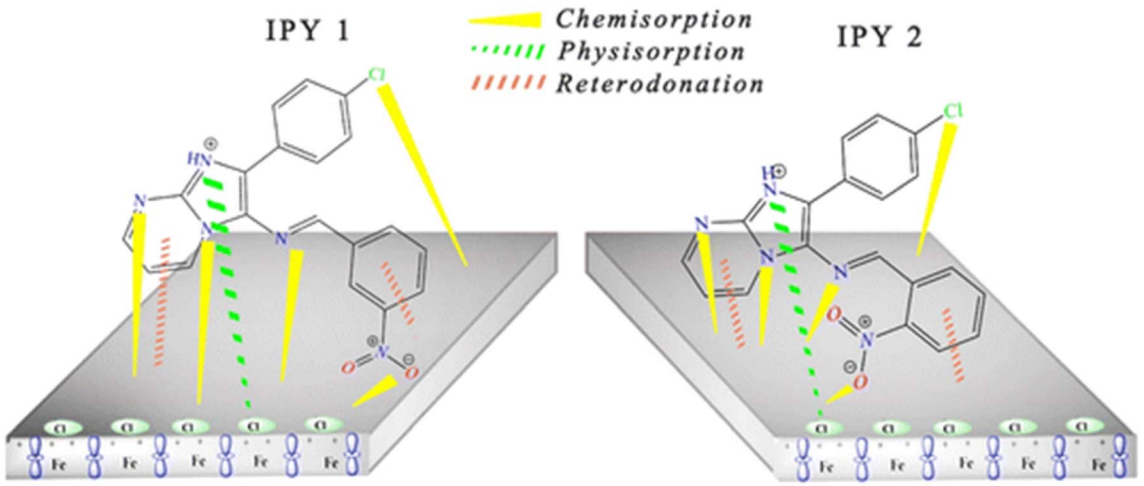

Fig. 27 A mechanistic pathway of corrosion inhibitors through different kind of interactions, reproduced from ref. 72 with permission from [RSC] [*RSC Adv.*, 2025, **15**, 12342–12363] copyright 2025.

corrosion in strong acidic environment as shown in Fig. 25. As the temperature increased, the specimen surface become more rougher due to increased attack Fig. 26. Furthermore, the surfaces exposed to the plant extract incorporated acidic media at all evaluated temperatures had far smoother morphologies than those of the uninhibited surfaces. The effect of temperature over time during immersion has a significant influence on the corrosion inhibition effectiveness of plant-based green inhibitors in comparison to conventional inhibitors. As the temperature fluctuates, the corrosion rate goes up because of the increased randomness in molecules movement around the metallic surface, which could make the inhibitor layer less stable. Because they effectively stick to metal surfaces, green inhibitors that contain bioactive chemicals with functional groups like –OH, –COOH, and $–NH_2$ can withstand higher temperatures. Conventional inhibitors, which often use synthetic chemicals, may not work as well at higher temperatures because they break down faster. Research has demonstrated that organic inhibitors sustain a consistent adsorption mechanism during prolonged immersion across many temperatures, indicating their exceptional resilience and environmental compatibility. The ability to withstand temperature-induced deterioration illustrates the potential of green inhibitors for long-term industrial applications. Additional comparative research emphasises the necessity of exploring sustainable

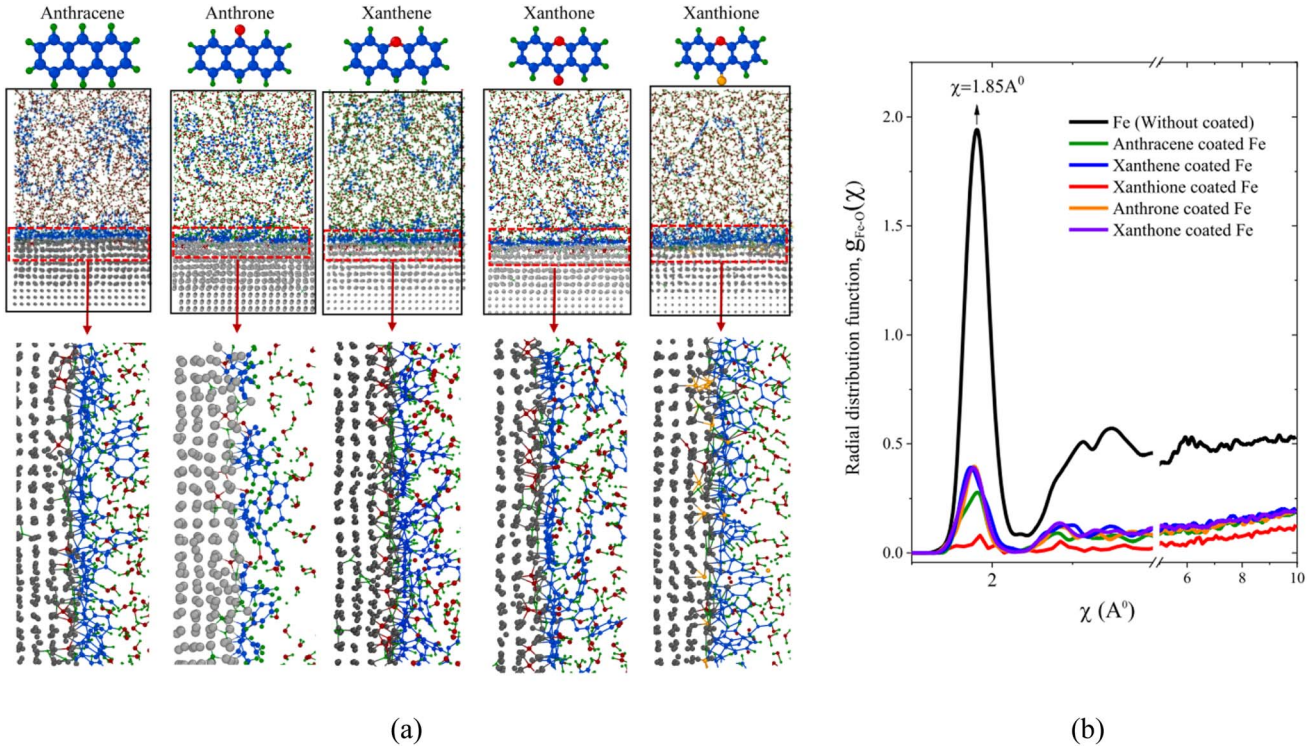

Fig. 28 (a) Snapshots of water interaction with the corrosion inhibitor-coated iron during reactive molecular dynamics simulation. The zoomed-in views show inhibitor layer at the iron–water interface. (b) The graph of the radial distribution function, $g_{Fe-O}(\chi)$, between the oxygen atom of water molecules and the coated iron surface. Blue, red, green, yellow and gray color atom depicts carbon, oxygen, hydrogen, sulfur and iron atoms, reproduced from ref. 74 with permission from [Elsevier] [*Surfaces and Interfaces*, 2025, **74**, 107647] copyright 2025.

alternatives to enhance efficiency and environmental compatibility.

Interaction of inhibitor molecules with metallic surface: theoretical approaches

Mechanistic pathway. CIs protect metal surfaces against rusting *via* a variety of ways. The creation of a coating that adheres to the metal surface is one method. In order to keep corrosive species from getting into touch with the metal, this coating serves as a barrier. The production of corrosion products that serve as passivators and provide a shield of protection on the metal surface is another method. Additionally, CIs can produce precipitates which assist in the removal or inactivation of aggressive components that exist in corrosive environments. These inhibitors work by removing water or other corrosive species from the metal surface by physical or chemical adsorption phenomenon, and makes it easier to form a barrier coating. Because they include organic molecules with polar functional groups and heteroatoms like nitrogen (N), oxygen (O), sulphur (S), and chlorine (Cl) are recognized as strong inhibitors.[15,71] By acting as a shield, these functional groups keep aqueous corrosive substances away from the metal surface. In addition, surfactants, which include polar hydrophilic and nonpolar hydrophobic groups are frequently used as CIs. By adhering to the metal surface, the hydrophilic group further shields it from corrosive substances.[72] In general, CIs function by creating barrier coatings, generating corrosion products that are passivated, and repelling corrosive species from the metal surface. These inhibitors are more effective in preventing corrosion as they contain heteroatoms and surfactants. A proposed mechanistic pathway of OCIs through different kinds of adsorption and interactions are demonstrated as Fig. 27.

A recent work[73] has clearly demonstrated the interaction of water molecules with the iron surface is significantly blocked in the presence of a protective layer formed by various organic compounds namely: anthracene (ANC), anthrone (AEN), xanthene (XEN), xanthone (XAN), and xanthione (XION) as inhibitors. In first step, water molecules gradually adsorb onto the coated iron surface as depicted by the reactive molecular dynamic simulations. With the progression of simulation, water molecules entered into the weakly adsorbed inhibitor coating, leading to desorption of loosely bound molecules into the water. However, inhibitor molecules strongly chemisorbed remained intact, continuing to provide long-standing protection. Fig. 28a shows the stable and atomically thin inhibitor film persists on the surface, effectively reducing water-induced corrosion. The above observation is supported by radial density distribution function, $g(\chi)$, for iron (with and without coated) and oxygen of water molecule $g_{Fe-O}(\chi)$ as quantitatively given in Fig. 28b. It is found that the height of first peak of $g_{Fe-O}(\chi)$ found maximum for Fe (without coated) at $\chi = 1.85$ Å and minimum for Fe coated with XION at $\chi = 1.92$ Å, which is specifying that oxygen atom able to interact with Fe (without

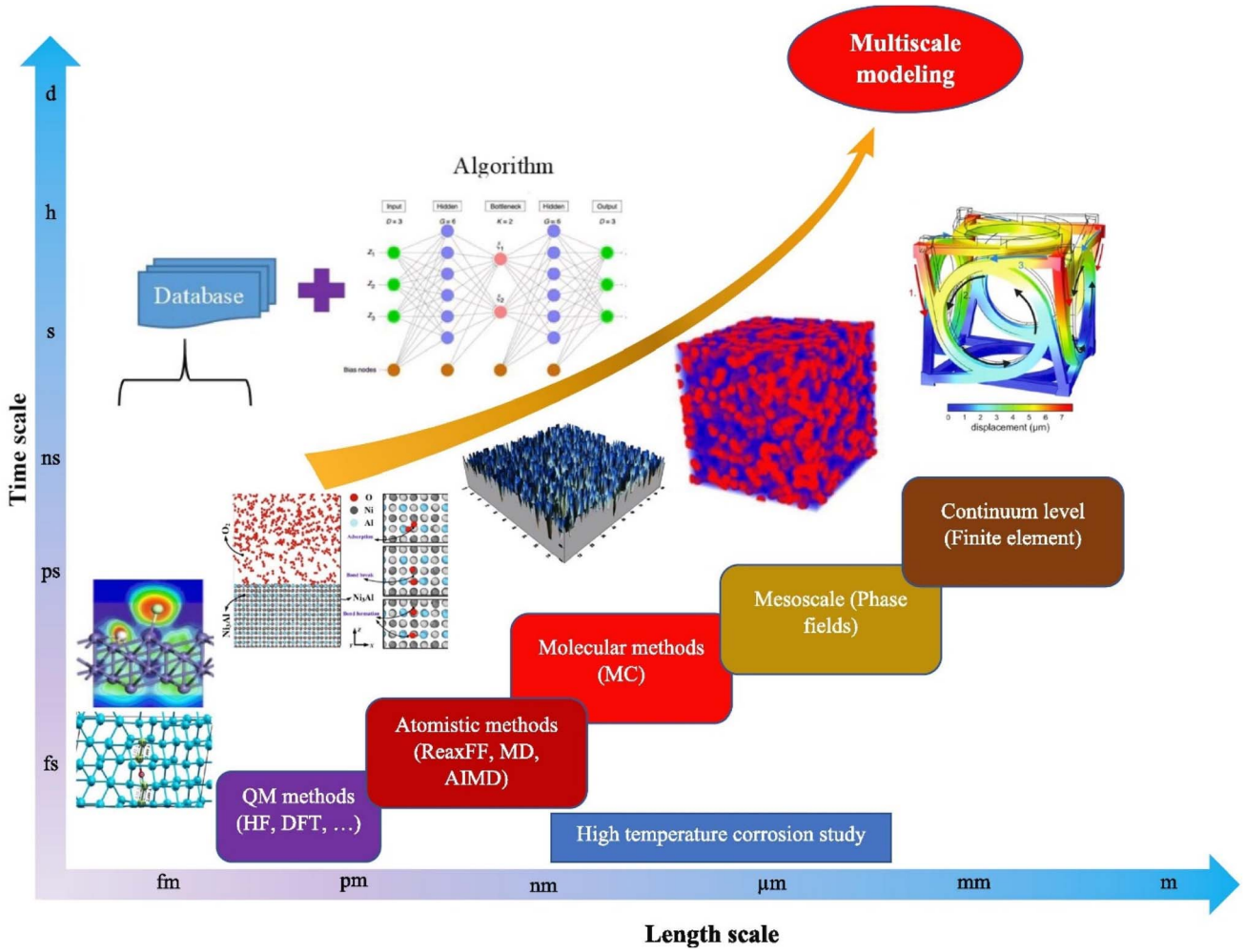

Fig. 29 Multi-scale simulation strategies for corrosion-related investigation. The *x*- and *y*-axis of flowchart shows the length and time scale respectively, reproduced from ref. 76 with permission from [Elsevier] [*Prog. Mater. Sci.*, 2025, **148**, 101359] copyright 2025.

coated) freely and forming various kinds of iron oxide compounds. From these simulation results, we can conclude that the XION corrosion inhibitor molecule successfully restricts and prevent the oxygen (associated with water) to interact with iron surface.[74]

Theoretical background: molecular modelling. CIs typically contain elements with free electrons (lone pairs) namely – oxygen (O), nitrogen (N), phosphorus (P), and sulphur (S) – along with π-electron-rich aromatic rings and active functional groups like oxygen containing free lone pairs in carboxylic acids (–COOH), nitrogen having lone pairs in amines ($–NH_2$), active lone pairs of oxygen in alcohols (–OH), amino acids and phenols. All these functional groups consist of electron-rich atoms that can readily adsorb onto metal surfaces. It is able to form of coordinate covalent bonds between the lone pair (free electron pair) or π-electrons of the inhibitor and the unoccupied vacant d-orbitals of the metal surface. During the inhibition process, the inhibitor molecules travel from the bulk solution toward the metal surface, interact with the electric double layer (EDL), and dislocate pre-adsorbed water molecules and other solutes.[75] This results in the adsorption of the inhibitor and makes charge redistribution both at the metal interface and the inhibitor molecule. To fully understand these complex multi-step processes, multi-scale atomistic and artificial intelligence-based calculations are pretty vital. Such modelling and data-driven approaches not only deepen our mechanistic insight into each stage – adsorption, interaction with EDL, and charge migration but also play a crucial role in the discovery of new, more effective CIs.[76]

Numerous computational techniques depending on length and time scale, were established to evaluate the protective efficiency of CIs (as illustrated in Fig. 29). The quantum level examines the electronic interaction of the chemical corrosive compounds with the metallic substrate during the adsorption and desorption processes. The atomic level simulation provides information about the bond dissociation and formation, diffusion, or movement of atoms/molecules during the corrosion process. Kinetic Monte Carlo simulations study the microscale corrosion processes. The mesoscale evaluates the microstructural evolution during the corrosion process. The macro-scale, such as FEM, examines the component mechanical properties and surface degradation of materials after

corrosion. These multi-scale computational approaches consistently indicate that OCIs exert their protective effects primarily through adsorption onto the metal surface at the metal–electrolyte interface.

Molecular modelling, such as DFT and RMD simulations, has emerged as a very efficient tool to carry out mathematical modelling and simulation for the selection of corrosion inhibitor molecule and their inhibition mechanism.[77,78] These realistic models demonstrated six key features:

(a) Electronic properties of isolated CIs,

(b) Interaction of the CI with the surface of the substrate,

(c) Adsorption model,

(d) The effect of both anodic and cathodic zones on the surface,

(e) Type of solvents,

(f) Electrodes potential effects.

Concerning about feature (a), polarizability, lone-pair electrons, dipolar moment, HOMO–LUMO energy *etc.*, may influence the binding ability of the CI to the surface. Feature (b) will provide information about the robustness of the interaction between inhibitor and surface. Feature (c) is also significant for the manipulation of surface–inhibitor interactions and its wettability. Feature (d) can play a vital role in modelling of CIs since the different polarity affect the inhibitor–surface interaction. Feature (e) will study how the inhibitor dislocates the solvent molecules from the metallic surface to be adsorbed on it. Feature (f) allows for system polarization: metallic interface, inhibitor, and the solvent.

Electronic properties of isolated inhibitors

Frontier molecular orbitals. The energy of FMO (energy of highest occupied molecular orbital, HOMO *i.e.* E_{HOMO}) and (energy of lowest unoccupied molecular orbital, LUMO *i.e.* E_{LUMO}) of a CIs are very essential for the defining its reactivity with metallic surface. A noble correlation found between the efficiency of corrosion inhibition and energy of FMOs, which is frequently associated with the atomic charge migration ability of the molecule. Hence, higher value of E_{HOMO} is likely to show an affinity of the inhibitor molecule to donate electrons to the

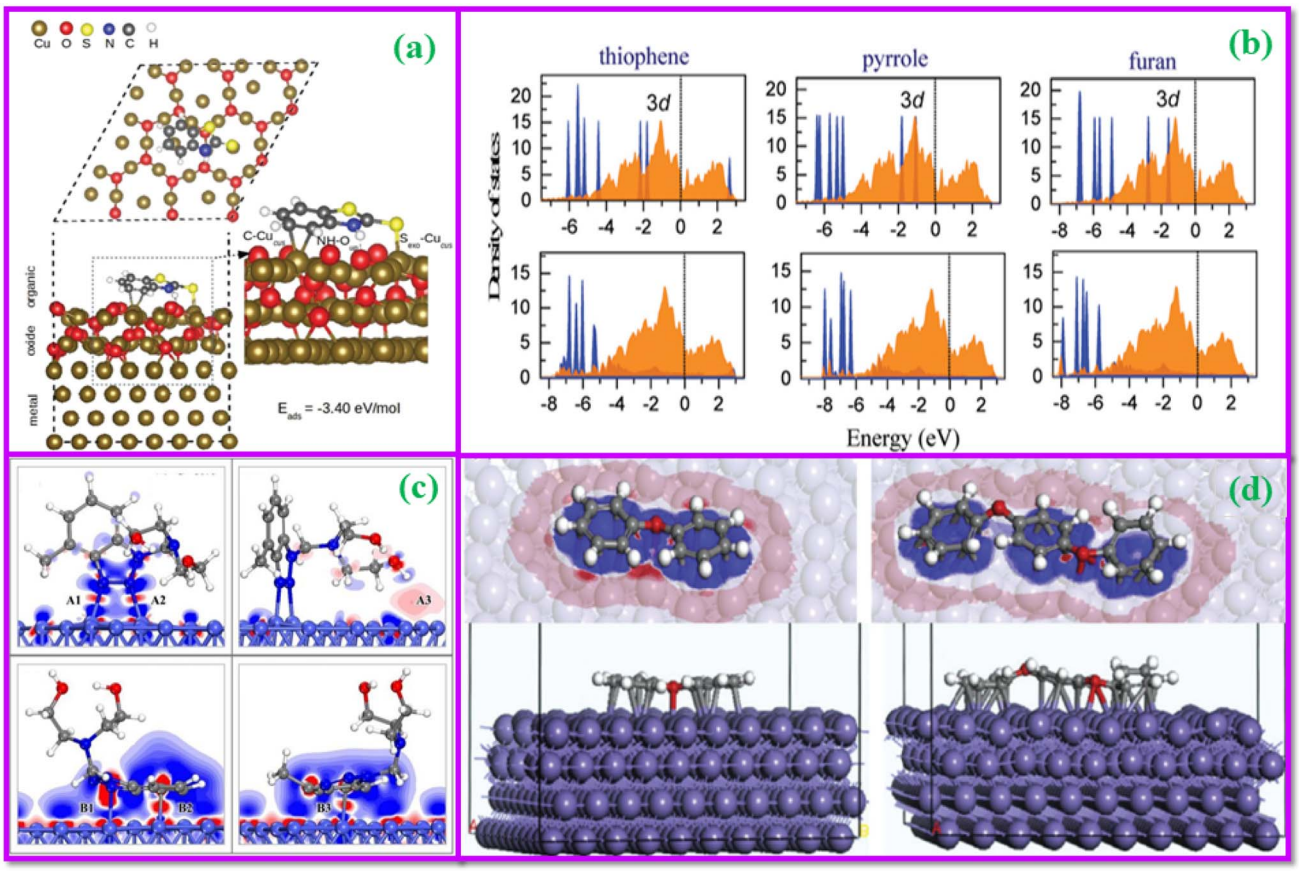

Fig. 30 Notable atomistic simulation work related to adsorption of corrosion inhibitor over the metallic surface: (a) snapshot and adsorption energy of the most stable configuration of 2-mercaptobenzothiazole on Cu and Cu_2O surface, reproduced from ref. 84 with permission from [IOP Science] [*J. Electrochem. Soc.*, 2020, **167**, 161506] copyright 2025, (b) densities of states of three inhibitors before (upper panel) and after (lower panel) the adsorption on Fe(110) surfaces, reproduced from ref. 85 with permission from [Elsevier] [*Appl. Surf. Sci.*, 2017, **406**, 301–306] copyright 2017, (c) two-dimensional cross-section of the charge density differences at critical bonding locations for Co adsorption systems, reproduced from ref. 86 with permission from [Elsevier] [*Colloids Surfaces A Physicochem. Eng. Asp.*, 2020, **605**, 125392] copyright 2020 and (d) equilibrium adsorption configurations and the corresponding charge density differences for 1-phenoxybenzene and 1,4-diphenoxybenzene moieties on the Fe(110) plane, reproduced from ref. 87 with permission from [Elsevier] [*Corros. Sci.*, 2019, **146**, 134–151] copyright 2019.

acceptor of lower empty molecular orbital energy. High values of E_{HOMO} facilitates adsorption and accordingly improves the inhibition efficiency whereas lower values of $E_{LUMO,}$ indicates the ability of the molecule to accept electrons. Further, the value of the energy gap ($\Delta E = E_{LUMO} - E_{HOMO}$) also helps us to quantify the reactivity of CIs. Low values of the ΔE (energy gap) will provide good inhibition efficiency, as the energy to remove an electron from the last occupied orbital for donation to the unoccupied d orbitals of the metallic substrates will be low. However, conventional DFT methods are known to provide unreliable absolute HOMO–LUMO energies due to self-interaction errors and incorrect long-range exchange behavior. The appropriate approach is to employ range-separated hybrid functionals, where the range–separation parameter is tuned to satisfy the DFT–Koopmans' theorem.[79–81] According to this principle, the negative of the HOMO energy should equal the vertical ionization potential, and the negative of the LUMO energy should approximate the electron affinity of the molecule. Tuning the functional to enforce this condition significantly improves the accuracy of calculated orbital energies and band gaps. In addition, other functional approaches, such as the widely used B3LYP method–Becke's three-parameter hybrid exchange functional (B3) combined with the Lee–Yang–Parr (LYP) correlation functional-are also frequently applied for HOMO–LUMO energy estimation. This hybrid functional, which mixes exact Hartree–Fock (HF) exchange with DFT exchange-correlation terms, provides an optimal compromise between computational cost and accuracy for organic and organometallic systems.[82,83]

Global hardness and softness. Hardness can be calculated in respect of the energies of HOMO and LUMO orbitals as:

$$\eta = \frac{E_{LUMO} - E_{HOMO}}{2}$$

The relationship between the hardness parameter and the energy gap is established numerically. It is reported that the CI molecules with a larger energy gap (*i.e.*, higher hardness) are less chemically reactive, while those with a smaller gap (*i.e.*, lower hardness) exhibit higher reactivity. Consequently, softer molecules are generally more effective as CIs, due to their greater tendency to interact with the metal surface. Hard molecules attain a high HOMO–LUMO gap, whereas soft molecules have a small energy gap, and thus soft base chemical species-based inhibitors are the most effective for corrosion inhibition of metallic substrates.

Mulliken population analysis. The Mulliken population analysis is a widely employed method to identify the active adsorption centers of corrosion inhibitor molecules. It is generally accepted that heteroatoms bearing a more negative Mulliken charge possess a higher tendency to adsorb onto metal surfaces *via* donor–acceptor interactions, where lone pair electrons from the heteroatoms are donated to the vacant d-orbitals of the metal. Using density functional theory (DFT), Obot *et al.*[83] performed Mulliken population analysis on xanthone in both its neutral and protonated forms to evaluate the origin of its inhibitive performance on mild steel in an acidic medium. Their study aimed to determine whether the

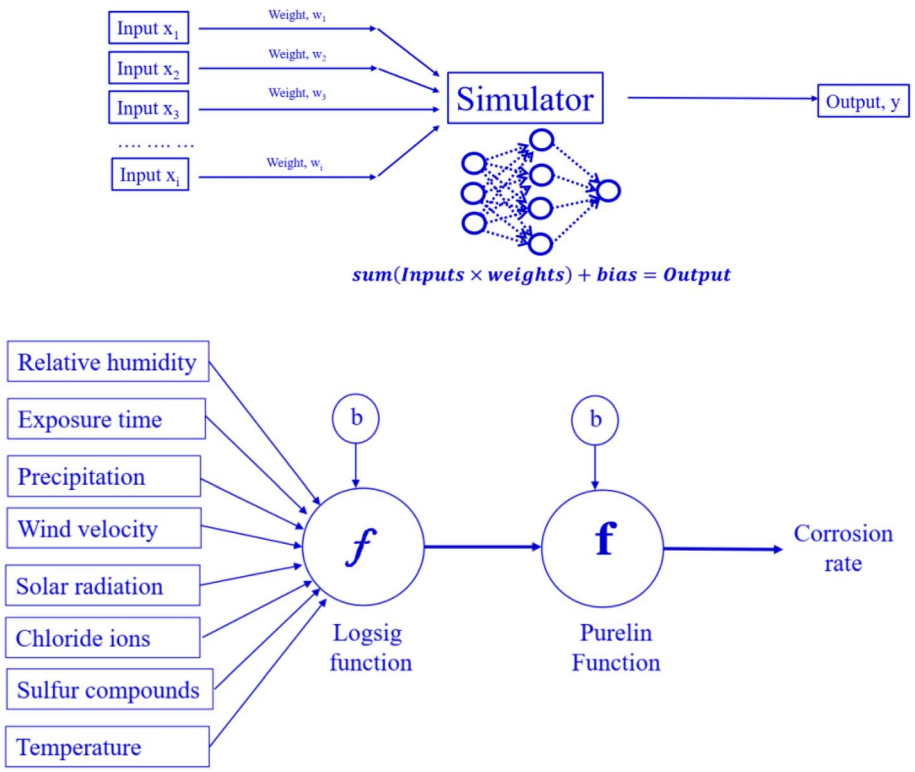

Fig. 31 Artificial Neural Network (ANN) model with linear and sigmoidal functions to predict environmental parameters.

neutral or protonated form of xanthone predominantly contributes to its corrosion inhibition efficiency.

In recent years, first-principles calculations based on quantum mechanical principles used to describe the behaviour of electrons, atoms, ions, and molecules have proven to be effective tools in studying corrosion inhibition mechanisms. Several notable applications have emerged from this approach. For instance, Chiter and colleagues[84] conducted density functional theory (DFT) simulations to explore how 2-mercaptobenzothiazole (MBTH, in its thione form) interacts with Cu surfaces coated by Cu_2O oxide layers. As illustrated in Fig. 30a, their results revealed that MBTH adsorbs nearly flat on the surface with a slight tilt. The calculated adsorption energy was approximately 3.40 eV mol^{-1}. The sulphur atom of MBTH forms a bond with a copper atom at a distance of about 2.17 Å, and two carbon atoms from the cyclic aromatic ring contribute to the surface interaction. Their findings suggest that MBTH can effectively replace surface-bound water and hydroxyl groups, thereby forming a stable protective film over the oxidized copper surface in aqueous conditions.

Guo and co-workers[85] conducted a thorough research on the adsorption characteristics of three common heterocyclic compounds: N-containing pyrrole, O-based furan, and S-containing thiophenone, on Fe(110) surfaces. As shown in Fig. 30b, adsorption of these molecules onto the iron surface leads to a slight broadening of their molecular density of states (DOS) peaks, which is attributed to orbital hybridization between the inhibitor and the metal substrate. This interaction also results in a shift of the DOS profiles for both the inhibitors and the iron surface toward lower energy levels. Their findings support an established empirical trend in efficiency of corrosion inhibition related to heteroatoms, indicating the order of effectiveness as O < N < S. Zang *et al.*86 explored the performance of corrosion inhibition of TT-LYK molecules in the context of chemical–mechanical polishing (CMP) of cobalt barrier by employing the CASTEP module within the Materials Studio software. Their simulation results demonstrated that TT-LYK can adsorb onto the cobalt surface in two distinct configurations: vertically, involving coordination through the N9 and N10 atoms and the formation of O17–H···Co hydrogen bonds; and parallelly, where both the benzene and triazole rings lie flat against the surface. As depicted in Fig. 30c, the charge density difference maps reveal significant electronic redistribution at the interface regions of charge depletion are shown in blue, while areas of charge accumulation appear in red confirming strong interaction between the inhibitor and the cobalt surface. To reduce computational cost, Murmu *et al.*[87] employed Density Functional Tight Binding (DFTB) simulations to study the adsorption behavior of two specific inhibitor segments on the Fe(110) surface. As illustrated in Fig. 30d, the charge density difference maps highlight regions of electron accumulation and depletion, suggesting a stronger donor–acceptor interaction for 1,4-diphenoxybenzene compared to 1-phenoxybenzene. These computational insights align well with the experimental observations, supporting the higher inhibition efficiency of the former molecule.

Prediction of corrosion rate using artificial neural networks (ANNs)

ANNs are computational models stimulated by the functioning of the human brain, containing of interconnected processing units called neurons. Each ANN is defined by three vital elements: behavior of individual nodes, network architecture, and learning algorithm. The behavior of a node is determined by factors such as the number of inward and outward signals, the weights allocated to these connections, and the activation function used to process the weighted inputs. The architecture defines how the nodes are arranged and linked together, while the learning rule defines how connection weights are adjusted during training. A simplified representation of a neural network, shown in Fig. 31, shows how each artificial neuron obtains multiple input signals modified by a weight, which can be either positive or negative. These inputs are shared and passed through an activation function to yield the neuron's output. The activation function, often a sigmoid function due to

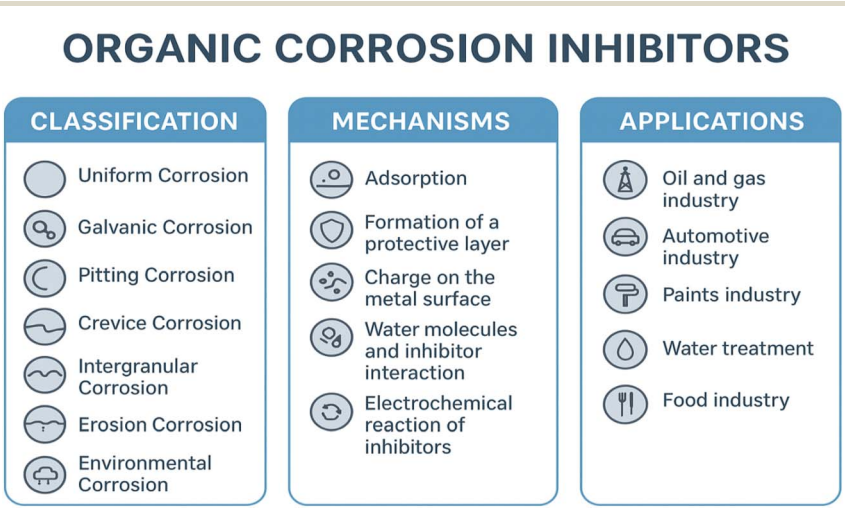

Fig. 32 Overall summary of the classification, mechanism and applications of organic corrosion inhibitors.

its bounded, smooth, and differentiable nature, determines the final output.

Typically, ANNs are organized into three main layers: (a) the input layer, (b) one or more hidden layers, and (c) the output layer. A most commonly used model is the multilayer perceptron (MLP), which is a feed-forward network that uses backpropagation for learning, as depicted in Fig. 31. Input data are usually scaled to a range of 0 to 1 to ensure efficient learning and to avoid overwhelming the hidden neurons. In supervised learning, the network adjusts the weights based on the variance of predicted and actual outputs by propagating the error backwards through the network, refining the weights iteratively to minimize the error. Since the early 1990s, ANNs have been widely applied to predict corrosion inhibition performance. For example, Rosen and Silverman[88] combined ANNs with expert systems to predict various types of corrosion based on Tafel curve parameters. Their model used input features such as passivation potential, passive current density, pitting potential *etc.* to assess the likelihood of general, crevice, and pitting corrosion. In another study, a quantitative structure–activity relationship (QSAR) model was developed to assess the inhibition efficiency of 17 α-amino acids against copper corrosion in acidic medias.[89] Molecular descriptors derived from DFT and MC simulations including global hardness (ω), LUMO energy (ELUMO), electron-donating capacity (DN), and total negative charge (TNC) were used as inputs for both multiple linear regression (MLR) and ANN models. The ANN model outperformed MLR in predictive accuracy and was further used to design and evaluate 10 new molecular derivatives. Additionally, the corrosion inhibition performance of 31 aromatic hydrazide and Schiff base molecules was modelled using ANNs. Input variables included a range of quantum chemical parameters such as EHOMO, ELUMO, total energy (TE), dipole moment (μ), molar volume (MV), and partition coefficient (P). The ANN used was a feed-forward backpropagation model implemented in MATLAB (version 7), which achieved a great correlation coefficient ($R = 0.968$), indicating excellent predictive performance compared to traditional methods. Given the inherently complex and nonlinear nature of corrosion processes, conventional analytical methods often fall short in capturing the full spectrum of variables involved. ANN models, with their powerful learning and generalization capabilities, have emerged as effective tools for modelling, predicting, and understanding corrosion behaviour across diverse materials and environmental conditions.

In summary, Fig. 32 provides an overview of the classification, mechanisms, and applications of OCIs. The type of corrosion is classify based on its inherent nature and properties. The mechanism involves adsorption, protective layer formation, charge on the metal–surface, interaction between water molecule and inhibitor, different types of electrochemical reactions of inhibitor. These are the possible mechanistic pathways to inhibit any metallic substrate. These inhibitors are extensively used in automobile sectors, oil and gas industries, food industries, water treatments, paint industries and many more.

Corrosion inhibitors and environmental regulations

Effect of conventional inhibitors on the environment. Although, imidazolines and quaternary amines are most common industrially active and effective OCIs but they may be hazardous to the environment if they are poisonous or bioaccumulative. Marine ecosystems may be harmed by their release into the environment, especially in offshore activities. Phosphonates are helpful in reducing scale and corrosion, but they may also lead to nutrient pollution in water bodies, which can cause problems like eutrophication.

Regulatory structures. Operators are required by rules to utilise chemicals with minimal toxicity and high biodegradability in areas such as the North Sea. The Oslo-Paris (OSPAR) Commission and other regulatory agencies must evaluate and authorise the substances used. REACH laws in the European Union mandate thorough reporting and assessment of chemicals, including CIs, to make sure they do not present intolerable dangers to human health and the environment.

Change to environmentally friendly inhibitors. Usage of green CIs made from organic or biodegradable materials is becoming more and more popular. These "green" inhibitors preserve performance standards while having a smaller negative impact on the environment. Through regulatory incentives, more stringent compliance standards, and sanctions for noncompliance, governments and regulatory organisations promote the use of environmentally friendly inhibitors.

Relative cost of corrosion inhibitors

The global CIs market size was projected 8.82 million USD in 2024 and is predicted to increase from 9.19 million USD in 2025 to approximately 13.34 million USD by 2034.[1,2] The economic cost of corrosion may be assessed directly from the operation, application and maintenance of corrosion resistant technologies such as protective coatings, corrosion-resistant materials, corrosion inhibitors, cathodic/anodic protection and corrosion inspection including monitoring tools; or indirectly from the loss of productivity, compensation for casualties and environmental pollution, and any other cost that is not directly incurred within that industry. The cost analysis of any process is a prominent parameter before its implementation towards society. There are two important points in a cost analysis (1) it should be a short term expenses and (2) long term savings. In terms of short-term expenses, although the initial cost of using traditional inhibitors may be lower, there may be unanticipated expenses related to environmental harm, regulatory compliance, and potential liabilities. The consideration of long-term savings by lessening environmental impact, enhancing worker safety, and adhering to increasingly stringent environmental requirements, organic inhibitors – while perhaps costlier initially – can save money overall. Additionally, the reputation of an industry might be improved and the chance of regulatory fines decreased.

Conclusions and prospects

In conclusion, a viable approach to addressing the problems initiated by corrosion is the development and installation of green CIs for industrial applications. Traditional CIs may be ineffective in a variety of corrosive circumstances and sometimes affect both the environment and the health of human beings. Green inhibitors provide an eco-friendly and sustainable alternative, such as biopolymers made from renewable resources, plant extracts, and chemical medicines from natural source and exhibit a number of desired qualities, such as affordability, little environmental harm, and compatibility with sustainable practices. Biopolymers like chitosan and cellulose, which may create protective barriers at the metal-environment interface, have demonstrated significant corrosion prevention effectiveness. With their electron-rich centres and high solubility, plant extracts are an attractive alternative, and the complex molecular structures of chemical medicines produced from natural sources provide these products with remarkable anti-corrosion properties. Industries can efficiently prevent corrosion in metals and alloys while minimising their environmental impact by considering these factors and using the appropriate green inhibitors. The development of more effective and long-lasting CIs might result from more research and development in this area, which would enhance industrial operations overall and save priceless assets.

The next generation organic biodegradable corrosion inhibitors are the prime necessity. As academics, industries, research and development continue to investigate and expand the development of OCIs, the future of these materials is quite promising. Metal assets and structures are protected by OCIs, whose future application are influenced by a number of events and trends include sustainable solutions, customizations, new delivery methods, advances testing with modelling and next generation applications as per the specific requirement of the industry:

- *Green and sustainable solution*: due to environmental concerns, there is a significant shift in focus toward eco-friendly, sustainable inhibitors. Under the basic principles of green chemistry, more products are produced from bio-based, renewable resources that are less harmful and have a lesser environmental impact.
- *Industry-specific solutions*: future development will be highly tailored because it has been established an approach, which fits all industries, is ineffective. We will see inhibitors designed especially to address the particular difficulties faced by sectors including oil and gas, maritime engineering, and aerospace.
- *The potential of nanotechnology*: the performance and efficiency of inhibitors will be enhanced by nanotechnology. Stronger, more durable corrosion protection can be obtained by combining nanoparticles and nanocomposites, as well as by developing hybrid materials that combine organic inhibitors with materials like polymers.
- *Intelligent, self-healing solutions*: in future, whole world will look for inhibitors that have the ability to respond to its environment and even heal itself. These "smart" inhibitors, which will be possible by advances in materials science, would significantly increase the lifespan of metal structures by automatically adapting to corrosive conditions and repairing any damage to their protective layer.[90]
- *Smarter delivery systems*: the usage guidelines and procedure for any inhibitor matters just as much as its make-up. The inhibitor will be released gradually and under control, recognitions to new delivery techniques including encapsulation and nanocarriers. This translates to less frequent reapplication and more extended protection.
- *Improved prediction through modelling & AI*: gaining a better grasp of the molecular mechanisms underlying inhibitors through sophisticated computer modelling and simulations. This will expedite development and increase accuracy by enabling researchers to forecast an inhibitor's activity in particular conditions.

To put it briefly, the future seems promising. The next generation of OCIs will better safeguard our essential metal infrastructure by embracing sustainability, personalization, and state-of-the-art technology, guaranteeing a more robust and sustainable future for present and upcoming generations.

Conflicts of interest

There are no conflicts to declare.

Data availability

No primary research results, software or code have been included and no new data were generated or analysed as part of this review.

Appendices

Appendix A

Table 1 Year wise description of different type of organic CIs reported in literature

Plant or source	Metal	Corrosive environment	Corr. inhibition efficiency/%	Inhibitor conc.	Year	Ref
Henna leaves	MS	1.0 M HCl	90.34 @ 25 °C	1.2 g L^{-1}	2000	91
Olive dry leaves	CS	2.0 M HCl	93 @ 25 °C	0.9 g L^{-1}	2007	92
Streptomycin	MS	1.0 M HCl	88.5 @ 35 °C	0.5 g L^{-1}	2009	93
Aspidosperma album bark	C38 steel	1.0 M HCl	90 @ 25 °C	0.1 g L^{-1}	2011	94

Table 1 (*Contd.*)

Plant or source	Metal	Corrosive environment	Corr. inhibition efficiency/%	Inhibitor conc.	Year	Ref
Palicoureaguianensis leaves	C38 steel	1.0 M HCl	89 @ 25 °C	0.1 g L^{-1}	2011	95
Schinopsislorentzii tree powder	Low CS	1.0 M HCl	66	0.2 g L^{-1}	2012	96
Piper guineense seeds	MS	0.5 M H_2SO_4	97.7	0.9 g L^{-1}	2012	97
Propolis	CS	NaCl (10 ppm) & $Al_2(SO_4)_3$ (35 ppm)	92.7 @ 30 °C	0.6 g L^{-1}	2013	98
Neolamarckiacadamba bark	MS	1.0 M HCl	91 @ 30 °C	0.005 g L^{-1}	2013	99
11% w/v extract of *ethanolicpropolis*	MS	3.5% NaCl	–N.A.–	13 gm	2014	100
Citrus peel	Al	0.5 to 2.0 M HCl	91 @ 10 °C	8.0 g L^{-1}	2015	101
Pectin from apples	X60 steel	0.5 M HCl	78.7 @ 25 °C	1.0 g L^{-1}	2015	102
Ascorbic acid	MS	H_2SO_4 @ pH 4	71.5 @ 20 °C	10 mol L^{-1}	2015	103
Retamamonosperma (L.) Boiss. Seeds	CS	1.0 M HCl	94.42 @ 30 °C	0.4 g L^{-1}	2015	104
Watermelon seeds	MS	1.0 M HCl	86.08	2.0 g L^{-1}	2015	105
Cryptostegia grandiflora leaves	MS	1.0 M H_2SO_4	83.54 @ 30 °C	0.5 g L^{-1}	2016	106
Citrus peel	MS	1.0 M HCl	94.2 @ 45 °C	2.0 g L^{-1}	2016	107
Pectin from tomato	X60 steel	0.5 M HCl	75.4 @ 25 °C	0.5 g L^{-1} pectin & 5 mM CeO_2	2016	108
Salvia hispanica seeds	Bronze	Simul. soln. of acid rain	95	0.4 g L^{-1}	2017	109
Grains of *Peganumharmala*	Al alloy	1.0 M HCl	91.78 @ 25 °C	0.025 g L^{-1}	2017	110
Bark of *Rhizophoraapiculata*	MS	1.0 M HCl	57.9	0.1 g L^{-1}	2017	111
Scenedemusalge	MS	1.0 M HCl	95.1	0.035 g L^{-1}	2018	112
Solid waste: Banana leaves Sugarcane Watermelon	MS	1.0 M HCl	69.60, 68.41 and 58.15 @ 25 °C	10% v/v	2018	113
Shrimps shell waste	CS	1.0 M HCl	88.50 @ 25 °C	10 M	2018	114
Cladodes of *Opuntia Ficus indica*	Steel	1.0 M HCl	94 @ 35 °C	1.0 g L^{-1}	2020	115
Tomato peel waste	Sn	2% NaCl + 1% acetic acid + 0.5% citric acid	72.98 @ 25 °C	4.0 g L^{-1}	2020	116
Piper guineense seeds	MS	1.0 M HCl	88.4	1.0 g L^{-1}	2021	117
Opuntia Dillenii seed oil	Iron	Acid rain	98.37 ± 0.08	1.0 g L^{-1}	2021	118
Thevetia peruviana flower	MS	1.0 M HCl	91.2	0.2 g L^{-1}	2021	119
Paederia Foetida leaves	MS	1.0 M HCl	73.77	—	2021	120
Rhoeo discolor leaves	MS	0.5 M HCl	87.72 @ 35 °C	2.0 g L^{-1}	2022	121
Ocimum basilicum seed	MS	1.0 M HCl	95.12	1.0 g L^{-1}	2022	122
Azadirachta indica leaves	MS	5.0 M HCl	89.25	4.0 g L^{-1}	2022	123
Turnip peel extract	Copper	3.5 wt% NaCl	92 @ 25 °C	20% v/v	2022	124
Dysphania ambrosioides	MS	1.0 M HCl	81.69 @ 30 °C	1.5 g L^{-1}	2022	125
Artemisia argyi leaves	CS	1.0 M HCl	97.1 @ 25 °C	0.5 g L^{-1}	2022	126
Jatropha curcas	MS	3.5% NaCl	90.26	4.0 g L^{-1}	2022	127
Hibiscus sabdariffa (Roselle)			81.32	1.48 g L^{-1}		
Colocasia esculenta	(SS)-410	0.5 M H_2SO_4	93	0.5 g L^{-1}	2023	128
Verbena officinalis	CS	0.5 M H_2SO_4	91.1	1.0 g L^{-1}	2024	129
Citrullus colocynthis	CS	1.0 M HCl	91.8 @ 30 °C	0.5 g L^{-1}	2024	130
Mahonia nepalensis	MS	1.0 M H_2SO_4	87.86	0.005 g L^{-1}	2024	131
Photinia leaves	CS	1.0 M HCl	97.82	1.0 g L^{-1}	2025	132
Aleppo pine fibers	MS	1.0 M HCl	84.3	1.0 g L^{-1}	2025	133

Appendix B

Table 2 Year wise list of already reported CIs with source and protective metals

Inhibitor source	Metal	Year	Ref
Natural honey	Cu	2000	134
Aqueous extract of *Rosmarinus officinalis*	Al–Mg alloy	2000	135
Opuntia extract	Al	2003	136
Extract of khillah (*Ammivisnaga*) seeds	SX 316 steel	2006	137
Prosopis—cineraria (khejari)	Al	2006	138
Carica papaya leaves extract	Mild steel	2007	139
Hibiscus sabdariffa (Calyx extract)	Steel	2008	140
Musa sapientumpeels (banana peels)	Mild steel	2008	141
Saccharides—mannose and fructose	Al and Zn	2008	142
Citric acid	Al	2008	143
Lawsonia extract (henna)	C-steel, Ni, Zn	2009	144
Neem leaves extract (*Azadirachtaindica*)	Mild steel	2010	145
Mango/orange peels	Steel	2010	146
Vanillin	Al	2010	147
Emblica officinalis	Steel	2010	148
Gum exudates	Mild steel	2012	149
Vernonia amygdalina (bitter leaf)	Al	2012	150
Garcinia kola seed	Mild steel	2013	73
Aloe leaves	Steel	2013	151
Rosemary	Steel	2014	152
Terminalia bellerica	Steel	2014	153
Tobacco plant extract and its parts	Al, steel	2014	154
Pomegranate juice and peels	Steel	2015	155
Amino acids & aspartic acid	Al	2016	156
Tamarind	Steel	2018	157
Tea leaves	Steel	2018	158
Rutin and quercetin	Al	2018	159
Eucalyptus oil	Steel	2019	160
Saponin	Al	2019	161
Acacia concianna	Al	2020	162
Benzoic acid	Fe, Al	2020	163
$CeCl_3$ and mercaptobenzothiazole (MBT)	Al	2020	164
Tannin beetroot	Al	2022	165
Acacia catechu	Mild steel	2022	166
Artabotrys odoratissimus	Mild steel	2022	167
Pichia sp. biofilm	Mild steel	2022	168
Camellia chrysantha flower	Steel	2023	169
Datura stramonium plant	Mild steel	2023	170
Feverfew root	Carbon steel	2023	171
Walnut husk	Carbon steel	2024	172
Chlorella vulgaris	Steel	2024	173
Artemisia argyi	Steel	2025	174
Chrysanthemum indicum			
Centipeda minima			
Corynocarpus laevigatus	Mild steel	2025	175
Helianthus tuberosus L.	Al	2025	176
Poria cocos			
Peganum harmala	Iron	2025	177
Potentilla erecta	Carbon steel	2025	178
Vicia faba	Mild steel	2025	179

Appendix C

Table 3 Significance of data derived from various experiments

Technique	Outcomes	Significance	Reference
Conventional immersion exposures	• If corrosion rate decreases with the increase in inhibitor concentration	• Excellent adsorption along with high surface coverage	46, 62 and 180
	• Inhibition efficacy decreases with the increase in temperature	• Increased desorption rate and possibility of inhibitor film disintegration higher temperatures	
	• Inhibition efficiency increases with addition of multiple compounds	• Synergism	
Electrochemical impedance spectroscopy	• Increase in polarization resistance	• Formation of a protective layer thereby reduced charge transfer at metal–electrolyte interface	181–186
	• Decrease in double layer capacitance	• Reduced dielectric constant due to increased thickness of the electric double layer	
	• Nyquist plots semicircle diameter increases with increase in inhibitor concentration	• Decrease in corrosion rate	
	• Phase angle in the bode plot for inhibited samples greater than uninhibited samples	• Formation of inhibitor's film (protective) on metal surface	
Potentiodynamic polarization	• Deviation in E_{corr} values	• Change in E_{corr} compare to uninhibited surface	180 and 182
	• A decrease in the i_{corr}	>85mv; anodic or cathodic inhibitor. <85mv; mixed type inhibitor	
	• Alteration in the cathodic and anodic Tafel slope towards lower values due to inhibitor addition	• Excellent protection & formation of a protective film • Mixed type inhibitor; retarding both cathodic and anodic reactions	

Appendix D

Table 4 Various models for explaining the adsorption isotherms

Isotherms	Equation	Plot	Reference
Freundlich	$\log\theta = \log K_{ads} + n\log C$	$\log\theta$ *vs.* $\log C$	187
Langmuir	$C\theta^{-1} = K_{ads}{}^{-1} + C$	$C\theta^{-1}$ *vs.* C	188
Temkin	$K_{ads}\, C = e^{f\theta}$	θ *vs.* $\log C$	186
Frumkin	$B\, C\, e^{2ae} = \theta\,(1-\theta)^{-1}$	θ *vs.* $\log C$	189
Flory–Huggins	$\log(C\theta^{-1}) = \log K_{ads} + x\log(1-\theta)$	$\log(C\theta^{-1})$ *vs.* $\log(1-\theta)$	184
El-Awady	$\log\{\theta\,(1-\theta)^{-1}\} = \log K + Y\log \mathrm{C}$	$\log\{\theta\,(1-\theta)^{-1}\}$ *vs.* $\log C$	190

Appendix E

Table 5 Physical significance of various thermodynamic–kinetic parameters

Parameters	Significance	Reference
$\Delta G_{ads}{}^{0}$	Insight on the adsorption process spontaneousity Type of adsorption $\Delta G_{ads}{}^{0} \leq -20$kj/mol; physisorption $\Delta G_{ads}{}^{0} \leq -40$ KJ mol; chemisorption -20 kj mol$^{-1} \leq \Delta G_{ads}{}^{0} \leq -40$kjmol^{-1}; both physical and chemical adsorption	64
$\Delta H_{ads}{}^{0}$	$\Delta H_{ads}{}^{0} > 0$; endothermic adsorption process $\Delta H_{ads}{}^{0} < 0$; exothermic adsorption process	
$\Delta S_{ads}{}^{0}$	$\Delta S_{ads}{}^{0} > 0$; adsorption is supported by randomness increase $\Delta S_{ads}{}^{0} < 0$; adsorption is supported by randomness decrease as reactant converted to activated complex	
E_a	The presence of an inhibitor leads to an elevation in activation energy (E_a), indicating physical adsorption	

Appendix F

Table 6 Langmuir isotherm parameters for different concentrations of *Ziziphora* leaves extract in 1 M HCl solution[54] (reproduced from ref. 54, copyright, Elsevier, 2020)

Concentration (ppm)	Immersion time (h)	K_{ads} (M^{-1})	$\Delta G_{ads}{}^{0}$ (kJ mol^{-1})
200	0.5	36 666	−35.9
	2.5	36 666	−35.9
	5.0	33 461	−35.7
400	0.5	14 166	−33.6
	2.5	22 500	−34.7
	5.0	16 730	−34.0
600	0.5	13 484	−33.5
	2.5	16 851	−34.0
	5.0	15 000	−33.7
800	0.5	14 375	−33.6
	2.5	16 607	−34.0
	5.0	14 375	−33.6

Acknowledgements

The corresponding author is grateful to Director, CSIR-NML for his support and encouragement through a research grant OLP-0452 project.

References

1 C. Verma, D. S. Chauhan, R. Aslam, P. Banerjee, J. Aslam, T. W. Quadri, S. Zehra, D. K. Verma, M. A. Quraishi, S. Dubey, A. AlFantazi and T. Rasheed, *Green Chem.*, 2024, **26**, 4270–4357.
2 S. Zamindar, S. Mandal, M. Murmu and P. Banerjee, *Mater. Adv.*, 2024, **5**, 4563–4600.
3 C. Yin, M. Kong, J. Zhang, Y. Wang, Q. Ma, Q. Chen and H. Liu, *ACS Omega*, 2020, **5**, 2620–2629.
4 L. T. Popoola, *Corros. Rev.*, 2019, **37**, 71–102.
5 C. Verma, E. E. Ebenso, M. A. Quraishi and C. M. Hussain, *Mater. Adv.*, 2021, **2**, 3806–3850.
6 I. E. Uwah, P. C. Okafor and V. E. Ebiekpe, *Arab. J. Chem.*, 2013, **6**, 285–293.
7 N. Hossain, M. Aminul Islam and M. Asaduzzaman Chowdhury, *Results Chem.*, 2023, **5**, 100883.
8 B. R. Fazal, T. Becker, B. Kinsella and K. Lepkova, *npj Mater. Degrad.*, 2022, **6**, 5.
9 A. Zakeri, E. Bahmani and A. S. R. Aghdam, *Corros. Commun.*, 2022, **5**, 25–38.
10 S. Almi, Z. Rais, S. Seridi, R. Benakcha, K. Almi, R. Hadjeb, H. Menasra and F. Adjal, *New J. Chem.*, 2025, **49**, 5639–5664.
11 B. D. B. Tiu and R. C. Advincula, *React. Funct. Polym.*, 2015, **95**, 25–45.
12 D. Li, Z. Zhang, B. Sukhbat, X. Wang, X. Zhang, J. Yan, J. Zhang, Q. Zhang, Y. Li, H. Wang and Y. Yan, *RSC Appl. Polym.*, 2025, **3**, 532–548.
13 M. A. Ahmed, S. Amin and A. A. Mohamed, *RSC Adv.*, 2024, **14**, 31877–31920.
14 Y. Liu, F. Chen, Z. Wang, H. Ma and Y.-C. Wu, *Mater. Today Commun.*, 2025, **46**, 112759.
15 M. Jiang, X. Liu, Y. Xu, S. Li, X. Liu, X. Niu, L. Lu, X. Sun, Z. Xie, Z. Wang and S. Cui, *ACS Sustain. Chem. Eng.*, 2025, **13**, 2411–2428.
16 M. Li, F. Liu, F. Mou, Z. Guo, W. Wang, Y. Zeng, L. B. Sim and B. Chen, *ACS Omega*, 2025, **10**, 24628–24641.
17 A. Omari Alaoui, W. Elfalleh, B. Hammouti, A. Titi, M. Messali, S. Kaya, B. EL IBrahimi and F. El-Hajjaji, *RSC Adv.*, 2025, **15**, 12645–12652.
18 M. A. Quraishi and D. Jamal, *J. Am. Oil Chem. Soc.*, 2000, **77**, 1107–1111.
19 M. Quraishi and D. Jamal, *Mater. Chem. Phys.*, 2001, **68**, 283–287.
20 M. A. Quraishi and D. Jamal, *Mater. Chem. Phys.*, 2001, **71**, 202–205.
21 A. Yıldırım and M. Çetin, *Corros. Sci.*, 2008, **50**, 155–165.
22 A. Ostovari, S. M. Hoseinieh, M. Peikari, S. R. Shadizadeh and S. J. Hashemi, *Corros. Sci.*, 2009, **51**, 1935–1949.
23 A. K. Satapathy, G. Gunasekaran, S. C. Sahoo, K. Amit and P. V. Rodrigues, *Corros. Sci.*, 2009, **51**, 2848–2856.
24 H. Ashassi-Sorkhabi, M. Majidi and K. Seyyedi, *Appl. Surf. Sci.*, 2004, **225**, 176–185.

25 H. Nakajima, P. Dijkstra and K. Loos, *Polymers*, 2017, **9**, 523.
26 J. Hidalgo, L. Hidalgo, C. D. Serrano Aguiar, D. B. García Madroñero, I. Galambos, J. E. Vilasó-Cadre, I. A. Reyes-Domínguez, A. M. V. Brânzanic, N. Ignat and G. L. Turdean, *Langmuir*, 2025, **41**, 9406–9421.
27 A. Rizi, A. Sedik, A. Acidi, K. O. Rachedi, H. Ferkous, M. Berredjem, A. Delimi, A. Abdennouri, M. ALAM, B. Ernst and Y. Benguerba, *ACS Omega*, 2023, **8**, 47224–47238.
28 J. Lopez de Lacalle, D. Minudri, M. L. Picchio, A. Gallastegui, D. Mantione, M. Forsyth and D. Mecerreyes, *RSC Sustain.*, 2024, **2**, 1809–1818.
29 M. Marinescu, *BMC Chem.*, 2019, **13**, 136.
30 G. Gece, *Corros. Sci.*, 2011, **53**, 3873–3898.
31 M. Abdallah, K. A. Soliman, M. Alfakeer, H. Hawsawi, A. M. Al-bonayan, S. S. Al-Juaid, S. Abd El Wanees and M. S. Motawea, *ACS Omega*, 2023, **8**, 34516–34533.
32 S. Abd El Maksoud, A. E. A. Fouda and H. Badawy, *Sci. Rep.*, 2024, **14**, 9052.
33 R. A. El-Nagar, M. I. Nessim, N. A. Khalil and S. I. Elewa, *Sci. Rep.*, 2024, **14**, 11484.
34 C. Verma, S. H. Alrefaee, M. A. Quraishi, E. E. Ebenso and C. M. Hussain, *J. Mol. Liq.*, 2021, **321**, 114484.
35 Q. Wang, Y. Sang, J. Yang and H. Liu, *Polymers*, 2025, **17**, 422.
36 S. Kumar, D. Sharma, P. Yadav and M. Yadav, *Ind. Eng. Chem. Res.*, 2013, **52**, 14019–14029.
37 N. F. H. Mahmoud and A. El-Sewedy, *J. Chem.*, 2018, **2018**, 1–9.
38 C. Verma, M. A. Quraishi, K. Kluza, M. Makowska-Janusik, L. O. Olasunkanmi and E. E. Ebenso, *Sci. Rep.*, 2017, **7**, 44432.
39 S. KM, B. M. Praveen and B. K. Devendra, *Results Surf. Interfaces*, 2024, **16**, 100258.
40 K. Shalabi, H. M. Abd El-Lateef, M. M. Hammouda and A. A. Abdelhamid, *ACS Omega*, 2024, **9**, 18932–18945.
41 R. Oukhrib, Y. Abdellaoui, A. Berisha, H. Abou Oualid, J. Halili, K. Jusufi, M. Ait El Had, H. Bourzi, S. El Issami, F. A. Asmary, V. S. Parmar and C. Len, *Sci. Rep.*, 2021, **11**, 3771.
42 G. Khan, W. J. Basirun, S. N. Kazi, P. Ahmed, L. Magaji, S. M. Ahmed, G. M. Khan, M. A. Rehman and A. B. B. M. Badry, *J. Colloid Interface Sci.*, 2017, **502**, 134–145.
43 Q. Deng, J. M. Castillo-Robles, E. de Freitas Martins, P. Ordejón, J.-N. Gorges, P. Eiden, X.-B. Chen, P. Keil and I. Cole, *Mol. Syst. Des. Eng.*, 2024, **9**, 29–45.
44 J. Tan, L. Guo, H. Yang, F. Zhang and Y. El Bakri, *RSC Adv.*, 2020, **10**, 15163–15170.
45 I. B. Obot, E. E. Ebenso and M. M. Kabanda, *J. Environ. Chem. Eng.*, 2013, **1**, 431–439.
46 S. Bashir, A. Thakur, H. Lgaz, I. M. Chung and A. Kumar, *Surf. Interfaces*, 2020, **20**, 100542.
47 A. K. Singh, S. Mohapatra and B. Pani, *J. Ind. Eng. Chem.*, 2016, **33**, 288–297.
48 S. Bashir, V. Sharma, H. Lgaz, I.-M. Chung, A. Singh and A. Kumar, *J. Mol. Liq.*, 2018, **263**, 454–462.
49 A. Biswas, S. Pal and G. Udayabhanu, *J. Adhes. Sci. Technol.*, 2017, **31**, 2468–2489.
50 N. A. Negm, N. G. Kandile, E. A. Badr and M. A. Mohammed, *Corros. Sci.*, 2012, **65**, 94–103.
51 E. A Badr, H. H. H. Hefni, S. H. Shafek and S. M. Shaban, *Int. J. Biol. Macromol.*, 2020, **157**, 187–201.
52 B. S. Mahdi, M. K. Abbass, M. K. Mohsin, W. K. Al-azzawi, M. M. Hanoon, M. H. H. Al-kaabi, L. M. Shaker, A. A. Al-amiery, W. N. R. W. Isahak, A. A. H. Kadhum and M. S. Takriff, *Molecules*, 2022, **27**, 4857.
53 N. Leslie and J. Mauzeroll, in *Encyclopedia of Solid-Liquid Interfaces*, Elsevier, 2024, pp. 461–478.
54 A. Dehghani, G. Bahlakeh, B. Ramezanzadeh and M. Ramezanzadeh, *Constr. Build. Mater.*, 2020, **245**, 118464.
55 S. Bashir, H. Lgaz, I. I. I. M. Chung and A. Kumar, *Chem. Pap.*, 2019, **73**, 2255–2264.
56 A. Nahle, R. Salim, F. El Hajjaji, M. R. Aouad, M. Messali, E. Ech-chihbi, B. Hammouti and M. Taleb, *RSC Adv.*, 2021, **11**, 4147–4162.
57 Q. A. Yousif, M. A. Bedair, A. M. Abuelela, A. Ansari, S. S. Malhotra and Z. Fadel, *RSC Adv.*, 2025, **15**, 28666–28688.
58 H. Tristijanto, M. N. Ilman and P. Tri Iswanto, *Egypt. J. Pet.*, 2020, **29**(2), 155–162.
59 P. Mourya, S. Banerjee and M. M. Singh, *Corros. Sci.*, 2014, **85**, 352–363.
60 B. P. Markhali, R. Naderi, M. Mahdavian, M. Sayebani and S. Y. Arman, *Corros. Sci.*, 2013, **75**, 269–279.
61 O. A. Akinbulumo, O. J. Odejobi and E. L. Odekanle, *Results Mater.*, 2020, **5**, 100074.
62 S. A. Umoren, U. M. Eduok and E. E. Oguzie, *Port. Electrochim. Acta*, 2007, **26**, 533–546.
63 H. Lgaz, K. Subrahmanya Bhat, R. Salghi, Shubhalaxmi, S. Jodeh, M. Algarra, B. Hammouti, I. H. Ali and A. Essamri, *J. Mol. Liq.*, 2017, **238**, 71–83.
64 S. Sharma and A. Kumar, *J. Mol. Liq.*, 2021, **322**, 114862.
65 A. Dehghani, G. Bahlakeh, B. Ramezanzadeh and M. Ramezanzadeh, *J. Taiwan Inst. Chem. Eng.*, 2019, **102**, 349–377.
66 B. Tan, B. Xiang, S. Zhang, Y. Qiang, L. Xu, S. Chen and J. He, *J. Colloid Interface Sci.*, 2021, **582**, 918–931.
67 A. Dehghani, G. Bahlakeh, B. Ramezanzadeh and M. Ramezanzadeh, *J. Mol. Liq.*, 2019, **277**, 895–911.
68 Z. Song, H. Cai, Q. Liu, L. Jiang and H. Chu, *J. Ind. Eng. Chem.*, 2022, **111**, 464–479.
69 A. R. Simović, B. N. Grgur, J. Novaković, P. Janaćković and J. Bajat, *Metals*, 2023, **13**, 508.
70 Y. Qiang, S. Zhang, B. Tan and S. Chen, *Corros. Sci.*, 2018, **133**, 6–16.
71 J. Zhang, F. Yang, Y. Dai, Y. Liu, Y. Yu and S. Wang, *Langmuir*, 2023, **39**, 18043–18051.
72 S. Y. Mosavian, Z. Hamidi, N. Sabbaghi, M. Shahabi, M. Noroozifar, M. A. Karimi Zarchi and H. Raissi, *Polym. Bull.*, 2023, **80**, 7569–7598.
73 A. I. Ikeuba, P. C. Okafor, U. J. Ekpe and E. E. Ebenso, *Int. J. Electrochem. Sci.*, 2013, **8**, 7455–7467.

74 S. Kumar, N. Kumar, L. K. Meena, A. Kumar, R. Kumar, V. S. Yadav and L. M. Pandey, *Surf. Interfaces*, 2025, **74**, 107647.
75 M. A. V. Devanathan and B. V. K. S. R. A. Tilak, *Chem. Rev.*, 1965, **65**, 635–684.
76 T. Wenga, D. D. Macdonald and W. Ma, *Prog. Mater. Sci.*, 2025, **148**, 101359.
77 P. Liu, Q. Xu, Q. Zhang, Y. Huang, Y. Liu, H. Li, R. Zhang and G. Lei, *J. Adhes. Sci. Technol.*, 2024, **38**, 1563–1584.
78 E. E. Ebenso, C. Verma, L. O. Olasunkanmi, E. D. Akpan, D. K. Verma, H. Lgaz, L. Guo, S. Kaya and M. A. Quraishi, *Phys. Chem. Chem. Phys.*, 2021, **23**, 19987–20027.
79 M. E. Foster and B. M. Wong, *J. Chem. Theory Comput.*, 2012, **8**, 2682–2687.
80 L. N. Anderson, M. B. Oviedo and B. M. Wong, *J. Chem. Theory Comput.*, 2017, **13**, 1656–1666.
81 R. S. Bhatta, G. Pellicane and M. Tsige, *Comput. Theor. Chem.*, 2015, **1070**, 14–20.
82 A. Nakata, Y. Imamura, T. Otsuka and H. Nakai, *J. Chem. Phys.*, 2006, **124**, 094105.
83 I. B. Obot, D. D. Macdonald and Z. M. Gasem, *Corros. Sci.*, 2015, **99**, 1–30.
84 F. Chiter, D. Costa, V. Maurice and P. Marcus, *J. Electrochem. Soc.*, 2020, **167**, 161506.
85 L. Guo, I. B. Obot, X. Zheng, X. Shen, Y. Qiang, S. Kaya and C. Kaya, *Appl. Surf. Sci.*, 2017, **406**, 301–306.
86 X. Zhang, G. Pan, L. Hu, H. Wang and C. Wang, *Colloids Surf., A*, 2020, **605**, 125392.
87 M. Murmu, S. K. Saha, N. C. Murmu and P. Banerjee, *Corros. Sci.*, 2019, **146**, 134–151.
88 E. M. Rosen and D. C. Silverman, *Corrosion*, 1992, **48**, 734–745.
89 B. El Ibrahimi, A. Jmiai, K. El Mouaden, R. Oukhrib, A. Soumoue, S. El Issami and L. Bazzi, *J. King Saud Univ., Sci.*, 2020, **32**, 163–171.
90 H. Zhao, X. Zhang, L. Ji, H. Hu and Q. Li, *Corros. Sci.*, 2014, **83**, 261–271.
91 H. Al-Sehaibani, *Materwiss. Werksttech.*, 2000, **31**, 1060–1063.
92 A. Y. El-Etre, *J. Colloid Interface Sci.*, 2007, **314**, 578–583.
93 S. K. Shukla, A. K. Singh, I. Ahamad and M. A. Quraishi, *Mater. Lett.*, 2009, **63**, 819–822.
94 C. R. M. Faustin, M. Lebrini and F. Robert, *Int. J. Electrochem. Sci.*, 2011, **6**, 4095–4113.
95 F. R. M. Lebrini and C. Roos, *Int. J. Electrochem. Sci.*, 2011, **6**, 847–859.
96 H. Gerengi and H. I. Sahin, *Ind. Eng. Chem. Res.*, 2012, **51**, 780–787.
97 E. E. Oguzie, C. B. Adindu, C. K. Enenebeaku, C. E. Ogukwe, M. A. Chidiebere and K. L. Oguzie, *J. Phys. Chem. C*, 2012, **116**, 13603–13615.
98 S. F. A and H. B. A, *African J. Pure Appl. Chem.*, 2013, **7**, 350–359.
99 P. B. Raja, A. K. Qureshi, A. Abdul Rahim, H. Osman and K. Awang, *Corros. Sci.*, 2013, **69**, 292–301.
100 K. Agarwal, *J. Mater. Sci. Surf. Eng.*, 2014, **1**, 44–48.
101 N. Chaubey, V. K. Singh and M. A. Quraishi, *Int. J. Ind. Chem.*, 2015, **6**, 317–328.
102 S. A. Umoren, I. B. Obot, A. Madhankumar and Z. M. Gasem, *Carbohydr. Polym.*, 2015, **124**, 280–291.
103 M. A. Chidiebere, E. E. Oguzie, L. Liu, Y. Li and F. Wang, *J. Ind. Eng. Chem.*, 2015, **26**, 182–192.
104 N. El Hamdani, R. Fdil, M. Tourabi, C. Jama and F. Bentiss, *Appl. Surf. Sci.*, 2015, **357**, 1294–1305.
105 N. A. Odewunmi, S. A. Umoren and Z. M. Gasem, *J. Environ. Chem. Eng.*, 2015, **3**, 286–296.
106 M. Prabakaran, S.-H. Kim, V. Hemapriya and I.-M. Chung, *J. Ind. Eng. Chem.*, 2016, **37**, 47–56.
107 L. M. P. Dolabella, J. G. Oliveira, V. Lins, T. Matencio and W. L. Vasconcelos, *J. Coatings Technol. Res.*, 2016, **13**, 543–555.
108 A. N. Grassino, J. Halambek, S. Djaković, S. Rimac Brnčić, M. Dent and Z. Grabarić, *Food Hydrocoll.*, 2016, **52**, 265–274.
109 A. K. Larios-Galvez, J. Porcayo-Calderon, V. M. Salinas-Bravo, J. G. Chacon-Nava, J. G. Gonzalez-Rodriguez and L. Martinez-Gomez, *Anti-Corros. Methods Mater.*, 2017, **64**, 654–663.
110 D. Amar, *J. Chem. Pharm. Res.*, 2017, **9**, 311–318.
111 M. A. Asaad, M. Ismail, P. B. Raja and N. H. A. Khalid, *Surf. Rev. Lett.*, 2017, **24**, 1850013.
112 A. Khanra, M. Srivastava, M. P. Rai and R. Prakash, *ACS Omega*, 2018, **3**, 12369–12382.
113 S. Marzorati, L. Verotta and S. Trasatti, *Molecules*, 2018, **24**, 48.
114 A. A. Farag, A. S. Ismail and M. A. Migahed, *Egypt. J. Pet.*, 2018, **27**, 1187–1194.
115 R. Boulmerka and S. Abderrahmane, *Bull. Mater. Sci.*, 2020, **43**, 242.
116 J. Halambek, I. Cindrić and A. Ninčević Grassino, *Carbohydr. Polym.*, 2020, **234**, 115940.
117 D. I. Njoku, C. N. Njoku, H. Lgaz, P. C. Okafor, E. E. Oguzie and Y. Li, *J. Mol. Liq.*, 2021, **330**, 115619.
118 M. Rehioui, S. Abbout, B. Benzidia, H. Hammouch, H. Erramli, N. A. Daoud, N. Badrane and N. Hajjaji, *Heliyon*, 2021, **7**, e06674.
119 J. Haque, C. Verma, V. Srivastava and W. B. W. Nik, *Sustain. Chem. Pharm.*, 2021, **19**, 100354.
120 N. Hossain, M. A. Chowdhury, A. K. M. P. Iqbal, M. S. Islam, N. Y. Sheikh Omar and A. Z. A. Saifullah, *Curr. Res. Green Sustain. Chem.*, 2021, **4**, 100191.
121 N. Gayakwad, V. Patil and B. M. Rao, *Mater. Today Proc.*, 2022, **49**, 536–541.
122 Y. Fernine, R. Salim, N. Arrousse, R. Haldhar, F. El Hajjaji, S.-C. Kim, M. Ebn Touhami and M. Taleb, *J. Mol. Liq.*, 2022, **355**, 118867.
123 H. Kumar, V. Yadav and A. Kumari, *J. Phys. Chem. Solids*, 2022, **165**, 110690.
124 M. H. Fekri, F. Omidali, M. M. Alemnezhad and A. Ghaffarinejad, *Mater. Chem. Phys.*, 2022, **286**, 126150.
125 W. Daoudi, A. El Aatiaoui, N. Falil, M. Azzouzi, A. Berisha, L. O. Olasunkanmi, O. Dagdag, E. E. Ebenso, M. Koudad,

A. Aouinti, M. Loutou and A. Oussaid, *J. Mol. Liq.*, 2022, **363**, 119839.
126 Q. Wang, L. Liu, Q. Zhang, X. Wu, H. Zheng, P. Gao, G. Zeng, Z. Yan, Y. Sun, Z. Li and X. Li, *Sustain. Chem. Pharm.*, 2022, **27**, 100710.
127 M. A. A. Abdul Aziz, E. Hamzah and M. Selamat, *Mater. Today Proc.*, 2022, **51**, 1344–1349.
128 R. Singh, D. Prasad, Z. Safi, N. Wazzan and L. Guo, *J. Bio-Tribo-Corrosion*, 2023, **9**, 76.
129 A. E.-A. S. Fouda, A. F. Molouk, M. F. Atia, A. El-Hossiany and M. S. Almahdy, *Sci. Rep.*, 2024, **14**, 16112.
130 M. Tabyaoui, M. Tourabi, H. Zarrok, C. Jama, F. Benhiba, A. Zarrouk and F. Bentiss, *Environ. Sci. Pollut. Res.*, 2024, **31**, 43757–43780.
131 A. Kumari Das, S. Neupane, K. Kumar Nayak, S. Shrestha, N. Karki, D. Kumar Gupta and A. Prasad Yadav, *Results Chem.*, 2024, **12**, 101866.
132 H. Mei, B. Zhou, S. Hu, C. Wu and H. Cen, *J. Adhes. Sci. Technol.*, 2025, **39**, 2384–2405.
133 E. M. Saoudi Hassani, R. Salim, E. Ech-chihbi, H. Zejli, I. Mehdaoui, R. Mahmoud, Y. A. Younous, G. A. Shazly, A. Aqdas, A. Taleb, M. Taleb and Z. Rais, *Sci. Rep.*, 2025, **15**, 12164.
134 A. Y. El-Etre and M. Abdallah, *Corros. Sci.*, 2000, **42**, 731–738.
135 M. Kliškić, J. Radošević, S. Gudić and V. Katalinić, *J. Appl. Electrochem.*, 2000, **30**, 823–830.
136 A. Y. El-Etre, *Corros. Sci.*, 2003, **45**, 2485–2495.
137 A. Y. El-Etre, *Appl. Surf. Sci.*, 2006, **252**, 8521–8525.
138 M. K. Sharma, S. Kumar, R. Ratnani and S. P. Mathur, *Bull. Electrochem.*, 2006, **22**, 69–73.
139 P. C. Okafor and E. E. Ebenso, *Pigment Resin Technol.*, 2007, **36**, 134–140.
140 E. E. Oguzie, *Port. Electrochim. Acta*, 2007, **26**, 303–314.
141 E. E. Eddy and N. O. Ebenso, *African J. Pure Appl. Chem.*, 2008, **2**, 46–54.
142 P. B. Raja and M. G. Sethuraman, *Mater. Lett.*, 2008, **62**, 113–116.
143 R. Solmaz, G. Kardaş, B. Yazıcı and M. Erbil, *Corros. Eng., Sci. Technol.*, 2008, **43**, 186–191.
144 M. A. S. Rajendran, R. B. Devi, B. S. Devi, K. Rajam and J. Jeyasundari, *Zašt. Mater.*, 2009, **50**, 77–84.
145 P. C. Okafor, E. E. Ebenso and U. J. Ekpe, *Int. J. Electrochem. Sci.*, 2010, **5**, 978–993.
146 J. C. da Rocha, J. A. da Cunha Ponciano Gomes and E. D'Elia, *Corros. Sci.*, 2010, **52**, 2341–2348.
147 R. Rosliza, A. Nora'aini and W. B. Wan Nik, *J. Appl. Electrochem.*, 2010, **40**, 833–840.
148 V. G. V. R. Saratha, *E-J. Chem.*, 2010, **7**, 677–684.
149 M. A. Abu-Dalo, A. A. Othman and N. A. F. Al-Rawashdeh, *Int. J. Electrochem. Sci.*, 2012, **7**, 9303–9324.
150 F. A. Ayeni, I. A. Madugu, P. Sukop, A. P. Ihom, O. O. Alabi, R. Okara and M. Abdulwahab, *J. Miner. Mater. Charact. Eng.*, 2012, **11**, 667–670.
151 R. N. V. Sribharathy, S. Rajendran and P. Rengan, *Eur. Chem. Bull.*, 2013, **2**, 471–476.
152 M. A. Velázquez-González, J. G. Gonzalez-Rodriguez, M. G. Valladares-Cisneros and I. A. Hermoso-Diaz, *Am. J. Anal. Chem.*, 2014, **5**, 55–64.
153 E. E. Oguzie, M. A. Chidiebere, K. L. Oguzie, C. B. Adindu and H. Momoh-Yahaya, *Chem. Eng. Commun.*, 2014, **201**, 790–803.
154 A. S. Fouda, G. Y. Elewady, K. Shalabi and S. Habouba, *Int. J. Adv. Res.*, 2014, **2**, 817–832.
155 H. Ashassi-Sorkhabi, S. Mirzaee, T. Rostamikia and R. Bagheri, *Int. J. Corros.*, 2015, **2015**, 1–6.
156 M. A. Migahed, S. M. Rashwan, M. M. Kamel and R. E. Habib, *J. Mol. Liq.*, 2016, **224**, 849–858.
157 N. B. Iroha and A. O. James, *J. Chem. Soc. Niger.*, 2018, **43**, 510–517.
158 A. B. Hamdan, Suryanto and F. I. Haider, *IOP Conf. Ser.: Mater. Sci. Eng.*, 2018, **290**, 012086.
159 D. Sukul, A. Pal, S. K. Saha, S. Satpati, U. Adhikari and P. Banerjee, *Phys. Chem. Chem. Phys.*, 2018, **20**, 6562–6574.
160 G. Fekkar, F. Yousfi, H. Elmsellem, M. Aiboudi, M. Ramdani, I. Abdel-Rahman, B. Hammouti and L. Bouyazza, *Int. J. Corros. Scale Inhib.*, 2020, **9**, 446–459.
161 A. I. Ikeuba and P. C. Okafor, *Pigment Resin Technol.*, 2019, **48**, 57–64.
162 R. Haldhar, D. Prasad and N. Bhardwaj, *Arab. J. Sci. Eng.*, 2020, **45**, 131–141.
163 M. Alahiane, R. Oukhrib, Y. A. Albrimi, H. A. Oualid, H. Bourzi, R. A. Akbour, A. Assabbane, A. Nahlé and M. Hamdani, *RSC Adv.*, 2020, **10**, 41137–41153.
164 A. C. Balaskas, M. Curioni and G. E. Thompson, *J. Electroanal. Chem.*, 2020, **863**, 114081.
165 A. Kumar, J. Kumar and Nishtha, *Mater. Today Proc.*, 2022, **64**, 141–146.
166 R. Karki, A. K. Bajgai, N. Khadka, O. Thapa, T. Mukhiya, H. B. Oli and D. P. Bhattarai, *Electrochem*, 2022, **3**, 668–687.
167 M. R. Rathod, R. L. Minagalavar and S. K. Rajappa, *J. Indian Chem. Soc.*, 2022, **99**, 100445.
168 B. Tamilselvi, D. S. Bhuvaneshwari, S. Padmavathy and P. B. Raja, *J. Mol. Liq.*, 2022, **359**, 119359.
169 J. Dai and X. An, *Int. J. Electrochem. Sci.*, 2023, **18**, 100080.
170 K. Hjouji, E. Ech-chihbi, I. Atemni, M. Ouakki, T. Ainane, M. Taleb and Z. Rais, *Sustain. Chem. Pharm.*, 2023, **34**, 101170.
171 Z. Zhou, X. Min, S. Wan, J. Liu, B. Liao and X. Guo, *Results Eng.*, 2023, **17**, 100971.
172 M. Akbari Shahmirzadi and M. Azadi, *Heliyon*, 2024, **10**, e29962.
173 E. Almanza, L. Del Carmen Gutierrez Pua, Y. Pineda, W. Rozo, M. Marquez and A. Fonseca, *Heliyon*, 2024, **10**, e39717.
174 T.-S. Chu, W.-J. Mai, H.-Z. Li, B.-X. Wei, Y.-Q. Xu and B.-K. Liao, *Int. J. Mol. Sci.*, 2025, **26**, 561.
175 A. I. Obike, K. S. Eze, I. Abdel-Rahman, A. I. Ikeuba, I. K. Nwokolo and C. Aghalibe, *Curr. Res. Green Sustain. Chem.*, 2025, **10**, 100447.
176 R. Ao, J. Liu, X. Ren, Y. Liu and Y. Jia, *J. Alloys Compd.*, 2025, **1010**, 177977.

177 H. Hamidi, F. Shojaei, H. Eslami, R. Aliabadi, M. Pourfath and M. Vaez-Zadeh, *Langmuir*, 2025, **41**, 3249–3258.
178 H. M. Hassan, *Int. J. Electrochem. Sci.*, 2025, **20**, 101028.
179 S. Ben Dlala, M. Haj Romdhane, S. Lakard, B. Lakard, D. Le Cerf, H. Majdoub, N. Jaffrezic-Renault and H. Ben Halima, *Int. J. Biol. Macromol.*, 2025, **310**, 143149.
180 Z. Bensouda, E. H. El Assiri, M. Sfaira, M. Ebn Touhami, A. Farah and B. Hammouti, *J. Bio- Tribo-Corrosion*, 2019, **5**, 84.
181 G. A. Swetha, H. P. Sachin, A. M. Guruprasad, B. M. Prasanna and J. Fail, *Anal. Prev.*, 2019, **19**, 1113–1126.
182 A. M. Guruprasad, H. P. Sachin, G. A. Swetha and B. M. Prasanna, *Int. J. Ind. Chem.*, 2019, **10**, 17–30.
183 X. Luo, S. Zhang and L. Guo, *Int. J. Electrochem. Sci.*, 2014, **9**, 7309–7324.
184 A. Singh, K. R. Ansari and M. A. Quraishi, *Int. J. Hydrogen Energy*, 2020, **45**, 25398–25408.
185 S. John and A. Joseph, *Mater. Chem. Phys.*, 2012, **133**, 1083–1091.
186 P. Dohare, D. S. Chauhan, A. A. Sorour and M. A. Quraishi, *Mater. Discov.*, 2017, **9**, 30–41.
187 E. E. Oguzie, *Corros. Sci.*, 2007, **49**, 1527–1539.
188 A. Singh, N. Soni, Y. Deyuan and A. Kumar, *Results Phys.*, 2019, **13**, 102116.
189 A. A. El-Awady, B. A. Abd-El-Nabey and S. G. Aziz, *J. Electrochem. Soc.*, 1992, **139**, 2149–2154.
190 I. B. Obot, N. O. Obi-Egbedi and S. A. Umoren, *Int. J. Electrochem. Sci.*, 2009, **4**, 863–877.